Electrophysiological characterisation and expression pattern of ion channels in astrocytes before and after traumatic brain injury

Stefanie Götz

Graduate School of Systemic Neurosciences
LMU Munich

Dissertation der Graduate School of Systemic Neurosciences der

Ludwig-Maximilians-Universität München

22nd July 2019

Electrophysiological characterisation and expression pattern of ion channels in astrocytes before and after traumatic brain injury

Dissertation der Graduate School of Systemic Neurosciences der

Ludwig-Maximilians-Universität München

Stefanie Götz

22nd July 2019

1st reviewer: PD Dr. Lars Kunz

2nd reviewer: Prof. Dr. Benedikt Grothe

External reviewer: Prof. PhD Alfonso Araque

Date of Submission: 12.03.2019

Date of Defense: 08.07.2019

Table of content

Abstract

After traumatic brain injury (TBI) astrocytes perform various beneficial tasks like the reorganisation and support of the blood-brain barrier (BBB), the remodelling of synapses and neural circuits and controlling inflammation. They do this by becoming reactive under these conditions. Astrocyte reactivity includes, but is not limited to hypertrophy, polarization, the upregulation of glial fibrillary acidic protein (GFAP) in astrocytic processes as well as proliferation of astrocytes surrounding the lesion site. In the somatosensory cortex of mice juxtavascular astrocytes, which have their soma directly adjacent to blood vessels are more prone to proliferate in response to TBI, whereas non-juxtavascular astrocytes with the cell soma further away from the vasculature are less likely to do so. Nevertheless, the underlying mechanism of this selective proliferation is still not well understood. It is known that ion channels play an important role in cell cycle progression in different cell types and at different developmental stages. Especially potassium (K^+) channels have been shown to be key players. To determine whether there are differences present between the two astrocyte subtypes per se, in this study K^+ channel expression patterns and electrophysiological properties were characterized in juxtavascular astrocytes and compared with the ones of non-juxtavascular astrocytes in the unlesioned somatosensory cortex of Aldh1l1-eGFP mice. Furthermore, ion channel expression patterns were compared five days after astrocyte reactivity was induced by a stab wound lesion.

Whole-cell patch-clamp recordings in somatosensory cortex slices of healthy Aldh1l1-eGFP mice revealed great heterogeneity in the resting membrane potential (V_r), the resting membrane conductance (G_r) and the input resistance (R_{in}) of different astrocytes. 70% of non-juxtavascular and 81% of juxtavascular control astrocytes displayed typical Ohmic passive current patterns with linear IV-curves. Blocking of inwardly rectifying $K_{ir}4.1$ ion channels in electrophysiological recordings as well as immunohistochemical stainings revealed a homogeneous expression of $K_{ir}4.1$ channels in astrocytes across all cortical layers. Heterogeneous expression of $K_{ir}6.2$ and $K_v4.3$ channels in somatosensory cortex astrocytes was revealed by means of immunohistochemistry. Moreover, heterogeneous expression of hyperpolarization-activated cyclic nucleotide-gated 1 (HCN1) channels in somatosensory cortex astrocytes of the unlesioned brain was detected by immunohistochemistry, but could

not be confirmed in electrophysiological recordings. All dissimilarities mentioned above could not be related to whether an astrocyte is non-juxtavascular or juxtavascular in nature.

A stab wound lesion and the subsequent reactive astrogliosis triggered a downregulation of $K_{ir}4.1$ in proliferating reactive astrocytes as well as the upregulation of $K_v4.3$ channels on polarized astrocytic processes. This was accompanied by a shift especially in juxtavascular astrocytes towards non-passive current response patterns. This proposed an important role of these two K^+ channel subtypes in astrocyte proliferation suggesting that these reactive astrocytes might resemble immature astrocytes with proliferative potential. Astrocyte reactivity and proliferation had no impact on $K_{ir}6.2$ and HCN1 channel expression. HCN2 channels, which were absent in astrocytes in control conditions were upregulated on processes of a subset of reactive polarizing astrocytes independently of non-juxtavascular and juxtavascular position as well as proliferative behaviour. These finding are of great interest for therapeutic approaches since there is increasing evidence that astrocyte proliferation positively affects healing processes and axon regeneration after traumatic brain injury.

1 Introduction

1.1 Glia cells

1.1.1 Evolution of glia cells

At some point in life history on earth and especially with the evolution of bilateral body organization centralized brains appeared in combination with condensed ganglia that were more complex than the so far present nerve nets of the radial symmetric phyla Cnidaria and Ctenophora: This allowed animals to react to more advanced external stimuli and complex environments. In addition, a new cell type arose, the so called glia cells (Bullock & Horridge, 1965; Hartline, 2011). The most likely scenario is that glia cells evolved parallel to the appearance of sensory systems. For example in Planarians and Polychaeta larvae light detecting neurons are accompanied by supporting pigment cells (Gehring & Ikeo, 1999), which might already resemble a form of glia cells. During evolution, the amount of glial cells in the brain increased. In invertebrate species like *Drosophila* and *Caenorhabditis* around 10 % of cells in the central nervous system are glia cells (Pereanu et al., 2005; Beckervordersandforth et al., 2008; von Hilchen et al., 2008; Oikonomou & Shaham, 2011) whereas the amount of glia cells appears to increase with brain complexity. The general opinion is, that the bigger the brain, the higher the ratio of glia cells to neurons (Reichenbach, 1989). And indeed, studies have shown, that there is a dominance of glia cells in comparison to neurons in larger brains (Ransom et al., 2003). For a long time it has been thought, that in the highly advanced and large human brains, glia cells outnumber neurons up to ten times (Kandel et al., 2000; Ullian et al., 2001; Doetsch, 2003; Nishiyama et al., 2005; Noctor et al., 2007). But newer studies show, that the human brain bears nearly the same number of neurons and non-neuronal cells, with the latter being comprised of glia cells, mesenchymal cells as well as endothelial cells and that the ratios in humans resemble the ones in other primates (Azevedo et al., 2009). The ratio of non-neuronal cells to neurons differs immensely for different brain regions. For example in the cerebral cortex the ratio is 0.99 non-neuronal cells/neurons, whereas in the cerebellar cortex the ratio is only 0.23. In the rest of the brain, non-neuronal cells outnumber neurons by an astonishing ratio of 11.35 (Azevedo et al., 2009). This is in line with other studies in the human brain, where it has been shown that in subcortical areas like the thalamus, the glia to neuron ratio is 17:1 (Pakkenberg & Gundersen, 1988). Recent studies in mammals highlight that the

ratio of glial cells to neurons depends on neuronal density and not on brain size (Herculano-Houzel, 2014).

1.1.2 Historic background of neuroglia

The concept of glia cells was established in 1856 by the German scientist Rudolf Virchow. He named these cells after the greek word “glia” referring in this case to "putty", due to him believing that these neuroglia cells were an acellular mass that functions as connective brain tissue, the so called “Nervenkitt” or “Zwischenmasse” in which the neurons of the brain are embedded (Virchow, 1856, 1858). The first glia cell type was identified namely the Müller glia cells in the retina (Müller, 1851) followed by the discovery of cerebellar Bergmann glia in 1857 (Bergmann, 1857). In 1865 white and grey matter stellate glia cells were described by Otto Deiters (Deiters, 1865). Later, using his silver-chromate impregnation technique, Camillo Golgi described grey matter glia cells as cells with a round soma and a high amount of fine stellate processes. Moreover, he defined glia as a distinct cellular population that stays in close contact to blood vessels and he showed the existence of heterogeneous glia cell populations throughout the brain, as well as glial networks and radial fibres now known as radial glia cells (Golgi, 1870). In 1920, Cajal implemented the astrocyte-specific gold chloride-sublimate staining and described a variety of astrocyte types (Ramon y Cajal, 1920). Also oligodendrocytes and microglia were identified and described around that time (Del Rio-Hortega, 1919, 1920). Another type of neuroglia, the NG2 glia cells are a much more recent discovery (Stallcup, 1981).

1.1.3 Definition of glia cells

All non-neuronal cells of the nervous system, except cells that are part of the vasculature, are pooled under the umbrella term neuroglia. In contrast to neurons, which are defined as cells that generate action potentials, it is quite difficult to find a simple and universally applicable definition to define a glia cell. They are often said to be non-excitable, delineating them from excitable neurons, but exceptions to this rule are present. Newer approaches define glia according to their functions as homeostasis-maintaining cells that show high amounts of heterogeneity regarding their origin, structure and especially their function (Parpura & Verkhratsky, 2014). In invertebrates, glia cells are defined as cells that have a close association

with neurons and they separate neuronal compartments from the mesoderm. They arise from ectodermal layers and are named macroglia (Bullock & Horridge, 1965; Radojcic & Pentreath, 1979; Hartline, 2011; Parpura & Verkhratsky, 2014). Studies in Drosophila have shown that these macroglia cells can be subdivided into different classes and perform various functions like constituting the blood-brain barrier (BBB), enwrapping axons, ensuring the proper layering of neurons during development, the maintenance of neurons, axon guidance and many more (Hartenstein, 2011). In invertebrates macroglia cells also function as brain macrophages. In contrast, vertebrate brain immune cells, the so called microglia cells originate from the mesoderm and migrate into the central nervous system (CNS) during embryogenesis (Saijo & Glass, 2011). In the mammalian nervous system, glial cells are classified in peripheral nervous system (PNS) glia originating from the neural crest and CNS glia with neuroectodermal origin (Parpura & Verkhratsky, 2014; Prasad & Charney, 2019). PNS glia comprises satellite glial cells that ensheathe neuronal cell bodies in sympathetic, parasympathetic and sensory ganglia (Hanani, 2005, 2010), olfactory ensheathing cells that enwrap non-myelinated neurons in the olfactory nervous system (Ramón-Cueto & Avila, 1998) as well as enteric glia which is present in the nervous system of the gastrointestinal tract and has stunning similarities to astrocytes in the CNS (Coelho-Aguiar et al., 2015). Non-myelinating Remak Schwann cells that enwrap small axons in Remak fibres are crucial for the proper development and function of the PNS as well as regeneration after peripheral nerve damage (Harty & Monk, 2017). One more type of non-myelinating Schwann cells are perisynaptic Schwann cells, that enwrap the neuromuscular junction (Ko & Robitaille, 2015). Myelinating Schwann cells, that are the counterpart of oligodendrocytes in the CNS, form the myelin sheath of sensory and motor neurons to enable saltatory conduction along the nodes of Ranvier (Kidd et al., 2013). In the CNS also several types of glia cells are present (Allen & Barres, 2009) that can be divided into macroglia cells with neuroectodermal origin and microglia cells that stem from the mesoderm (Parpura & Verkhratsky, 2014). These glia cell types will be introduced in the following paragraph.

1.2 Glia cell types

1.2.1 Microglia

New studies show, that microglia progenitor cells are derived from CD-45 c-kit positive erythromyeloid precursors in the extra-embryonic yolk sac, the first site where haematopoiesis takes place and are generated in mice during early embryogenesis (Kierdorf et al., 2013). These cells subsequently invade the CNS and colonize all regions via tangential and radial migration (Mosser et al., 2017), where they differentiate into microglia cells in a transforming growth factor (TGF)-β-dependent process (Butovsky et al., 2014). Microglia cells (Figure 1) function as the resident immune cells of the brain (Allen & Barres, 2009). In humans, depending on the studies, they are estimated to provide 5 to 10 % or even up to 15 % of glia cells (Mittelbronn et al., 2001; Pelvig et al., 2008). Microglia cells can transform into different states depending on the functional need. Ramified microglia cells are present throughout the healthy CNS in a resting state, non-phagocytic and phagocytic activated microglia appear in the pathological CNS and dystrophic microglia cells are present in the aging brain (Gehrmann et al., 1995; Angelova & Brown, 2018). Microglia cells are organised in distinct non-overlapping domains (Kreutzberg, 1995) forming a massive network constantly scanning the surrounding neural tissue with their thin processes throughout an organisms` lifetime (Lawson et al., 1990). They use this scanning mechanism to sense damage, infectious agents and debris from dead cells, as well as to conduct housekeeping tasks (Hickman et al., 2018). Their roles in housekeeping mechanisms comprise the remodelling of synapses during development and neurodegeneration (Zhan et al., 2014; Lui et al., 2016; Vasek et al., 2016), maintaining myelin homeostasis (Healy et al., 2016), as well as reacting to lesions and cell death by migrating towards debris and phagocytosing it (Fuhrmann et al., 2010). Another important function of microglia cells is the protection against damaging events. They do this by mediating defence mechanisms against pathogens, detrimental self-proteins and tumours. This is mediated by pathogen sensing receptors and the according receptor mediated pathways. Upon activation, neuroinflammatory responses are triggered in microglia cells, as well as the upregulation of antigen presenting complexes like the major histocompatibility complex (MHC) II to interact with T-lymphocytes (Almolda et al., 2011; Hickman et al., 2018). The proper functioning of microglia cells is

essential for brain development and function and when disrupted has detrimental effects on the CNS (Parpura & Verkhratsky, 2014).

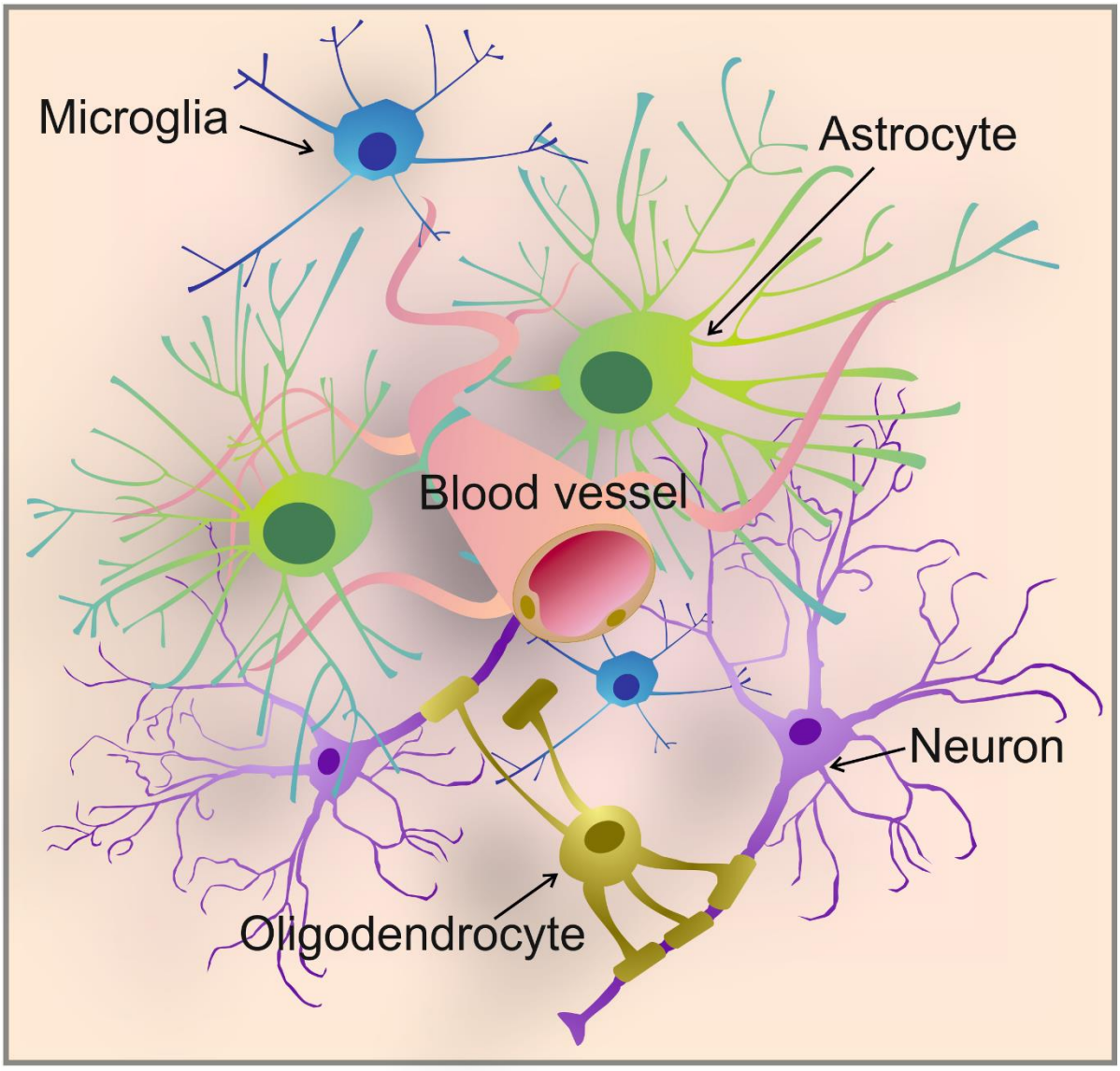

Figure 1: Schematic illustration of the main glial cell types in the central nervous system
Astrocytes (green) are in contact with the brain vasculature via endfeet. Microglia cells (blue), the immune cells of the brain, constantly scan their surrounding via small processes in the ramified resting state. Oligodendrocytes (yellow) enwrap axons of several neurons (lilac) and form the myelin sheath.

Macroglia

During the development of the CNS, neurons are generated first in a process called neurogenesis which is followed by gliogenesis where macroglia cells are made (Deneen et al., 2006; Kang et al., 2012). Gliogenesis takes place from late embryonic to even postnatal stages (Goldman, 2004). The switch from neurogenesis to gliogenesis occurs at embryonic day 12.5 in the spinal cord and around embryonic day 16-18 in the cerebral cortex of mice under the control of the transcription factors Sox9 and NFIA (Stolt et al., 2003; Deneen et al., 2006; Kang et al., 2012). Moreover, other factors like Notch-signalling pathways, histone methylation, the methylase Dntm1 and N-CoR, which is a repressor of transcription, play direct and indirect roles in the switch to gliogenesis (Molofsky and Deneen, 2015).

1.2.2 NG2 glia

NG2 glia cells are a subtype of macroglia cells that are positive for the nerve/glia antigen (NG2), which is a chondroitin sulphate proteoglycan. They are present in white and grey matter regions of the developing and adult brain (Nishiyama et al., 2009), as well as in neurogenic niches like the dentate gyrus and subventricular zone (Aguirre, 2004; Aguirre et al., 2004; Passlick et al., 2013). Studies in mice have shown, that during brain development NG2 glia cells appear in three different waves originating from different neural precursors. The first wave emerges around E11.5 in the ventral forebrain from Nkx2.1 precursors in the medial ganglionic eminence (MGE). The second wave has its origin in the lateral and caudal ganglionic eminences (LGE; CGE) around E15 and are generated by Gsh2 precursors. The NG2 glia cells generated during the first two waves populate the embryonic telencephalon and cerebral cortex. The third wave arises postnatally in the cerebral cortex from Emx1 precursors (Kessaris et al., 2006). During development and even during adulthood NG2 glia cells generate oligodendrocytes and hence make up the greatest population of resident progenitor cells in the adult brain (Dimou & Gallo, 2015). They have a highly branched morphology and are capable to react to injury by repopulating lesioned areas (Aguirre et al., 2007; Simon et al., 2011; Whittaker et al., 2012; Filous et al., 2014; Scafidi et al., 2014). NG2 glia cells are the only glia cells that receive direct inhibitory and excitatory input from neuronal synapses. This neurotransmitter-mediated signalling might mediate NG2 differentiation into oligodendrocytes (Gallo et al., 2008; Bergles et al., 2010; Fröhlich et al., 2011; Sakry et al., 2011). Moreover,

they have the capacity to give rise to astrocytes or persist self-renewing NG2 glia cells dependent on the brain region they reside in and their developmental stage (Zhu et al., 2007; Zhu et al., 2008; Simon et al., 2011; Zhu et al., 2011).

1.2.3 Oligodendrocytes

Oligodendrocytes (Figure1) are characterized as neuroglia cells, with only few processes radiating from their soma (Pérez-Cerdá et al., 2015). They originate from NG2 glia cells that differentiate first into premyelinating oligodendrocytes and later become mature myelinating oligodendrocytes (Emery, 2010). Oligodendrocytes are only present in the CNS and their analogues in the PNS are Schwann cells (Kidd et al., 2013). Oligodendrocytes are smaller than astrocytes and lack cytoplasmic glycogen granules and intermediate filaments. Moreover, they have a high density in their cytoplasm and nuclei with densely packed chromatin and their processes have a high amount of microtubules (Afifi, 1991; Lunn et al., 1997). Myelinating oligodendrocytes extend 1 to 40 processes (depending on the CNS region) that contact axons of different neurons and enwrap them to form the myelin sheath which is needed for fast action potential propagation as well as axon protection and trophic support (Bunge et al., 1961; Bunge et al., 1962; Bunge, 1968; Afifi, 1991; Fünfschilling et al., 2012; Saab et al., 2016). Additionally, satellite or also called perineuronal oligodendrocytes exist. Satellite oligodendrocytes are primarily non-myelinating cells present predominantly in the grey matter (Ludwin, 1979; Takasaki et al., 2010; Szuchet et al., 2011). They are located at the somal base close to the axon initial segment which is the action potential initiation site of a neuron (Kole & Stuart, 2012; Pérez-Cerdá et al., 2015). These cells are proposed to remyelinate axons after injuries (Ludwin, 1979), guard neurons from apoptosis (Taniike et al., 2002) and give them metabolic support (Takasaki et al., 2010). Moreover, it has been shown that satellite oligodendrocytes are integrated into a glial-syncytium with oligodendrocytes and astrocytes and constrain high-frequency activity of neurons (Battefeld et al., 2016).

1.3 Astrocytes

Astrocytes were named in 1895 by Michael von Lenhossék after the Greek words astron = star and kytos = cavity or cell meaning star like cell (Lenhossék, 1895). Later, Santiago Ramón y Cajal introduced the gold and mercury chloride-sublimate staining technique, which specifically stains glial fibrillary acidic protein (GFAP) of astrocytes and led him to confirm that astrocytes originate from radial glia cells (García-Marín et al., 2007). Already in the late 19th and early 20th century scientists assumed that astrocytes perform a plethora of different functions apart from just being a filler between neurons (Verkhratsky & Nedergaard, 2018). Nowadays it is known that astrocytes are a very heterogeneous group of cells with many different subtypes and an incredible amount of different functions they exert in the nervous system. The following paragraphs will exclusively discuss astrocytes in the mammalian brain.

1.3.1 Astrocyte definition

Astrocytes are extremely heterogeneous and as already discussed earlier, not only important in the mature brain but also play important roles during the development of the CNS by providing migratory pathways for neurons and supporting neuronal growth. They also serve as progenitors for neurons and other neural cells and play a critical role in synapse formation and development (Ransom et al., 2003). Therefore astrocytes drastically change their functions and properties over the course of development (Kimelberg, 2010) and it is hard to find general applicable criteria that define an astrocyte. Nevertheless, several criteria have been established (Barres, 2003; Ransom et al., 2003; Kimelberg, 2004c, b, a; Barres, 2008; Wang & Bordey, 2008; Kimelberg, 2009, 2010). Astrocytes are defined as non-excitable cells in the CNS with a high amount of potassium (K^+) channels in the cell membrane and hence have a resting membrane potential (V_r) close to the equilibrium potential for K^+ (E_K). They possess a large amount of intermediate filaments which are the origin of the astrocyte specific GFAP protein and many of the astrocytic processes are in close contact with synapses and surround them. Moreover, astrocytic endfeet contact the vasculature and they bare glycogen granules. They are able to take up the neurotransmitters glutamate and gamma-aminobutyric acid (GABA) via astrocyte-specific transporters and are highly coupled with other astrocytes by gap-junctions made of connexin 43 and 30. All of the criteria mentioned above can individually or in some degree of combination also be true for other glia cells. But the combination of all said criteria

is what identifies a neural cell as an astrocyte (Wang & Bordey, 2008; Kimelberg, 2010; Verkhratsky & Nedergaard, 2018).

1.3.2 Astrocyte origin and development

Radial glia cells in the embryonic ventricular zone operate as neural progenitor cells that produce neurons at earlier stages and when neuronal migration along their radial fibres is finished around birth, they morph into protoplasmic astrocytes (Schmechel & Rakic, 1979; Voigt, 1989; Malatesta et al., 2000; Noctor et al., 2001; DeAzevedo et al., 2003; Malatesta et al., 2003). Radial glia cells in the subventricular zone of the neonatal CNS are generating intermediate glial progenitor cells via asymmetric division that migrate into the cortex and develop into grey matter astrocytes and oligodendrocytes. Additionally, they have the potential to become white matter astrocytes (Levison et al., 1993; Levison & Goldman, 1993, 1997; Ganat et al., 2006). NG2 glia cells in the ventral forebrain are also capable of generating protoplasmic astrocytes that do not migrate to other brain areas but remain residential in the ventral forebrain. This generation of astrocytes starts prenatally around E17.5 most likely from the Emx1positive NG2 glia cells mentioned in paragraph 1.2.2 (Kessaris et al., 2006; Zhu et al., 2007; Zhu et al., 2011). Another type of neural progenitors which reside in the marginal zone of the embryonic and neonatal cortex give rise to astrocytes of cortical layer I-IV as well as to neurons and oligodendrocytes. This might explain differences that are present between astrocytes of superficial and deeper layers (Costa et al., 2007; Breunig et al., 2012). Nevertheless the main source of astrocytes generated in the postnatal brain is through symmetric proliferation of mature astrocytes throughout the CNS (Ge et al., 2012). Proliferation of astrocytes will be elucidated in detail later in this thesis (Paragraph 1.6.2 and 1.8).

1.4 Astrocyte types

As previously mentioned astrocytes comprise a highly heterogeneous group of glial cells with many subpopulations of different morphology and functions (Kimelberg, 2004c). Based on morphology, astrocytes are proposed to make up 20 to 40 % glia of the human brain (Pelvig et al., 2008). In this paragraph the main astrocyte subpopulations in the various regions of CNS are introduced.

1.4.1 Protoplasmic astrocytes

Protoplasmic astrocytes (Figure 1) are present in the grey matter of the CNS and have a very specific morphology with a small (approximately 10 µm) cell soma with radially extending processes that bare a massive amount of fine lamellar arborisations that occupy a more or less spheroid volume and make up for a high surface-to-volume ratio of up to 25 μm^{-1} and a surface area of 80.000 μm^2 (Bushong et al., 2002; Ogata & Kosaka, 2002; Kimelberg, 2004c, 2010; Reichenbach et al., 2010; Verkhratsky & Nedergaard, 2018). They are highly abundant with between 10.000 to up to 30.000 cells per mm^3 (Bushong et al., 2002; Ogata & Kosaka, 2002; Reichenbach et al., 2010). Moreover, they are greatly coupled through gap-junctions with other surrounding astrocytes via their smallest arborisations and occupy non-overlapping domains that resemble a syncytium like structure (Giaume & McCarthy, 1996; Bushong et al., 2002; Houades et al., 2008). In the cortex of rodents, protoplasmic astrocytes are in contact with up to 8 neurons and cover a plethora of synapses in addition to surrounding neuronal dendrites (Bushong et al., 2002; Halassa et al., 2007). Human astrocytes are the most complex ones in the mammalian kingdom. They are 2.55 fold larger in diameter and occupy a greater volume than their rodent counterparts. Hence, they are capable of covering way more synapses within a single astrocytic domain (Oberheim et al., 2006; 2009). Protoplasmic astrocytes have a tremendous heterogeneity in morphological features between and within different nuclei (Kimelberg, 2004c, 2010; Verkhratsky & Nedergaard, 2018). In addition to the morphological differences, protoplasmic astrocytes have a high amount of heterogeneity regarding functionality as well as physiological properties (Kimelberg, 2004c, 2010; Parpura & Verkhratsky, 2014; Verkhratsky & Nedergaard, 2015, 2018), which will be discussed in detail later.

1.4.2 Fibrous astrocytes

In mammals astrocytes that are present in the white matter tracts, the retinal nerve fibre layer and the optic nerve, are named fibrous astrocytes and they differ drastically from grey matter astrocytes regarding their morphology (Waxman, 1986; Butt et al., 1994). They have small cell somata that lay in rows between axon bundles in the white matter and are characterised by an elongated appearance due to their up to 100 µm long protruding processes that span radially along myelinated fibres (Lundgaard et al., 2014). Other morphological characteristics of fibrous astrocytes are overlapping domains with other astrocytes. They establish perinodal processes that contact the nodes of Ranvier and have endfeet associated with the vasculature and the pia (Verkhratsky & Nedergaard, 2015). In addition to the morphological differences to protoplasmic astrocytes; fibrous astrocytes differ in protein expression patterns as well. The hyaluronic acid receptor cluster of differentiation 44 (CD44) as well as the intermediate filament proteins vimentin and GFAP are predominantly and highly expressed in fibrous astrocytes (Kaaijk et al., 1997; Goursaud et al., 2009) compared to very little amounts being present in protoplasmic ones. Therefore, they are thought to play an important role for structural integrity among myelinated axon bundles. In contrast to protoplasmic astrocytes, where gap-junctional coupling is happening on average between 94 astrocytes, in fibrous astrocytes the degree of gap junctional coupling varies immensely between different brain regions from no to a few coupled astrocytes in the corpus callosum to up to 91 % of fibrous astrocytes forming a network in the optic nerve (Lee et al., 1994; Haas et al., 2006).

1.4.3 Müller glia

Müller glia cells, which were discovered and named by Heinrich Müller in 1851 are retinal cells that combine the characteristics of radial glia cells and protoplasmic astrocytes (Müller, 1851; Reichenbach & Bringmann, 2017). Their cell somata lie in the inner nuclear layer of the retina and they extend main processes that bare microvilli to the subretinal space and main processes that contain multivesicular bodies that project to the vitreal space. Smaller processes that emanate from the sides of the cell enwrap and contact neurons but also form endfeet that associate with blood vessels (Bringmann et al., 2006; Reichenbach & Bringmann, 2017). In addition to providing neuronal support and performing secretory and homeostatic functions,

Müller glia cells - due to their elongated shape - have a higher refractive index and are therefore able to provide a low scattering passage for light through the retina (Franze et al., 2007).

1.4.4 Bergmann glia

Bergmann glia cells support young granule cell migration from the external granular layer of the cerebellum comparable to radial glia cells in cortical development (Rakic, 1971; Gregory et al., 1988; Hatten, 1990; Hartmann et al., 1998). They have small somata located in the Purkinje cell layer of the cerebellum and extend radially aligned processes that span the molecular layer of most vertebrates, also known as Bergmann fibres (Grosche et al., 2002). Around 8 Bergmann glia cells surround one Purkinje neuron. They are responsible for proper functioning and the survival of neurons by exerting homeostatic functions as well as glutamate uptake (Chaudhry et al., 1995; Müller & Kettenmann, 1995; Reichenbach et al., 1995; Ruiz & Ortega, 1995; Cui et al., 2001; Grosche et al., 2002). The 3 to 6 Bergmann fibres that emanate from a Bergmann glia cell branch of complex side processes with a high surface-to-volume ratio which allow them to contact and ensheathe up to 8000 synapses (Grosche et al., 1999).

1.4.5 Radial glia

In mammals, radial glia cells are the glia of the developing brain. Their cell somata are located in the ventricular zone of the embryonic neural tube. They have a bipolar morphology with one process extending to the basal surface under the meninges and one reaching the apical surface, where they are in contact with the lumen of the ventricle (Cameron & Rakic, 1991; Bentivoglio & Mazzarello, 1999). They are connected among each other by adherent junctions (Shoukimas & Hinds, 1978; Møllgård et al., 1987; Aaku-Saraste et al., 1996). Moreover, radial glia cells bear glycogen granules, as also seen in adult astrocytes (Götz et al., 2002). Radial glia cells start developing from neuroepithelial cells depending on the basic helix-loop-helix Hes transcription factor at the embryonic stage E9.5 (Hatakeyama, 2004). Radial glia cells occupy a lot of different functions. On the one hand they support the migratory process of postmitotic neurons from the ventricular zone to their positions in basal parts of the neural tube (Rakic, 1988) by working as a scaffold for neurons to move along. On the other hand they make up the majority of precursor cells in the developing brain and start to divide during the neurogenic phase between E12-18 producing neurons between E14-16 and astrocytes from E18 on

(Malatesta et al., 2000; Hartfuss et al., 2001; Noctor et al., 2002; Malatesta et al., 2003). The generation of astrocytes by radial glia cells has already been shown by Voigt (1989), who used DiI tracer labelling of radial glia cell endfeet at the pial surface in the ferret cortex. This way he was able to follow labelled radial glia cells throughout development and shows that they become astrocytes later on (Voigt, 1989). Moreover it has been shown that radial glia cells also generate multiciliated ependymal cells which are present in the wall of the lateral ventricle (Spassky, 2005).

1.4.6 Other astrocyte types

Many other types of astrocytes can be found in the CNS. There is the subpopulation of surface-associated astrocytes that form the glia limitans in the posterior piriform cortex (Feig & Haberly, 2011). Tanycytes, which are bipolar astrocytes, form a bridge between the ventricular wall and the portal capillaries. They play a key role in brain-endocrine interactions (Rodríguez et al., 2005). Velate astrocytes are present in the granular layer of the cerebellum and in the olfactory bulb where small neurons are packed very densely (Chan-Palay & Palay, 1972; Valverde & Lopez-Mascaraque, 1991). Pituicytes in the neurohypophysis actively engage in controlling the ionic microenvironment (Hatton, 1999). Marginal and perivascular astrocytes form several layers of endfeet plates with blood vessels that are located close to the pia mater and therefore form the pial and perivascular glia limitans barrier (Liu et al., 2013). Moreover ependymocytes, choroid plexus cells and retinal pigment epithelial cells exist that line the ventricles and subretinal space. They are responsible for the production of the cerebrospinal fluid as well as its flow (Reichenbach & Bringmann, 2017). In the primate and human brain astrocyte types can be found that do not exist in other animals. First off, human protoplasmic astrocytes have much more complex arborisations and therefore occupy significantly larger domains than in rodents (Oberheim et al., 2006; Oberheim et al., 2009) . In primates, polarized astrocytes exist that have their cell somata located close to the corpus callosum and extend long processes into superficial cortical layers (Oberheim et al., 2009). Vice versa interlaminar astrocytes exist in old world monkeys, apes and humans that have a small cell soma located in cortical layer I that project up to two very long process into cortical layer IV and several smaller processes into cortical layer II to IV (Oberheim et al., 2009). Being an exclusive feature in humans, varicose projection astrocytes are bushy astrocytes residing in layer V and VI and

project long unbranched processes in all directions through the deeper cortical layers that bare evenly distributed varicosities along these projections (Oberheim et al., 2009).

1.5 Astrocyte functions in the healthy brain

During the development of the nervous system astrocytes already play important roles in synaptogenesis by providing regulatory factors and structural components in the perinatal brain (Eroglu & Barres, 2010; Pfrieger, 2010; Clarke & Barres, 2013; Verkhratsky & Nedergaard, 2018). In the adult brain specialised astrocytes exist in neurogenic niches that function as adult stem cells capable of neurogenesis (Ihrie & Alvarez-Buylla, 2008; Kriegstein & Alvarez-Buylla, 2009).

During late embryogenesis protoplasmic astrocytes start to divide the grey matter into non-overlapping parcels in a process called tiling. This generates micro-anatomical domains that are restricted by the reach of the astrocytic processes. The processes are in contact with multiple neurons and their respective synapses and connect them to the vasculature in said domain hence creating the so called neurovascular unit (Iadecola & Nedergaard, 2007). These astrocyte domains are connected with each other via gap-junctional coupling forming astroglial syncytia that are segregated themselves within anatomical structures like for example the barrels of the somatosensory cortex (Houades et al., 2008).

1.5.1 Homeostatic functions

When neurons are active, depolarisation leads to an accumulation of K^+ ions in the surrounding extracellular space. If K^+ is not removed it would have detrimental effects like continuous neuronal depolarisation, hyperexcitability and seizures (Wang & Bordey, 2008). Astrocytes are capable of taking up the excess K^+ from the extracellular space via inwardly rectifying potassium channels (K_{ir}), as well as Na^+/K^+ and K^+/Cl^- transporters and distribute it through the gap-junctional syncytium where it is subsequently released at sites with lower extracellular K^+ concentration (Ballanyi et al., 1987; Karwoski et al., 1989). This mechanism is called K^+ spatial buffering (Figure 2c) (Kuffler & Nicholls, 1966). In addition to K^+ spatial buffering astrocytes also execute homeostatic functions by regulating the extracellular chloride (Cl^-) concentrations (Kettenmann et al., 1987; Egawa et al., 2013), calcium (Ca^{2+}) concentrations (Zanotti & Charles, 1997) as well as the pH by hydrogen (H^+) removal from and hydrogen carbonate (HCO_3^-) release into the extracellular space (Rose & Ransom, 1996; Deitmer & Rose, 2010). Astrocytes are also able to prevent reactive oxygen species (ROS) toxicity in the

brain (Winkler et al., 1994; Desagher et al., 1996; Dringen et al., 1999; Rice, 2000). They regulate the volume of and the water flow in the extracellular space via aquaporin 4 channels (Amiry-Moghaddam & Ottersen, 2003; Yao et al., 2008; Haj-Yasein et al., 2011; Nagelhus & Ottersen, 2013). Astrocytes are also performing transmitter homeostasis (Figure 2a) to prevent excitotoxicity (Verkhratsky & Nedergaard, 2018). They take up glutamate from the synaptic cleft via the excitatory amino acid transporters (EAAT1/2) glutamate aspartate transporter (GLAST) and glutamate transporter 1 (GLT-1) (Danbolt, 2001; Hertz & Zielke, 2004; Hertz et al., 2007). The glutamate that has been cleared by astrocytes from the synaptic cleft is enzymatically broken down to glutamine via glutamine-synthetase (GS) and then released to be subsequently taken up by neurons that transform it back to glutamate and GABA (Westergaard et al., 1995; Sonnewald et al., 1998). In addition, astrocytes express equilibrating and concentrating transporters that allow them to accumulate adenosine internally where it is phosphorylated by the adenosine kinase (ADK) (Boison, 2008). Moreover, astrocytes have high affinity GABA transporters (GABA transporter 1 and 3 (GAT-1 and GAT-3) located in the cellular membrane close to the synaptic cleft and take up GABA, likely to control transmitter spillover. The internalised GABA can subsequently be released through GAT transporters depending on internal sodium (Na^+) concentration and depolarization of the cell (Gallo et al., 1991; Yee et al., 1998; Barakat & Bordey, 2002).

1.5.2 The tripartite synapse

Astrocytes enwrap synapses in the brain to different extent depending on the brain region, with up to 90 % of synapses in layer IV of the somatosensory cortex being ensheathed by astrocytic processes (Bernardinelli et al., 2014). Together with the endterminal of the presynaptic neuron and the postsynaptic neuron astrocytes form the so called tripartite synapse (Figure 2b) (Allen & Barres, 2009). Glutamate (Glu) that is released from the presynaptic neuron binds to astrocytic metabotropic glutamate receptors (mGluR) which results in intracellular Ca^{2+} elevation. Ca^{2+} subsequently triggers vesicular release of neuromodulators and neurotransmitters from the astrocyte. These neuromodulators and neurotransmitters interact with presynaptic and postsynaptic receptors of neurons which results in the modification of neuronal mechanisms and activity. One astrocyte can ensheathe and contact several thousand

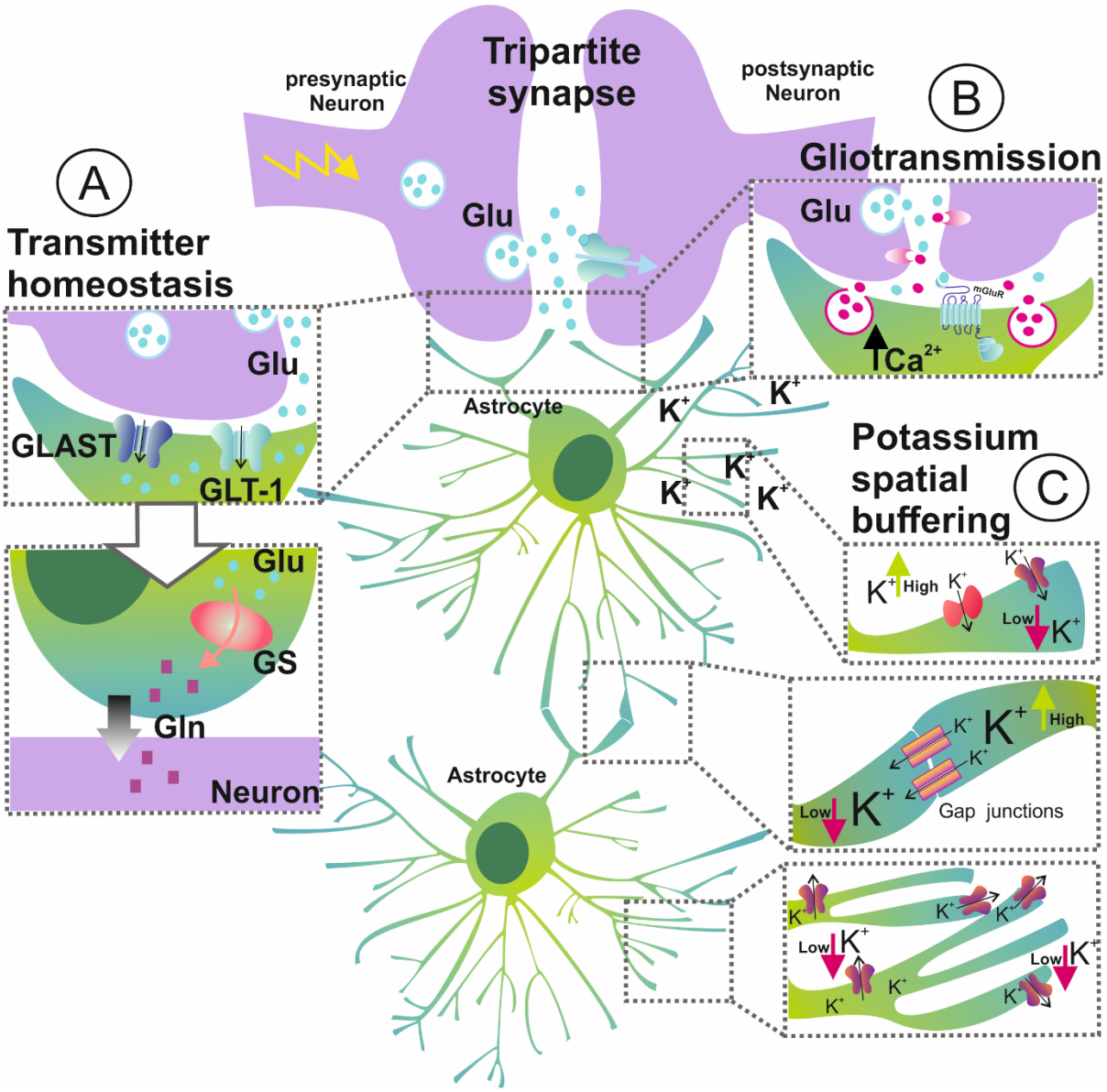

Figure 2: Astrocyte functions in the healthy brain
A: Astrocytes perform transmitter homeostasis.They take up glutamate (Glu) from the synaptic cleft via glutamate transporters GLAST and GLT-1. Glutamate is then broken down enzymatically via glutamine-synthetase (GS) into glutamine (Gln) which is released and subsequently taken up by neurons. **B:** Astrocytes enwrap synapses in the brain and together with the endterminal of the presynaptic neuron and the postsynaptic neuron they form the so called tripartite synapse. Glutamate (Glu) that is released from the presynaptic neuron binds to astrocytic metabotropic glutamate receptors (mGluR). Subsequently vesicular release of neuromodulators and neurotransmitters from the astrocyte is triggered to interact with presynaptic and postsynaptic receptors of neurons. **C:** Astrocytes perform K^+ spatial buffering by taking up excess K^+ from the extracellular space vir K_{ir} (lilac), as well as Na^+/K^+ and K^+/Cl^- transporters (red). Subsequently they distribute it via gap-junctions (long orange tunnels) through the astrocytic network where it gets released at sites with lower extracellular K^+ concentration.

synapses (Verkhratsky et al., 2012; Parpura & Verkhratsky, 2014; Verkhratsky & Nedergaard, 2018). They are able to release neuromodulators and neurotransmitters (e.g. Glutamate, GABA, adenosine triphosphate (ATP)) through several different mechanisms in a more spatially diffuse and much slower manner than neurons do hence modifying and regulating neuronal networks, mechanism and activity (Verkhratsky et al., 2012; Parpura & Verkhratsky, 2014). Furthermore, astrocytes play a role in synaptic pruning, the maintenance of synapses, regulation of synaptic plasticity as well as the integration of synaptic fields (Nedergaard & Verkhratsky, 2012; Schafer & Stevens, 2013). Thus, they are key players in higher brain functions like memory and learning, sleep, circadian rhythm and they are part of the glymphatic system that clears the brain from waste and toxins (Verkhratsky & Nedergaard, 2018).

1.5.3 Maintenance of the blood-brain barrier

Astrocytes play important roles in the formation, as well as the maintenance of the BBB (Figure 3). Their endfeet are in contact with the vasculature of the CNS and form the parenchymal part of the BBB (Abbott et al., 2010). They also regulate the tight-junctions that are formed between blood vessel endothelial cells (Abbott et al., 2006). Astrocytes release vasodilators and vasoconstrictors and therefore actively regulate blood flow (MacVicar & Newman, 2015). Due to their association with the brain vasculature astrocytes locally provide metabolic support to neurons (Figure 3). According to the astrocyte neuron lactate shuttle hypothesis they take up glucose from the blood stream and convert it into lactate, which is subsequently released from the astrocytes and taken up by neurons and fed into their tricarboxylic acid (TCA) cycle (Pellerin & Magistretti, 1994, 2012). In addition, studies in rats have shown that astrocytes are able to take up lactate from the extracellular space (Genda et al., 2011). Another way of metabolic support for neurons is the storage of glycogen by astrocytic glycogen granules. The glycogen is provided to neurons during phases of high neuronal activity (Brown & Ransom, 2007).

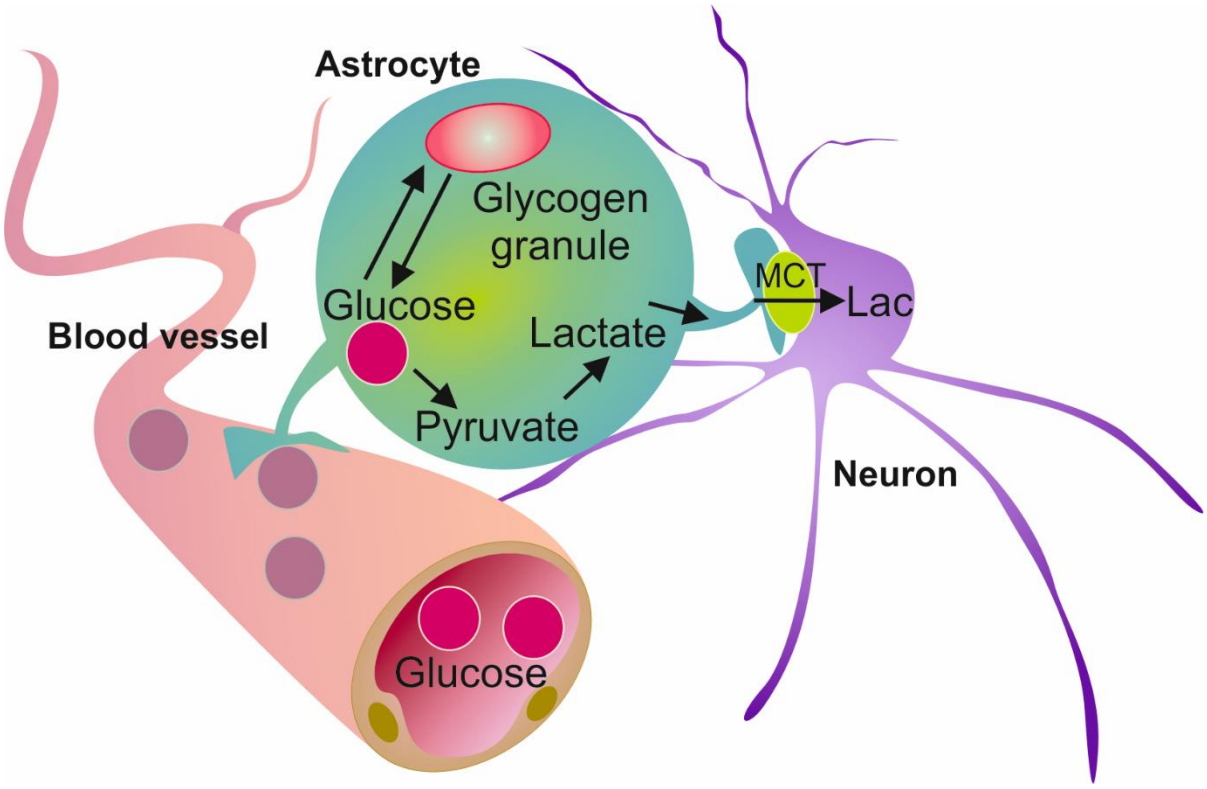

Figure 3: Astrocytes provide metabolic support for neurons
Astrocytes take up glucose from the blood stream. The glucose subsequently is converted during the glycolysis into pyruvate. Pyruvate is converted into lactate by the lactate dehydrogenase. Lactate is then transported from the astrocytes via the monocarboxylate transporter (MCT) to neurons. The glucose that is taken up by astrocytes can also be converted into glycogen and is stored in astrocytic glycogen granules. During phases of high neuronal activity the glycogen is converted back into glucose, transformed into lactate and then provide to neurons for metabolic support.

1.6 Astrocytes in the injured brain: Reactive astrogliosis

One major function of astrocytes is, that they are capable to react to neurological disorders, brain disease and injury with a multistage and graded process called reactive astrogliosis, which is still not fully understood (Pekny & Pekna, 2014).

Together with microglia cells astrocytes are important for the tissue response triggered by non-physiological and pathological changes in the brain environment (Pekny & Nilsson, 2005; Sofroniew, 2009; Buffo et al., 2010; Sofroniew & Vinters, 2010; Pekny & Pekna, 2014, 2016; Pekny et al., 2016; Pekny et al., 2018). So what exactly is reactive astrogliosis and what changes do astrocytes undergo after they become reactive? What triggers their activation and what are the effects, positive as well as negative, of this reactivity?

1.6.1 Astrocyte reactivity and reactive astrogliosis

Reactive astrogliosis in mammals is a multistep process, which is still not completely understood but the following definition has been proposed by Michael V. Sofroniew (2009): First, reactive astrogliosis can be considered as a series of functional and cellular changes in response to different intensities and forms of pathological events and insults to the CNS tissue. Second, the extent of these changes depends on the severity of the initiating events. Third, the changes undergone by reactive astrocytes are highly regulated by signalling molecules and fourth, these changes are accompanied either by loss or gain of functions that have either positive or negative effects on the surrounding tissue and cells (Sofroniew, 2009; Sofroniew & Vinters, 2010). It is important to keep in mind, that the reactive astrogliosis is a highly complex and graded process that proceeds continuously with different stages that blend into each other (Sofroniew & Vinters, 2010). First of all, mild to moderate reactive astrogliosis happens in response to either diffuse innate immune activation caused by bacterial or viral infection, mild trauma or in regions more distant to a bigger lesion. In these cases astrogliosis can be reversed after the underlying cause disappeared because no reorganization of tissue architecture takes place (Sofroniew & Vinters, 2010). In response to severe lesions, neurodegenerative stimuli and more serious infections, severe and diffuse astrogliosis kicks in accompanied by the loss of astrocytic domains and astrocyte proliferation. Lastly, severe astrogliosis in combination with glia scar formation is caused by severe penetrating or

contusive trauma, invasive infections or even abscesses, stroke, chronic neurodegeneration and tumours (Sofroniew & Vinters, 2010). Glial scar formation (Figure 4) is a process that also involves other neural cells apart from reactive astrocytes (Bundesen et al., 2003; Herrmann et al., 2008) where extracellular matrix collagens get deposited to form a molecular clue containing scar that inhibits cell migration as well as axonal growth (Silver & Miller, 2004). This is accompanied by pronounced and long lasting tissue reorganisation (Sofroniew & Vinters, 2010).

Reactive astrocytes can be triggered by many different molecular mediators excreted by other astrocytes and a variety of other cell types including leukocytes, oligodendrocytes, microglial cells, endothelial cells and also neurons (Sofroniew, 2009). Amongst these molecular triggers are different cytokines and growth factors (John et al., 2003; Di Giorgio et al., 2007), bacterial lipopolysaccharides (LPS) and toll-like receptor (TLR) ligands that are part of the innate immune response (Farina et al., 2007), molecules that get released by injured cells like ATP (Neary et al., 2003), ROS as well as glucose deprivation and hypoxia (Swanson et al., 2004), neurotransmitters and neuromodulators (Bekar et al., 2008), NH_4^+, which is a product of systemic metabolic toxicity (Norenberg et al., 2009), and also by factors that are associated with neurodegenerative diseases (Simpson et al., 2010). The mechanisms underlying the activation are equally diverse (for more information see (Sofroniew, 2009)). It has been shown in mouse models, that candidate pathways mediating astrocyte activation are the STAT3 pathway (Sriram et al., 2004), the deactivation of β1-integrin in astrocytes (Robel et al., 2009) as well as Ca^{2+}-dependent N-cadherin upregulation (Kanemaru et al., 2013). Moreover in rats, the activation of the epidermal growth factor receptor (EGFR) is important for the transition from non-reactive to reactive astrocytes (Planas et al., 1998; Erschbamer et al., 2007). Traumatic brain injury (TBI), which can be caused by many different stimuli like brain contusion and penetrating injuries, has different levels of severity (Graham et al., 2000) and is a special form of brain insult where mechanical forces are involved (Burda et al., 2016). In addition to the previously mentioned activation stimuli, in TBI astrocytes are also activated by the mechanical forces that result in tissue distortion and perforation and subsequently in strain. In rat cultures, this activates mechanotransducing and stretch-activated ion channels in the astrocytic membranes (Bowman et al., 1992; Islas et al., 1993; Cullen et al., 2011) which

allows rapid influx of extracellular Ca^{2+} and Na^{+} (Rzigalinski et al., 1997; Rzigalinski et al., 1998; Floyd et al., 2005).

There are different morphological and molecular features which define an astrocyte as a reactive one. First and foremost, they upregulate their expression of GFAP enormously. Even astrocytes in the cerebral cortex that do show only minimal or no GFAP positivity in the healthy brain upregulate this main element of intermediate filaments upon activation (Eng et al., 2000). One more characteristic of reactive astrocytes is the swelling of the cell soma and processes, an event called hypertrophy. In mild astrogliosis this happens within their distinct domains. Extension, overlap as well as disruption of different astrocytic domains occur in severe astrogliosis (Wilhelmsson et al., 2006; Sofroniew, 2009; Sofroniew & Vinters, 2010). Moreover, astrocytic process can be seen to polarize towards an injury site depending on the Rho guanosine triphosphate hydrolase enzyme (GTPase) cell division control protein 42 (*Cdc42)* of rodents *in-vivo* and *in-vitro* (Höltje et al., 2005; Etienne-Manneville, 2006; Robel et al., 2011a; Bardehle et al., 2013). In addition, *Cdc42*-dependent migration of astrocyte towards the site of injury has been shown in scratch wound assays *in-vitro* (Etienne-Manneville, 2006; Robel et al., 2011a; Zamanian et al., 2012).

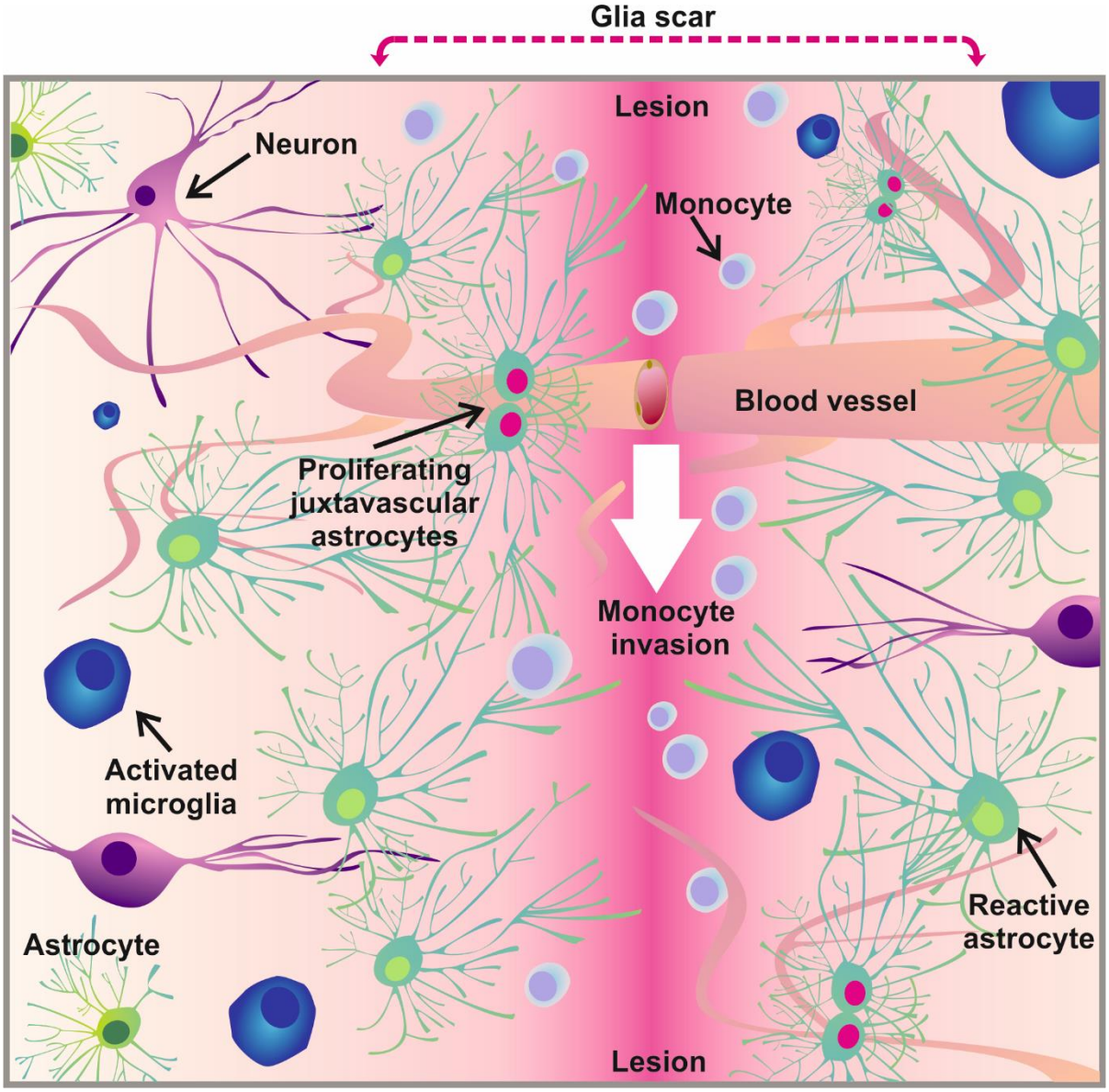

Figure 4: Reactive astrogliosis after traumatic brain injury
Glial scar formation is a process that also involves various neural cells where extracellular matrix collagens get deposited to form a molecular clue containing scar that inhibits cell migration as well as axonal growth. Astrocytes surrounding the lesion in a radius of 300µm upregulate GFAP and become reactive (dark green). Most of the reactive astrocytes also become hypertrophic and a subset of them polarizes towards the lesion site. A fraction of astrocytes surrounding the lesion start to proliferate. Proliferating astrocytes (dark green; pink nucleus) generate two closely associated daughter cells. Proliferation is mainly happening juxtavascular astrocytes. Also activated microglia cells (blue) are present at the lesion site in excessive amounts. Also monocytes (white) can be found that invade the brain tissue from the blood stream.

1.6.2 Astrocyte proliferation after injury *in-vivo*

As previously mentioned, one key component of astrogliosis is that a proportion of astrocytes proliferate (Figure 4) in response to invasive and traumatic brain injury like stab wounds or stroke which causes an increase in astrocyte numbers surrounding a lesion (Sofroniew, 2009; Buffo et al., 2010; Robel et al., 2011b). Isolation and subsequent *in-vitro* culturing of rodent astrocytes showed that a subset of these cells form neurospheres containing self-renewing and multipotent cells with neural stem cell potential (Lang et al., 2004; Buffo et al., 2008). A study in mice has shown, that the stem cell response pattern of astrocytes is triggered by sonic hedgehog (shh) from the plasma and cerebrospinal fluid (Sirko et al., 2013).

Because astrocyte migration and proliferation towards and surrounding an injury site has not been investigated *in-vivo* until then, Bardehle et al. in 2013 , used *in-vivo* 2pLSM (2 photon laser scanning microscope) live imaging techniques to observe the response behaviour of astrocytes to a traumatic brain injury in the mouse cortex (Bardehle et al., 2013). They found, that reactive astrocytes show great functional heterogeneity in their response patterns to a stab wound lesion, which can be interpreted as some kind of differentiation of labour. Via *in-vivo* monitoring they analysed the behaviour of the exact same astrocytes over the course of weeks. In response to a stab wound lesion, astrocytes surrounding the lesion in a radius of 300 µm upregulated GFAP and therefore became activated. Around 86 % of these reactive astrocytes were becoming hypertrophic. Polarization of astrocytic processes towards the lesion with a positive correlation between the amounts of polarization to the size of the lesion occurred in 45 % of astrocytes between 3 to 5 days post injury (dpi). This polarization of astrocytic processes is also seen in the epileptic mouse brain (Oberheim et al., 2008). Most important Bardehle et al. (2013) could show, that in stark contrast to what can be observed in *in-vitro* scratch wound assays in rodents, where astrocytes are moving towards the wound (Höltje et al., 2005; Etienne-Manneville, 2006; Robel et al., 2011a) that this is not the case *in-vivo* (Bardehle et al., 2013). In the cerebral cortex of mice astrocytes remain stationary even up to weeks after TBI (Bardehle et al., 2013). A very crucial observation they made, was that 14 % of astrocytes surrounding the lesion started to proliferate within the first 7 days post injury. Therefore, they concluded that the 20 % increase in astrocyte numbers surrounding a lesion in the cortex is solely due to the proliferation of these cells instead of migratory processes.

Proliferating astrocytes in the cortex generate two closely associated daughter cells and it is important to note that proliferation is mainly happening in astrocytes that have their cell soma directly adjacent to blood vessels in the brain parenchyma proper. This subset of cells is therefore called juxtavascular astrocytes (Bardehle et al., 2013). This lead to the conclusion, that the small subset of reactive astrocytes that undergo cell division after a traumatic brain injury, the so called juxtavascular astrocytes are especially important because they are the only source to increase astrocyte numbers in the grey matter of the somatosensory cortex in mice (Bardehle et al., 2013). In addition, selective ablation experiments, performed in the same study, suggested that this class of proliferating juxtavascular astrocytes plays a role in limiting leucocyte invasion into the injured brain (Bardehle et al., 2013). It has also been shown that astrocyte proliferation is common in response to a variety of pathological brain events in humans and especially to abscesses and demyelinating lesions like multiple sclerosis. However, a much smaller portion of astrocytes proliferate compared to their rodent counterparts (Dowling et al., 1997; Schönrock et al., 1998; Montana et al., 2005).

1.7 Positive and negative effects of astrogliosis

Reactive astrocytes perform various functions in response to CNS insults which will be discussed in the following paragraph. For long it has been assumed that due to the inhibition of neuronal regeneration beyond the glia scar, reactive astrocytes only play detrimental roles after brain insults and even that inhibition of reactive astrogliosis would be a valuable therapeutic strategy (Ramon y Cajal, 1928). Indeed, the inhibition of neuronal regeneration, especially if not resolved during the acute injury phase, can lead to negative effects (Rolls et al., 2009). Moreover in rat astrocyte cultures have shown, that astrocytic pattern recognition receptor induced NFκB (nuclear factor kappa-light-chain-enhancer of activated B cells) signalling leads to the swelling of cells and subsequently to cytotoxic oedema that are responsible for detrimental brain swelling after traumatic insults (Jayakumar et al., 2014). In the traumatically injured CNS of rodents proteins that constitute the perineuronal net, the chondroitin sulphate proteoglycans (CSPGs) aggrecan, versican and neurocan become upregulated in reactive astrocytes directly surrounding the lesion core which might impact synapse regeneration and neuronal sprouting in a negative way by thickening of the perineuronal net (Busch & Silver, 2007; Harris et al., 2009; Harris et al., 2010; Yi et al., 2012). Moreover, reactive astrocytes might be involved in the generation of seizures (Jansen et al., 2005; Tian et al., 2005), the production of excessive amounts of neurotoxic ROS (Swanson et al., 2004; Hamby et al., 2006) and trigger an intense inflammatory reaction by producing cytokines (Brambilla et al., 2005; Brambilla et al., 2009).

Nevertheless, other scientific research elucidates that reactive astrogliosis has a variety of positive effects on the injured brain (Sofroniew, 2009). Amongst these beneficial effects is the regulation and repair of the BBB, the separation of the damaged tissue to protect healthy surrounding tissue, the regeneration of neuronal circuits and synapse remodelling as well as controlling inflammatory processes (Burda et al., 2016), which will be discussed in detail in the following paragraphs.

1.7.1 Support and reorganization of the blood-brain barrier

It is known that newly proliferated astrocytes are crucial for the repair of the BBB in mice (Bush et al., 1999). They do so by releasing molecules like sonic hedgehog (shh) and retinoic acid that act on endothelial cells of the BBB to reduce its permeability and induce its repair (Alvarez et al., 2011; Alvarez et al., 2013; Mizee et al., 2014). Moreover, in early stages of reactive gliosis the ATP release from astrocytes and subsequent activation of microglia cells play a role in maintaining the BBB (Roth et al., 2014). Reactive astrocytes release vasoactive endothelial growth factor (VEGF) and apolipoprotein E (APOE) which leads to an increase in the permeability of the BBB boosting pro-inflammatory mechanisms and leucocyte infiltration in mice (Argaw et al., 2009; Argaw et al., 2012; Bell et al., 2012). Reactive astrocytes alter the expression pattern of aquaporin 4 (AQP4) channels on processes that are in contact with endothelial cells, which influences fluid homeostasis (Papadopoulos & Verkman, 2013). Moreover, reactive astrocytes release danger-associated molecular pattern (DAMP) molecules like the high-mobility group box 1 (HMGB1) that act on endothelial cells and promote the repair and remodelling of the BBB and vasculature in the lesioned brain of rodents (Hayakawa et al., 2012; Hayakawa et al., 2013).

1.7.2 Synapse and circuit remodelling

Reactive astrocytes regulate injury-induced remodelling of synapses by polarizing their processes towards traumatized neurons, which is beneficial for survival and promotes synapse recovery depending on STAT3 mediated thrombospondin-1 signalling in mice (Tyzack et al., 2014). Thrombospondin-1/2 becomes upregulated in murine astrocytes after stroke and promotes axonal sprouting (Liauw et al., 2008). After traumatic brain injury reactive astrocytes respond to a decrease in excitatory input from neighbouring neurons by releasing the cytokine tumour necrosis factor (TNF) α, which subsequently induces excitatory synaptic scaling in said neurons by increasing AMPA receptor density in synapses of rodents (Turrigiano et al., 1998; Beattie et al., 2002; Stellwagen & Malenka, 2006; Turrigiano, 2006). In addition, a study in an entorhinal denervation *in-vitro* model has shown that astrocytic TNFα release after injury leads to an increase in excitatory synaptic strength, which might be important to preserve neuronal excitability while the disturbed neuronal networks reorganize (Becker et al., 2015). Another mechanism for synaptic reorganization by astrocytes might be mediated by astrocytic

production of extracellular matrix molecules that form and modify the perineuronal net that is important for synapse stabilization (Wang & Fawcett, 2012). As previously mentioned, proteins that constitute the perineuronal net become upregulated after CNS insults (Busch & Silver, 2007; Burda et al., 2016). Conflicting data exists which shows that the upregulation of the extracellular matrix protein neurocan that is highly expressed by reactive astrocytes, inhibits axon development *in-vitro* (Friedlander et al., 1994) but is present in regions of excessive axonal sprouting *in-vivo* after TBI in the entorhinal cortex of rats (Haas et al., 1999). The same is true regarding tenascin-C, which inhibits axon outgrowth of olfactory sensory neurons of mice *in-vitro* but is present in regions with pronounced axonal sprouting after brain damage in the rat dentate gyrus (Deller et al., 1997; Treloar et al., 2009). This might be explained by the expression of α9 integrin in sprouting neurons after TBI, which is capable of increasing neurite outgrowth on tenascin-C rich substrates in cultures of rat dorsal root ganglion neurons (Andrews et al., 2009). In rats, the CSPGs aggrecan, versican and neurocan are upregulated in reactive astrocytes surrounding a lesion and are downregulated further away (Harris et al., 2009). This suggests a spatiotemporal regulation of these CPSGs; on the one hand to prevent the formation of unwanted synaptic connections with deleterious targets and on the other hand to promote axonal outgrowth towards constructive ones. This is influencing post-traumatic remodelling of neuronal circuits (Burda et al., 2016).

1.7.3 Control of inflammation

After focal tissue damage or extent inflammation, reactive astrocytes are able to segregate the injured tissue from healthy adjacent neural tissue by forming scars comprised of newly proliferated astrocytes that limit spreading of inflammation and mediate wound repair (Sofroniew & Vinters, 2010; Wanner et al., 2013; Burda & Sofroniew, 2014; Sofroniew, 2014). After traumatic brain injury in mice dying cells in the damaged region release ATP (Kim & Dustin, 2006). This ATP-release triggers $Ca2^{+}$ waves in astrocytes that subsequently triggers astrocytes to release ATP themselves through connexin-hemichannels. Extracellular ATP signalling in rodents was shown to be crucial for the rapid recruitment of microglial cells and neutrophils as well as inducing astrocyte reactivity *in-vitro* and *in-vivo* (Guthrie et al., 1999; Verderio & Matteoli, 2001; Davalos et al., 2005; Huang et al., 2012; Roth et al., 2014). Moreover, ATP released by astrocytes in the murine brain has neuroprotective functions and

is crucial for the survival of meningeal and parenchymal cells (Roth et al., 2014). Reactive astrocytes are also capable of releasing and reacting to inflammatory molecules like danger-associated molecular patterns (DAMP) and alarmins as well as immunomodulatory molecules like chemokines and cytokines. These signalling molecules limit and decrease the inflammatory response and encourage clearance of cytotoxic debris (Pedrazzi et al., 2010; Burda & Sofroniew, 2014). In addition, it has been shown in mouse astrocytes cultures that they also express TLRs and receptor for advanced glycation end products (RAGE) that are typically present in cells with immune functions like macrophages and microglia (Ponath et al., 2007; Gorina et al., 2011). It has been shown in rat glia cell cultures, that the activation of astrocytic RAGE by amyloid-beta results in astrocytes taking over phagocytic functions (Jones et al., 2013). The activation of astrocytic pattern recognition receptors by bacterial LPS leads to the expression of immunomodulatory and proinflammatory molecules, which is believed to increase pro-inflammatory signalling pathways resulting in recruitment of immune cells into the CNS (Lenz et al., 2007; Hoarau et al., 2011; Hamby et al., 2012). Experiments with cultured rat astrocytes have shown, that opposed to the deleterious effects that astrocytic pattern recognition receptor induced NFκB signalling can have after TBI, it can also be beneficial by resulting in the release of glio- and neuroprotective growth factors (Zaheer et al., 2001; Jayakumar et al., 2014).

Other beneficial functions of reactive astrocytes are the protection of neurons from ammonia toxicity being present in hepatic encephalopathy, Reye's syndrome, urea cycle disorders and other neurological conditions (Rao et al., 2005). In rodents reactive astrocytes produce glutathione to protect the tissue from oxidative stress (Chen et al., 2001; Shih et al., 2003; Swanson et al., 2004; Vargas et al., 2008), take up excess glutamate, which could otherwise be excitotoxic (Rothstein et al., 1996; Bush et al., 1999; Swanson et al., 2004) and they release ATP which leads to an accumulation of its catabolic neuroprotective product adenosine in the tissue (Lin et al., 2008).

1.8 Underlying cause of astrocyte proliferation

It has been shown via clonal Star Track analysis in mice that the heterogeneous reaction of reactive astrocytes is related to their developmental origin (Martín-López et al., 2013). As previously mentioned, astrocyte proliferation mainly occurs in lesions that affect the BBB, which led to the identification of several factors that are involved in the regulatory processes leading to proliferation like shh, endothelin-1, and fibroblast growth factor (FGF) signalling in rodents *in-vivo* and *in–vitro* as well as in human tissue (Gadea et al., 2008; Kamphuis et al., 2012; Zamanian et al., 2012; Behrendt et al., 2013; Götz & Sirko, 2013; Sirko et al., 2013; Dimou & Götz, 2014; Kang et al., 2014). Genome wide expression pattern analysis of murine grey matter proliferative reactive astrocytes shows that this subset of astrocytes upregulates the expression of genes comparable to neural stem cells extracted from the subependymal zone (Sirko et al., 2015). Amongst these are the two lectins galectin 1 and galectin 3 that are known to be highly expressed in neural stem cells as well as reactive astrocytes of rodents and upregulated after smaller injuries and in cancer (Camby et al., 2006; Sakaguchi et al., 2006; Kajitani et al., 2009; Yan et al., 2009; Beckervordersandforth et al., 2010; Le Mercier et al., 2010; Di Lella et al., 2011; Newlaczyl & Yu, 2011; Qu et al., 2011; Zamanian et al., 2012; Young et al., 2014; Sirko et al., 2015). Sirko et al. (2015) showed that these two lectins are expressed in a small subset of reactive astrocytes (25 %) after traumatic brain injury in the grey matter of mice with galectin 3 specifically labelling proliferating ones. These findings were further supported by experiments performed in *Lgals1*$^{-/-}$ (Lectin, Galactoside-Binding, Soluble, 1) and *Lgals3*$^{-/-}$ (Lectin, Galactoside-Binding, Soluble, 3) mice where they could show that reactive astrocyte proliferation, neurosphere formation and GFAP positivity was reduced in response to an insult (Sirko et al., 2015). All of the above could be fully rescued by supplementing galectin 3 *in-vitro*, indicating galectin 3 as a key player in promoting astrocyte proliferation after an injury (Sirko et al., 2015). Another factor that might influence the proliferation of juxtavascular astrocytes is a cross-regulation happening between astrocytes and invading monocytes. After a stab wound injury in mice that lack monocyte invasion, increased proliferation of astrocytes was observed (Frik et al., 2018). In addition, a reduced glial scar with less extracellular matrix deposition can be observed, which also led to higher amounts of neurons surrounding the smaller lesion site (Frik et al., 2018). Despite the higher

amount of proliferating astrocytes, less GFAP positive cells were observed at the lesion site (Frik et al., 2018).

1.9 Ion channels in cell cycle progression

Cell division is a process by which the DNA (deoxyribonucleic acid) has to be distributed between two daughter cells. In order to do so, the cell has to pass through the cell cycle that consists of a long interphase followed by a mitosis (M)-phase that comprises the mitosis itself, in which the replicated genome is separated into two new nuclei and the cytokinesis where the cytoplasm is duplicated. The interphase consists of the gap (G) 1-phase, during which the cell grows and prepares for the cell division. This is followed by the synthesis (S)-phase where DNA is synthesized and chromosomes are replicated. Finally, the G2-phase is reached in which the cell continues to grow and synthesizes proteins to form new organelles before it subsequently enters into the mitotic cell division phase (M-phase). After the M-phase, each daughter cell can either re-enter into the G1-phase of a new cell cycle or into a quiescent G0-state that for some cells lasts for the rest of their life, the so called end-differentiated ones (Campbell & Reece, 2008). To guarantee smooth proceeding of the cell cycle and prevent genetic inaccuracies from being propagated certain cell cycle checkpoints have to be hit throughout the proliferation process. Most importantly, a sensor to supervise that a task has been completed properly is needed before downstream events are initiated (Hartwell & Weinert, 1989). A malfunction of cell cycle checkpoints results in uncontrolled division of cells and can lead to a lot of health defects including cancer (Blackiston et al., 2009).

For instance, mitosis cannot start if DNA replication was unsuccessful during the S-phase. Also cell segregation cannot happen before all chromosomes are aligned properly on the mitotic spindle (Murray, 1992). Hence, cell cycle checkpoints are functioning as feedback control mechanisms for cell cycle divisors between G1- and S-phase, G2- and M-phase, as well as the transition from the M-phase either into a resting state (G0) or a new G1-phase. In vertebrates a main player in this downstream regulation are cyclin-dependant kinases (CDK) complexes that need to be expressed at certain points in time (Rieder, 2011). Another key mechanism that has been shown to influence cell-cycle progression is the transmembrane potential of a cell (Blackiston et al., 2009).

The transmembrane potential is determined by uneven distribution of ions between the extracellular fluids and the cytosol and the cells membrane permeability for said ions (Wright, 2004). Because ions are electrically charged the extracellular and intracellular side of the membrane has a distinct potential and the potential difference across the membrane is called resting membrane potential (V_r) (Wright, 2004). Ions can cross the hydrophobic lipid bilayer through channel proteins that are hydrophilic on the inside and therefore provide a passage, the so called channel pore (Hille, 1992). In non-excitable, as well as in excitable cells the V_r is mainly regulated by the K^+ conductance. Potential changes in excitable neurons are rapid and caused by the opening and closing of voltage-dependent ion channels. The potential changes that occur during the cell cycle are way slower and smaller and occur in a gradual manner due to variations in ion channel expression and activity in proliferative cells (Urrego et al., 2014). It has been shown in T lymphocytes that the blocking of K^+ channels leads to an arrest of proliferative processes (DeCoursey et al., 1984). Moreover, it has been established for a long time that K^+ channels vary in their expression pattern and activity depending on the cell cycle in cultured cells and *Xenopus* oocytes (Takahashi et al., 1993; Arcangeli et al., 1995; Brüggemann et al., 1997; Pardo et al., 1998).

The first hints that the membrane potential of a cell might be related to cell proliferation came in the early 1950s when it became clear that cells with a hyperpolarized resting membrane potential, like neurons and muscle cells are nearly never mitotic at all. But the underlying mechanism was not clear at that time (Binggeli & Weinstein, 1986). In the following years multiple studies highlighted that the V_r decreases in malignant cells as well as in highly growing cultured cells (Blackiston et al., 2009). When human endothelial cells are hyperpolarized by applying electric fields the cyclin inhibitor p27 gets upregulated in these cells accompanied by a downregulation of cyclin E and proliferation is arrested (Wang et al., 2003). In the 1960s, it has been shown that V_r fluctuates during the cell cycle correlating with the transitions from G1- to S-phase as well as G2- to M-phase in (Figure 5) sarcoma cells (Cone, 1969). This has been confirmed by changing a cells intracellular ion concentration to generate a hyperpolarized V_r resembling the one of non-proliferative neurons. This resulted in a reversible blockage of cell mitosis (Cone & Tongier, 1971).

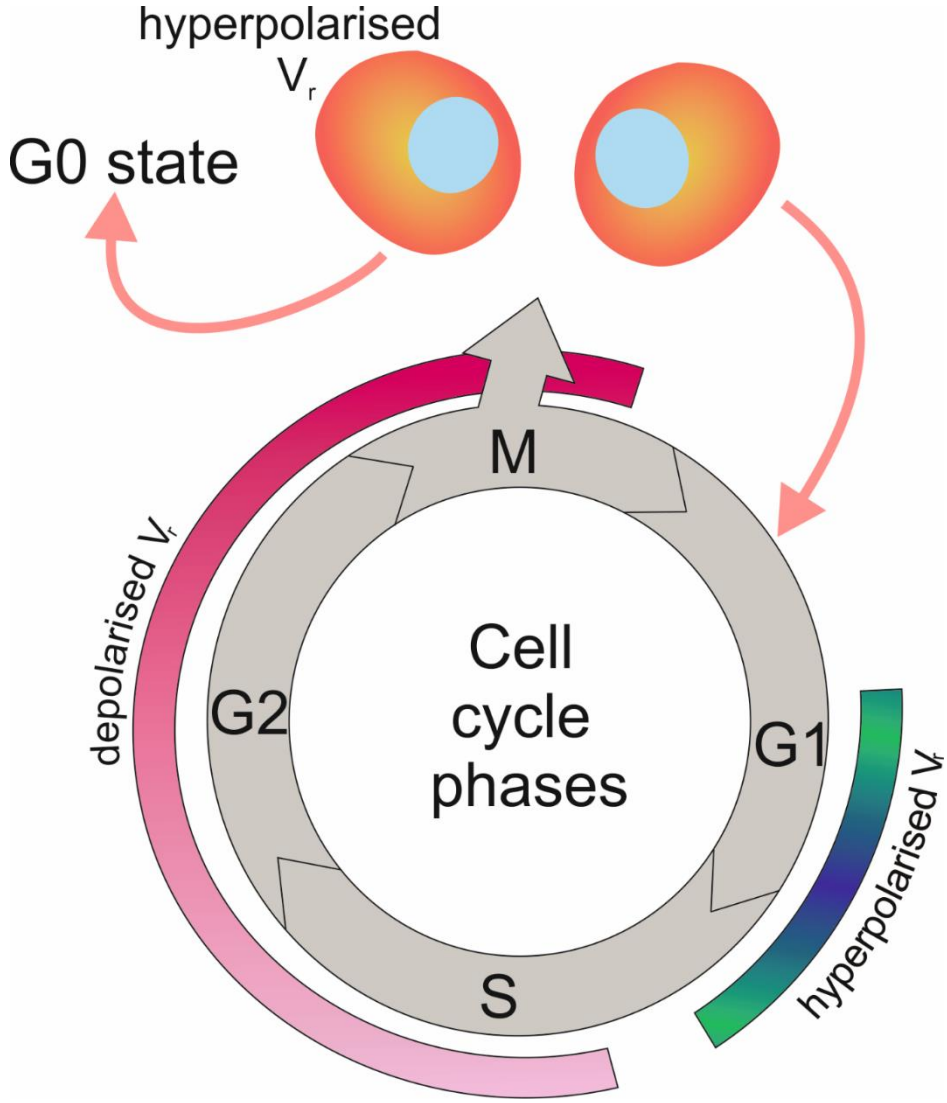

Figure 5: The membrane potential changes during the cell cycle
The membrane potential (V_r) of cells fluctuates throughout the cell cycle. Cells are hyperpolarised during the G1-phase and at the beginning of the S-phase. DNA synthesis starts when the membrane becomes depolarized. To transition from G2-phase to M-phase the cell membrane has to be depolarized to induce mitosis. Cells that are in the resting or end differentiated state (G0) tend to have a very negative V_r. Changes in a cells membrane potential are accompanied by changes in ion channel expression. In non-excitable, as well as in excitable cells the resting membrane potential is mainly regulated by the K^+ conductance hence especially K^+ conducting channels are involved in this process.

Alterations in extracellular ion concentrations leads to a depolarisation of the membrane and prevents Schwann cells, lymphocytes, fibroblasts and astrocytes from transitioning from the G1- into the S-phase (Orr et al., 1972; Canady et al., 1990; Freedman et al., 1992; Wilson & Chiu, 1993). Moreover, a continuous depolarization of neurons induced DNA synthesis and the following downstream events in otherwise non-proliferative mature neurons (Stillwell et

al., 1973; Cone & Cone, 1976). Inhibition of certain ion channels causes an arrest in the cell cycle of B-cell lymphocytes and other cell types, which is reversible (DeCoursey et al., 1984; Chiu & Wilson, 1989; Price et al., 1989; Amigorena et al., 1990; Wang et al., 1992). One of the main ion channel families that influence cell cycle progression are K^+ channels. When they are inhibited, some proteins alter their expression pattern including cell cycle relevant proteins like interleukin (IL)1/2 and transferrin (DeCoursey et al., 1984; Gelfand et al., 1987; Price et al., 1989; Amigorena et al., 1990; Freedman et al., 1992; Lin et al., 1993). Many cell types are less likely to proliferate after they are differentiated and the V_r of differentiated cells is much more hyperpolarised than in non-specified cells (Blackiston et al., 2009). This suggests a correlation between the V_r and the capacity to enter the cell cycle. In quail embryos neural crest cells have a depolarized V_r of -35mV in early stages but become more negative (-55mV) at later stages. These changes are due to a turnover in K^+ channels. In the early stages the main K^+ channel present in neural crest cells is the human Ether-a-go-go Related Gene (hERG) channel, which gets replaced by inwardly rectifying potassium channels (K_{ir}) later in development (Bauer & Schwarz, 2001). The same is true for human mesenchymal stem cells where artificial depolarization prevents them from entering into a differentiated state while hyperpolarisation leads to faster differentiation (Sundelacruz et al., 2008). When using K^+ channel inhibiting drugs, cultured intestinal epithelial cells enhance wound healing and therefore proliferation (Lotz et al., 2004). Also alterations in gap junctional communication is crucial for proliferation of adult stem cells in regenerative processes in Planaria (Oviedo & Levin, 2007). Not only do ion channels control proliferation via depolarization and hyperpolarization of the cell membrane, the cell cycle itself also influences the expression pattern of ion channels downstream of cell cycle checkpoints (Blackiston et al., 2009). For example, when cells are exposed to mitogens like epidermal growth factors (EGF) or LPS, expression and activity of different K^+ channels increases (Mummery et al., 1982; Deutsch et al., 1986; Enomoto et al., 1986; Decoursey et al., 1987; Magni et al., 1991; Lovisolo et al., 1992; Grissmer et al., 1993; Partiseti et al., 1993; Wilson & Chiu, 1993). Although the underlying mechanism for K^+ channel regulation after mitogen exposure are still unclear, an involvement of the serine/threonine-protein kinase (Raf), the rat sarcoma GTPase (Ras) as well as the cyclin-dependant-kinase inhibitor proteins $p21^{ras}$ has previously been shown (Huang & Rane, 1994).

Experiments in embryonic retinal cells have shown that the composition of ion channels changes during the G1-phase (Lenzi et al., 1991, 1993). Among the K^+ channels that change their expression and activity patterns along with the cell cycle are ATP-sensitive K^+ channels, Ca^{2+} activated K^+ channels and outwardly rectifying K^+ channels during the G1- to S-phase transition (Woodfork et al., 1995; MacFarlane & Sontheimer, 2000; Ouadid-Ahidouch et al., 2001; Ouadid-Ahidouch, 2004). Inhibiting as well as blocking and knock down of voltage-activated $K_v1.3$ and $K_v1.5$ channels in rat oligodendrocyte precursor cells leads to a cell cycle arrest in the G1-phase and the accumulation of cyclin-dependant-kinase inhibitor proteins $p27^{cip1}$ and $p21^{kip1}$ (Ghiani et al., 1999; Chittajallu et al., 2002). Hyperpolarization-activated cyclic nucleotide-gated (HCN) channels are also known to be involved in the cell cycle progression of embryonic stem cells. Blocking of these channels with ZD7288 decreased the amounts of cells in G0-state and G1-phase and increased the amount of embryonic stem cells in the S-phase suggesting that also HCN currents influence cell cycle progression (Lau et al., 2011). The depolarization of mouse macrophages induces the S-phase and an upregulation of the avian myelocytomatosis viral oncogene homolog (c-myc) and AP-1 transcription factor subunit (c-fos) transcription factors that are relevant for proliferative processes (Kong et al., 1991). Experiments in the breast cancer cell line MCF-17 confirmed that the V_r is hyperpolarized at the transition from G1- to S-phase as well as at the G2- and M-phase transition while cells are depolarized around the G0-state and G1-phase (Wonderlin et al., 1995). To transition from G2-phase to M-phase the cell membrane has to be depolarized (Blackiston et al., 2009). At this transition ether-à-go-go (r-eag) K^+ channel currents (Pardo et al., 1998) and voltage-activated Cl^- currents are also known to be involved (Valenzuela et al., 2000; Chen et al., 2002; Zheng et al., 2002).

1.10 Ion channels in astrocytes

It has been elaborated in the previous paragraphs that the underlying cause of why juxtavascular astrocytes are more likely to enter the cell cycle compared to non-juxtavascular ones in response to TBI is still not completely understood. As already discussed above it is known that ion channels play an important role in cell cycle progression in different cell types and at different developmental stages and especially K^+ ion channels are known to be a key player (Blackiston et al., 2009; Urrego et al., 2014). There are several types of K^+ channels present in astrocytes, some of which are known to be involved in astrocytic proliferation and others that change their expression pattern after a traumatic event (MacFarlane & Sontheimer, 1997, 2000; Rusnakova et al., 2013; Honsa et al., 2014; Verkhratsky & Nedergaard, 2018). This makes these channels, if differently expressed between non-juxtavascular and juxtavascular astrocytes, a great candidate to explain their distinct proliferative pattern in response to TBI.

1.10.1 The astrocytic membrane potential

The intracellular ion concentration is defined by the membrane permeability of the cell for certain ions, active transport via ion pumps and intracellular cytosolic buffering mechanisms for calcium (Verkhratsky & Nedergaard, 2018). In astrocytes, the intracellular ion concentrations are 120-140 mM for K^+, 15-20 mM for Na^+, 50-150 nM Ca^+ and around 30-60 mM Cl^- (Hansen, 1985; Jones & Keep, 1987; Bekar & Walz, 2002; Langer & Rose, 2009; Unichenko et al., 2012; Zheng et al., 2015; Rose & Verkhratsky, 2016; Verkhratsky & Nedergaard, 2018).

Astrocytes are known for expressing an excessive amount of inwardly rectifying $K_{ir}4.1$ ion channels in the astrocytic membrane which leads to a very hyperpolarized V_r around -80 mV close to the K^+ equilibrium potential (E_K = 98 mV) and a low input resistance between 5-20 MΩ (Mishima et al., 2007; Mishima & Hirase, 2010; Dallérac et al., 2013). Moreover, the high permeability for K^+ also shapes astrocytic current to voltage relationships making them almost linear. Hence, mainly passive current patterns are visible establishing it as a feature of adult astrocytes (Pastor et al., 1995; Isokawa & McKhann, 2005; Djukic et al., 2007; Adermark & Lovinger, 2008; Du et al., 2015; Fazel et al., 2018). The astrocytic syncytium, where

astrocytes are highly coupled with neighbouring astrocytes via gap-junctions, leads to isopotentiality in these networks, by equalizing an astrocytes V_r to the ones of neighbouring cells (Ma et al., 2016). The very negative astrocytic V_r is the driving force for membrane transporters, which is crucial for performing homeostatic functions that are associated with astrocytes (Verkhratsky & Nedergaard, 2018).

1.10.2 Inwardly rectifying potassium channels (K_{ir})

Inwardly rectifying K^+ channels are ion channels that are able to conduct K^+ ions more rapidly from the extracellular side to the cytosolic side of the cell membrane than the other way round (Doupnik et al., 1995; Reimann & Ashcroft, 1999). The main physiological role of K_{ir} channels is the stabilisation of the V_r close to E_K in cardiac as well as neural cells and they mediate the potassium flow across the cell membrane governed by a strong voltage-dependence of the Mg^{2+} and polyamine channel block (Nichols & Lopatin, 1997; Guo et al., 2003). The family of K_{ir} channels is comprised of seven major subfamilies $K_{ir}1$ to $K_{ir}7$ (Nichols & Lopatin, 1997). $K_{ir}2$ channels are strongly rectifying while the $K_{ir}1$, $K_{ir}4$, $K_{ir}5$ and $K_{ir}7$ subfamilies only have weakly rectifying properties. Moreover, $K_{ir}3$ are G-protein-coupled channels and the $K_{ir}6$ subfamily form ATP-gated channels by assembling with sulfonylurea receptors (Nichols & Lopatin, 1997; Roeper & Liss, 2001).

As mentioned above $K_{ir}4.1$ channels are the main type of K^+ channels expressed by astrocytes and responsible for maintaining their very negative V_r (Mishima et al., 2007; Mishima & Hirase, 2010; Dallérac et al., 2013). In the CNS, $K_{ir}4$ expression is predominantly found in astrocytes mainly in the hippocampus, cerebral cortex, Bergmann glia of the cerebellum, Müller glia in the retina, the optic nerve, deeper cerebellar nuclei and the ventral horn of the spinal cord. This was confirmed by either immunohistochemistry or by the presence of Cs^+ and Ba^+ sensitive currents in rodent astrocytes *in-vitro* and *in-vivo* (Nowak et al., 1987; Barres et al., 1990; Sontheimer et al., 1992; Tse et al., 1992; Ransom & Sontheimer, 1995; Poopalasundaram et al., 2000; Higashi et al., 2001; Kalsi et al., 2004; Olsen et al., 2007). The astrocytic $K_{ir}4.1$ channels are predominantly expressed in the processes and endfeet of astrocytes especially the ones that are perivascular or perisynaptic (Higashi et al., 2001) and in rats there is a developmentally regulated shift from somatic expression towards the processes between postnatal day 0 to 60, which has been shown in rodents (Moroni et al., 2015). This is

accompanied by an increase in $K_{ir}4.1$ channel density (Seifert et al., 2009). In addition, it has been shown that higher levels in $K_{ir}4.1$ channel expression in mature astrocytes are strongly linked to end-differentiation and a loss of proliferative potential (Sontheimer, 1994; Roy & Sontheimer, 1995; Bordey & Sontheimer, 1997; MacFarlane & Sontheimer, 1997; Higashimori & Sontheimer, 2007). Moreover, several studies have described the downregulation of $K_{ir}4.1$ in reactive astrocytes after a lesion in rodents *in-vitro* and *in-vivo* (MacFarlane & Sontheimer, 1997; Olsen et al., 2010; Gupta & Prasad, 2013) and could even link said downregulation to the proliferating astrocytes in spinal cord cultures of rats (MacFarlane & Sontheimer, 1997). This makes $K_{ir}4.1$ channels, if differently expressed between non-juxtavascular and juxtavascular astrocytes, a great candidate to explain their distinct proliferative pattern in response to TBI *in-vivo*.

The $K_{ir}6$ ion channel subfamily is able to assemble with the ATP-binding cassette transporter sub-family C (SUR) 1/2 to form ATP sensitive channels that open in response to a decrease in ATP concentration. Theses ATP-sensitive channels are known to be present in astrocytes and are speculated to play a role in the cells protection after metabolic stress as well as the regulation of gap junctional permeability (Thomzig et al., 2001; Wu et al., 2011). This makes them perfect candidates to be involved in the astrocytic reaction following an injury. In healthy rats, $K_{ir}6.1$ is present in astrocytes in the hippocampus, cerebellum and cortex as well as in Bergman glia (Thomzig et al., 2001). It has been shown, that $K_{ir}6.1$ mRNA is expressed in retinal Müller glia and the brainstem whereas $K_{ir}6.2$ mRNA is present in Müller glia, astrocytes in the cerebellar white matter and in the corpus callosum (Thomzig et al., 2001; Raap et al., 2002; Zhou et al., 2002):

1.10.3 Voltage-activated K^+ channels (K_v)

Voltage-activated K^+ (K_v) channels are represented by 12 subfamilies (K_v1-12) that are responsible for a plethora of different functions like electrical excitability in neurons and muscle cells, action potential frequency regulation, transmitter release, establishing the resting membrane potential as well as the rhythm of the heart and endocrine secretion (Pongs, 1999). Astrocytes show rapidly inactivating and activating A-type currents that are elicited at depolarized membrane potentials (-70 to-50 mV), but these A-type currents are most of the time masked by the much larger voltage- and time-independent $K_{ir}4.1$ currents (Bekar, 2004;

Seifert et al., 2009). In cultured rat hippocampal astrocytes, pharmacological experiments showed that around 70 % of A-type currents in these cells underlie the K_v4 channel subfamily, approximately 10 % originate from the K_v3 subfamily and the smallest amount, under 5 %, arise from the K_v1 subfamily (Bekar, 2004). $K_v3.4$ ion channels are predominantly localized on astrocytic processes while $K_v4.3$ channels are located in more somal regions, which might enable astrocytes to respond to high-frequency incoming signals from neurons with rapid membrane voltage oscillations to synchronize their function with neuronal activity (Bekar, 2004). In addition to A-type currents, astrocytes in the cerebellum, cortex, hippocampus and spinal cord of rats show delayed rectifying K^+ currents that are activated at around -20 mV (Bordey & Sontheimer, 2000). In young, immature rodent astrocytes, that are either still mitotic or have proliferative potential, the dominant currents are delayed rectifying (I_d) and transient (I_A) currents caused by voltage-activated K^+ channel (K_v) subfamilies (Bordey & Sontheimer, 1997; MacFarlane & Sontheimer, 2000; Seifert et al., 2009).

1.10.4 Hyperpolarization-activated cyclic nucleotide-gated channels (HCN)

HCN channels are encoded by four genes, the *Hcn1-4* genes and their proteins form hetero- and homotetrameric channels that are permeable for K^+ and Na^+ ions in a 4:1 ratio (Marx et al., 1999; Wahl-Schott & Biel, 2008). They are primarily present in neurons and are activated at a hyperpolarized V_r. HCN2 and 4 channels can be additionally activated by cyclic adenosine monophosphate (cAMP). In neurons these channels are responsible for the stabilization of the V_r, constraining long term potentiation (LTP), synaptic transmission and dendritic integration. Most importantly they mediate oscillation of the membrane potentials in neuronal and cardiac cells (Wahl-Schott & Biel, 2008; Lewis & Chetkovich, 2011). HCN channel transcripts are known to be present in neurons and have additionally been reported in primary astrocyte cultures and post-ischemic astrocytes of rodents and might therefore play a role in nonspecific cation influx (Rusnakova et al., 2013; Honsa et al., 2014). According to literature, HCN1 channels are present in astrocytes of the healthy rodent brain in small amounts. In the post ischemic brain reactive astrocytes have highly increased levels of HCN1-4 transcript and HCN1-3 channels were detected via immunohistochemistry in these cells (Rusnakova et al., 2013; Honsa et al., 2014).

1.11 Aim of the study

One major subclass of glia cells are astrocytes. Astrocytes play a major role after TBI and in several neurological diseases by becoming reactive under these conditions. This includes, but is not limited to hypertrophy, polarization, the upregulation of GFAP in astrocytic processes as well as proliferation of astrocytes surrounding the lesion site (Pekny & Pekna, 2014; Burda et al., 2016). Juxtavascular astrocytes, which have their soma directly adjacent to blood vessels are more prone to selectively proliferate after TBI in mice, whereas non-juxtavascular astrocytes rarely divide (Bardehle et al., 2013). Nevertheless, the underlying cause of this selective proliferation is still not well understood and especially why juxtavascular astrocytes are more likely to enter the cell cycle compared to non-juxtavascular ones. It is known that ion channels play an important role in cell cycle progression in different cell types and at different developmental stages. Especially K^+ ion channels are known to be key players (Blackiston et al., 2009; Urrego et al., 2014). There are several ion channels known to be present in astrocytes, which might also play an important role proliferation of astrocytes after a traumatic event.

Inwardly rectifying $K_{ir}4.1$ channels, which are mainly present in astrocytic processes and endfeet are responsible for maintaining the very negative V_r of astrocytes (Mishima & Hirase, 2010; Dallérac et al., 2013). Moreover, $K_{ir}4.1$ ion channel expression is known to be positively correlated with end differentiated cells and a downregulation of these potassium channels is known to happen in reactive astrocytes (MacFarlane & Sontheimer, 1997, 2000). The $K_{ir}6$ ion channel subfamily are ATP-sensitive channels known to be present in astrocytes and speculated to play a role in protecting the cell after metabolic stress as well as the regulation of gap junctional permeability (Thomzig et al., 2001). Moreover, it has been shown that delayed rectifying (I_d) and transient (I_A) currents caused by voltage-activated K^+ channel subfamilies (K_v ion channels) are dominant in young and immature astrocytes that are either still mitotic or have the potential to proliferate (Bordey & Sontheimer, 1997). These currents are also dominating in reactive proliferating astrocytes in spinal cord cultures (MacFarlane & Sontheimer, 1997). It is known, that HCN channels are involved in the cell cycle progression of embryonic stem cells. Blocking of these channels decreased the amount of cells in the G0-state and the G1-phase and increases the amount of embryonic stem cells in the S-phase suggesting that HCN currents influence cell cycle progression (Lau et al., 2011). Transcripts

of HCN channels are present in primary astrocyte cultures and known to be upregulated in post-ischemic astrocytes (Rusnakova et al., 2013; Honsa et al., 2014).

The aim of this doctoral thesis is to analyse if there are differences in ion channel composition present between non-juxtavascular and juxtavascular astrocytes that might be responsible for their differential behaviour after traumatic events. Therefore, the two astrocyte subtypes are characterised regarding their ion channel expression pattern and passive electrophysiological properties (resting membrane potential V_r, resting membrane conductance G_r and input resistance R_{in}) in the somatosensory cortex of adult transgenic Aldh1l1-eGFP mice.

In the first part of this study, it will be assessed by means of immunohistochemistry and electrophysiological whole-cell patch-clamp recordings whether there are inherent differences present between non-juxtavascular and juxtavascular astrocytes already in the healthy unlesioned somatosensory cortex.

In the second part, a stab wound lesion will be introduced into the brain to induce reactive astrogliosis. Immunohistochemistry and electrophysiological recordings will be used to work out whether the lesion induces a difference in the passive electrophysiological properties and ion channel expression patterns of non-juxtavascular and juxtavascular astrocytes. If dissimilarities are present, this might be the underlying cause for proliferation mainly occurring in reactive juxtavascular astrocytes.

Findings regarding a differential expression of certain subsets of ion channels that might be the underlying cause for the diverse proliferative behaviour of juxtavascular and non-juxtavascular astrocytes in response to traumatic brain injury would be of great interest for therapeutic approaches as it is known that astrocyte proliferation positively affects healing processes and axon regeneration after TBI.

1.12 Collaboration

This PhD project was done in the laboratory of Prof. Dr. Benedikt Grothe supervised by PD Dr. Lars Kunz and is a project funded by SyNergy (Munich Cluster for Systems Neurology) in collaboration with the group of Prof. Dr. Magdalena Götz at the Ludwig-Maximilians-University, Munich.

2 Materials and Methods

2.1 Animal rearing and license

The experimental animals were reared and housed according to the guidelines of the Bundesgesetzblatt Nr.37, Anhang A. The animals were housed and bred in the animal facility of the Department II of the LMU Biocenter (Martinsried). They were kept in an open Type II cage system in groups of no more than 8 animals and were provided with changing enrichment. The lighting was provided by an artificial light source and an artificial day and night cycle was generated by 12 hours of light and 12 hours without. A light intensity of 45 lux inside the cages was never exceeded. The room temperature in the housing facility lay between 20-24 °C and humidity was around 50 %. The animals were provided with food and water ad libitum and all conditions were in accordance with the RL2010/63/EU.

All experiments were in accordance with and approved according to the German Tierschutzgesetz.

2.2 Mouse strain

The BAC Aldh1l1-eGFP mouse line generated by GENSAT was used (provided by Prof. Dr. Magdalena Götz; BioMedical Center, Department of Physiological Genomics, Ludwig-Maximilians-Universität München) , which specifically expresses enhanced green fluorescent protein (eGFP) in nearly all astrocytes in the developing and adult CNS (Heintz, 2004). The aldehyde dehydrogenase 1 family, member L1 (Aldh1l1) is a highly expressed astrocyte specific gene that can be used as a specific marker to identify astrocytes in the CNS. It has high amounts of mRNA expression and its resulting proteins are present in the whole cell (Cahoy et al., 2008). The protein itself functions as a catalyser in the conversion of water, 10-formyltetrahydrofolate and nicotinamide adenine dinucleotide phosphate ($NADP^+$) to carbon dioxide, tetrahydrofolate and NADPH (Cook et al., 1991).

2.3 Surgery

2.3.1 Stab wound lesion

Surgical procedures were conducted under the Tierversuchsantrag Gz.: 55.2-1-54-2532-76-2016 (Regierung von Oberbayern). The experimental animals were briefly anesthetized with Isoflurane (IsoFlo®, 100% isoflurane; Zoetis Schweiz GmbH) until the righting reflex was lost and then put under general MMF anaesthesia with an intraperitoneal injection (i.p.) containing 0.5 mg/kg Medetomidin (Oreon Pharma; Domitor 1 mg/ml), 5 mg/kg Midazolam (Braun GmbH; 5 mg/ml) and 0.05 mg/kg Fentanyl (Jannsen Pharmaceutica; 0.05 mg/ml). Subsequently animals were put back into their cage and monitored constantly. The state of general anaesthesia was verified by the lack of the reflex to turn around as well as the lack of the blinking reflex. To guarantee working analgesia the paw pinch reflex was tested as well. When the animal had reached this condition, the eyes were covered with Bepanthen eye and nose cream (Bayer AG; active reagent 5 % Dexpanthenol) to prevent the cornea from drying out. During the whole procedure the animal was provided with dampened oxygen (Linde Gas Therapeutics GmbH; Conoxia ® GO_2X) through a breathing mask to facilitate breathing and guarantee proper ventilation.

To allow access to the operating area a small portion of fur was sheared from the animals head with an electric shaver. Then it was head fixed in a motorized stereotaxic stereo drive (NeuroStar GmbH; Serial#: SD214) and put onto a feedback controlled heating pad (Physitemp Instruments; TCAT-2DF controller and F040070504b 12 V/5.3 Ω/ 1408C-01 pad) set to 36°C. The skin on the head was opened with small scissors and a drill was used to perform a craniotomy in the region of the somatosensory cortex. A small cranial window was removed from the skull and kept aside to close the window later. To introduce the micro lesion a lancet was inserted 0.6 mm deep into the parietal cortex 1.5-2.5 mm parasagittal to the midline and then moved several times 1-1.5 mm caudally through the brain. After removing the lancet from the brain, the cranial window was closed with the small piece of skull, which was removed earlier in the procedure and a suture on the head was performed with surgical suture material (Feuerstein GmbH; Seide Schwarz 45cm USP 4/0 (m 1.5) HS 18) to close the operating area. To antagonize the anaesthesia, the animal was injected i.p. with AFB containing 2.5 mg/kg Atipamezol (CP Pharma; Revertor 5 mg/ml), 0.5 mg/kg Flumazenil (Hexal AG; 0.5 mg/ml)

and 0.1 mg/kg Buprenorphin (Bayer AG; Buprenorvet 0.3 mg/ml). Buprenorphin was used for post-surgery analgesia.

2.3.2 Post-surgery treatment

After the operation the animals were controlled regularly and 8 hours post-surgery they were again injected i.p with 0.1 mg/kg Buprenorphin (Bayer AG; Buprenorvet 0.3 mg/ml) to counteract wound pain. Consecutively, the animals were controlled daily and a total health score was determined every day post-surgery until the end of the experiment which was either 1, 3 or 5 dpi. The operated animals were housed together with their conspecifics of the same sex in a separate room with the same conditions as mentioned above. Solely during the phase while they were awakening from the anaesthesia they were housed individually in special prepared cages to prevent them from getting harmed by others. The post-surgical observation is conducted by the experimenter and, in addition, animals were controlled daily by the animal care takers.

2.4 Immunohistochemistry

2.4.1 Transcardial perfusion for tissue fixation

The supplier information of all the chemicals used in this study is listed in the appendix. Prior to the perfusion the experimental animals were injected i.p. with a lethal dose of Narcoren (400-800 mg/kg; (Merial GmbH; pentobarbital sodium 16 g/ml)). For post-mortem transcardial perfusion, the animals´ rib cage was opened and a needle was introduced into the bottom part of the left ventricle. Then the right atrium was cut open and perfusion started with Ringer solution containing 0.1 % heparin to prevent blood clotting so that the vascular system gets completely cleared from the blood. After 5 minutes the ringer solution is replaced with a solution containing 4 % PFA in 0.05 M PB (pH 7.4) for 20 minutes for tissue fixation. Subsequently the brain was removed from the skull and post-fixated for 2 hours in 4 % PFA solution at room temperature on a shaker.

2.4.2 Slice preparation and immunohistochemistry

PBS 0.02 M: 5 mM KH_2PO_4, 16 mM Na2HPO_4, 150 mM NaCl, 2.7 mM KCl (pH 7.4)

Washing solution: 1 % Saponin, 0.5 %TritonX100, 0.02 M PBS

Blocking solution: 1 % Bovine Serum Albumine, 1 % Saponin, 0.5 %TritonX100, 0.02 M PBS

After post-fixation brains were washed 3 times for 10-15 minutes in 0.02 M PBS on the shaker and then embedded in 4 % agar (dissolved in distilled water). 30 µm thick coronal sections of the somatosensory cortex were cut with a VT 1200S vibratome (Leica Microsysteme Vertrieb GmbH) and rinsed in 0.02 M PBS. Then the slices were transferred onto Thermo Scientific™ SuperFrost Ultra Plus™ Adhesion Slides and dried for at least 1 hour. Subsequently the slices were first encircled with an ImmEdge Hydrophobic Barrier PAP Pen (Vector Laboratories) to prevent spillage of staining solution and then washed for 5 minutes in washing tons filled with 0.02 M PBS on the shaker. After washing, the slices were incubated for 20 minutes in blocking solution to prevent unspecific antibody binding. Then this solution was replaced with new blocking solution that additionally contained the primary antibodies and slides were incubated 48 h at 4 °C in a wet chamber. Thereafter, slides were washed three times for 15-20 minutes in washing solution on the shaker at room temperature and then incubated with the secondary antibodies (diluted in blocking solution) over night at 4 °C in a wet chamber. For blood vessel labelling DyLight 649 labelled *Lycopersicon Esculentum* (Tomato) Lectin was added to the secondary antibody solution. The next day, slices were washed 3 times for 15-20 minutes in washing solution at room temperature and if nuclear labelling was needed stained with DAPI diluted in PBS for 20 minutes at room temperature. After thoroughly washing the slices 5 minutes in washing solution, the slides were mounted with VECTASHIELD Antifade Mounting Medium (Vector Laboratories) and cover slips and sealed with clear nail polish.

Primary antibodies

Anti-	Host	Dilution	Company	Catalogue #
K_{ir}4.1	rabbit	1:200	Alomone Labs	APC-035
K_{ir}6.1	rabbit	1:200	Alomone Labs	APC-105
K_{ir}6.2	rabbit	1:200	Alomone Labs	APC-020
K_v4.3	rabbit	1:200	Alomone Labs	APC-017
HCN1	rabbit	1:200	Alomone Labs	APC-030
HCN2	rabbit	1:200	Alomone Labs	APC-056
HCN3	rabbit	1:200	Alomone Labs	APC-057
Ki67	rat	1:100	ThermoFisher	14-5698-82
GFAP	mouse	1:500	Sigma	G3893
GFP	chicken	1:500	Aves Labs	GFP-1020

Secondary antibodies

Conjugate	Anti-	Host	Dilution	Company	Catalogue #
AMCA	Mouse	Donkey	1:100	Dianova	715-156-150
Alexa488	Chicken	Donkey	1:300	Dianova	703-546-155
Cy3	Rabbit	Donkey	1:400	Dianova	711-165-152
DyLight594	Rat	Donkey	1:200	Dianova	711-516-152

Unspecific markers

Marker	Dilution	Company	Catalogue #
DAPI	1:1000	Thermo Fisher	62248
DyLight 649 labeled *Lycopersicon Esculentum* (Tomato) Lectin	1:250	Vector Laboratories	DL-1178

2.5 Electrophysiology

ACSF slice: 120 mM sucrose, 25 mM NaCl, 25 mM $NaHCO_3$, 2.5 mM KCl, 1.25 mM NaH_2PO_4, 3 mM $MgCl_2$, 0.1 mM $CaCl_2$, 25 mM glucose, 0.4 mM ascorbic acid, 3 mM myo-Inositol, 2 mM Na-pyruvate (pH 7.4 by bubbling with 95 % O_2 and 5 % CO_2)

ACSF patch: 125 mM NaCl, 25 mM $NaHCO_3$, 2.5 mM KCl, 1.25 mM NaH_2PO_4, 2 mM $CaCl_2$, 1 mM $MgCl_2$, 25 mM glucose, 0.4 mM ascorbic acid, 3 mM myo-Inositol, 2 mM Na-pyruvate (pH 7.4 by bubbling with 95 % O_2 and 5 % CO_2)

Intracellular solution: 130 mM K-Gluconate, 20 mM Hepes, 10 mM EGTA, 13 mM Na_2-ATP, 1 mM $MgCl_2$ (Osmolarity:290 +/- 2 mOsm; pH 7.25-7.28 that was achieved via titration with either 1 M NaOH or 1 M KOH)

For all electrophysiological recordings of non-lesioned animals the mice were anesthetized with Isoflurane (IsoFlo®, 100 % isoflurane; Zoetis Schweiz GmbH) and quickly decapitated under anaesthesia. All lesioned animals were first quickly anesthetized with Isoflurane (IsoFlo®, 100 % isoflurane; Zoetis Schweiz GmbH) and then put under general anaesthesia using MMF i.p. (0.5 mg/kg Medetomidin (Oreon Pharma; Domitor 1 mg/ml), 5 mg/kg Midazolam (Braun GmbH; 5 mg/ml) and 0.05 mg/kg Fentanyl (Jannsen Pharmaceutica; 0.05 mg/ml)). When animals were under general anaesthesia, 50 µl Texas Red® labelled dextran (Molecular Probes Inc.; LOT: 1756567; 70000MW; 10 mg/ml in NaCl) was injected into the tail vein (i.v.) for blood vessel labelling. After 10-15 minutes incubation the animals were decapitated under general anaesthesia. The brains of all experimental animals were dissected from the skull and placed in ice cold artificial cerebrospinal fluid (ACSF) slice solution where the meninges were removed with very thin forceps. Then 200 µm thick coronal brain sections were cut with a Leica VT1200S vibratome (Leica Microsysteme Vertrieb GmbH) in ice-cold carbonated ACSF slice solution. The tissue slices were then transferred onto a net inside a beaker filled with ACSF patch solution. The beaker is placed into a water bath heated to 36 °C and slices were incubated for 45 minutes while being continuously bubbled with 95 % O_2 and 5 % CO_2. Subsequently, the slices were stored at room temperature and used for electrophysiological experiments after they had rested for at least 20 minutes.

To perform electrophysiological recordings the slices were transferred and weighed down with a slice anchor into a recording chamber that was mounted onto an Olympus BX51WI microscope (Olympus Europa Holding GmbH). The microscope is equipped with a light source

(Olympus TH4-200; Olympus Europa Holding GmbH) and an infrared filter for bright field microscopy and a white light source (LEj GmbH) for fluorescent imaging. For visual identification of cells an Orca –R^2 Digital Camera C10600 with the corresponding Hokawo software (Hamamatsu Photonics K.K) was installed and Olympus objectives with a 4x (Plan N 0.1; Olympus Europa Holding GmbH) and a 60x (PlanFL N 1.0; Olympus Europa Holding GmbH) magnification were used. To guarantee the health of the slices, the chamber was constantly perfused with freshly carbonated recording solution (ACSF patch) during the whole time of the experiments. All the electrophysiological recordings were performed at room temperature. For voltage-clamp whole-cell recordings, borosilicate glass capillaries (BM150F-10P with filaments, 1.5mm OD/0.86mm ID/100mm L; BioMediacal Instruments) were pulled using a DMZ Universal Electrode Puller (Zeitz Instrumente Vertriebs GmbH) to achieve a resistance between 3.5-5.5 MΩ when filled with intracellular solution. The recordings were acquired with a double patch clamp EPC 10 *USB* amplifier (HEKA Elektronik Dr. Schulz GmbH). The patched astrocytes were identified by fluorescent labelling with eGFP and their location towards blood vessels was either identified by bright field microscopy or by fluorescent blood vessels labelling (see above). For the identification a dual band GFP/mCherry ET Filterset was used (F56-019; AHF Analysentechnik AG). The capacitive artefact (C-fast) of the recording electrode was compensated in all recordings. All obtained data were corrected for a liquid junction potential of -16 mV. Data were acquired with a sampling rate of 20 kHz and Bessel filtered at 2.9 kHz and 10 kHz. The recording protocols were created with the help of the pulse generator in the PatchMaster software (HEKA Elektronik Dr. Schulz GmbH). The astrocytes were clamped to the V_r measured in current-clamp mode and subsequently injected with 200 ms long voltage steps ranging from -176 mV to +174 mV in 10 mV increments to obtain the current response from the patched cell for passive electrophysiological parameter identification. For all further analysis only cells that showed stable recordings and constant parameters were taken into account.

For pharmacological identification of $K_{ir}4.1$ channels astrocytes were clamped to their V_r measured in current-clamp mode and subsequently injected with 200 ms long voltage steps ranging from -176 mV to +174 mV in 10 mV increments to obtain the current response. Afterwards the $K_{ir}4.1$ channel blocker $BaCl_2$ dihydrate (200 µM) diluted in recording solution was washed into the recording chamber for 10 minutes.

For pharmacological identification of HCN channels in astrocytes the cells were clamped to the cells V_r measured in current clamp mode and then subsequently injected with 1 s long voltage steps ranging from -176 mV to -16 mV in 10 mV increments. Consecutively a selective HCN channel blocker ZD7288 [4-(N-ethyl-N-phenylamino)-1.2-dimethyl-6-(methylamino) pyrimidinium chloride] (50µM) diluted in recording solution was washed into the recording chamber for 10 minutes.

2.6 Microscopy

For a first evaluation of the immunohistochemical stainings a fluorescent microscope (Nikon Eclipse 80i; Nikon Instruments Inc.) equipped with Nikon Plan Fluor 109/0.3 (10x) and a Plan Fluor 209/0.50 (20x) objective was used. All final images shown here were then acquired with a Leica TCS SP-5 confocal laser scanning microscope (Leica Microsystems Vertrieb GmbH) using either a HCX PL APO Lambda Blue 20x 0.7 immersion objective or a HCX PL APO Lambda Blue 63x 1.4 oil immersion objective. The virtual slices were set constantly to 0.5 µm z-step size and an image size of 512x512 pixels. The bidirectional scanning mode was chosen and laser scanning frequency varied between 400 and 1000 Hz depending on the zoom factor for the corresponding picture. The line average was calculated from three subsequent line scans and the size of the pinhole was automatically adjusted by the software. The microscope used the following lasers: a diode laser (405 nm; 25 mW), an argon laser (458 nm, 467 nm, 488 nm, 514 nm; 5 mW), a DPSS laser (561 nm; 10 mW), a HeNe laser (594 nm; 2.5 mW) and another HeNe laser (633 nm; 10 mW) to visualise the different fluorescence labels. Before scanning, the laser power and the gain were adjusted to ensure an optimal fluorescence signal.

2.7 Data analysis

Igor

Electrophysiological data (*.dat files) acquired with the PatchMaster software (HEKA Elektronik Dr. Schulz GmbH) was loaded into the IGOR PRO 6.35A software (WaveMetrics Inc.) with the help of the Patchers Power Tools 2.19 extension (Dr. Francisco Mendez and Frank Würrihausen; Max-Planck-Institut für biophysikalische Chemie Göttingen). The raw current traces were further analysed with custom written IGOR PRO procedures.

GraphPad prism 5

GrapPad Prism 5 (GraphPad Software) was used to further process data, to perform statistical analysis on electrophysiological data, cell counting analysis and for graph design. For all data-sets non-Gaussian distribution was assumed and the results were presented as the median. For comparison of passive electrophysiological properties, statistical significance was determined by Kruskal-Wallis-tests or Mann-Whitney-tests depending on the datasets. To check for differences in the number of astrocytes that possess certain features with the help of contingency analysis either a two-sided Fisher´s exact test or a two-sided Chi-square test was used. For analyses of experiments with more than two groups, a Kruskal-Wallis test was performed to clarify if there is a difference between all respective groups. If the Kruskal-Wallis test was significant, a Mann-Whitney test was used for further testing of groups that were of interest. In these cases a Bonferroni-Correction was applied to determine the adequate p value. In case of experiments, in which a cells´ parameters were compared before and after application of an ion channel blocker, the Wilcoxon matched pairs test was used.

To analyse the expression pattern of ion channels in the healthy somatosensory cortex, astrocytes in cortex slices of adult mice were counted in the according cortical layers and the mean percentage of ion channel expressing non-juxtavascular and juxtavascular astrocytes for each animal was plotted in a bar chart. Then the median percentage of the different animals was determined for each layer. The criteria for a homogenous expression pattern was met, if the median percentage did not diverge more than 5 % from a complete homogeneity. Homogeneity was defined as 100% of the counted astrocytes being positive for the ion channels marker. A Kruskal-Wallis test was used to check for differences in ion channel expression between different cortical layers and between the two astrocyte subtypes.

In all statistical tests the significance level was set at $p<0.05$, except for Bonferroni corrected ones.

2.8 Image processing

ImageJ

All images acquired with the Leica TCS SP-5 confocal laser scanning microscope (Leica Microsysteme Vertrieb GmbH) were further processed and analysed with ImageJ software (Wayan Rasband, National Institutes of Health, USA). Image Stacks were corrected for a z chromatic shift between colour channels. For cell counting, the ImageJ manual counting tool was used and all optical sections of one stack were analysed individually. Images were produced by making z-stack maximum projections of a certain number of optical sections and brightness and contrast was adjusted for optimal signal to noise ratio.

Figures

All multi-panel figures and drawings in this study were produced with the help of the vector graphic image processing program CorelDRAW® Graphics Suite X8 (64-bit; Corel GmbH).

3 Results

3.1 Characterization of non-juxtavascular and juxtavascular astrocytes in the somatosensory cortex of the healthy brain

Juxtavascular astrocytes with their soma directly adjacent to blood vessels are prone to selectively proliferate after TBI in the somatosensory cortex of mice, whereas non-juxtavascular astrocytes are less likely to divide (Bardehle et al., 2013). It is known, that ion channels and especially K^+ channels play important roles in cell cycle progression and therefore division (Blackiston et al., 2009; Urrego et al., 2014). Hence it was of great interest to assess, whether there is an inherent difference between non-juxtavascular and juxtavascular astrocytes regarding their electrophysiological properties, as well as their ion channel composition in the healthy, unlesioned brain present.

3.1.1 Electrophysiological characterization of astrocytes in the healthy somatosensory cortex

In order to characterize non-juxtavascular and juxtavascular astrocytes regarding their passive properties in the healthy brain, electrophysiological voltage-clamp experiments were performed on somatosensory cortex slices of 25 adult BAC Aldh1l1-eGFP transgenic mice at ages between p24 and p48. Astrocytes were identified by the green fluorescence of the intracellularly expressed Aldh1l1-eGFP as seen in Figure 6a and a´. To distinguish non-juxtavascular from juxtavascular astrocytes the blood vessels were identified either by green fluorescence, which was due to astrocytic processes enwrapping larger blood vessels excessively (Figure 6a, red arrows), or with the help of bright field microscopy (Figure 6a). Juxtavascular astrocytes were defined by direct opposition of their somata to the blood vessel (Figure 6a, cyan arrow), whereas the somata of non-juxtavascular astrocytes were not directly adjacent to the vasculature (Figure 6a, white arrow). After identification, astrocytes were patched with a borosilicate glass electrode filled with intracellular solution, which also contained Alexa568® hydrazide sodium salt to label patched astrocytes with red fluorescence (Figure 6a´). In total, for unlesioned control animals, 74 astrocytes have been analysed of which 58 % were non-juxtavascular astrocytes and 42 % juxtavascular in nature (Figure 6b).

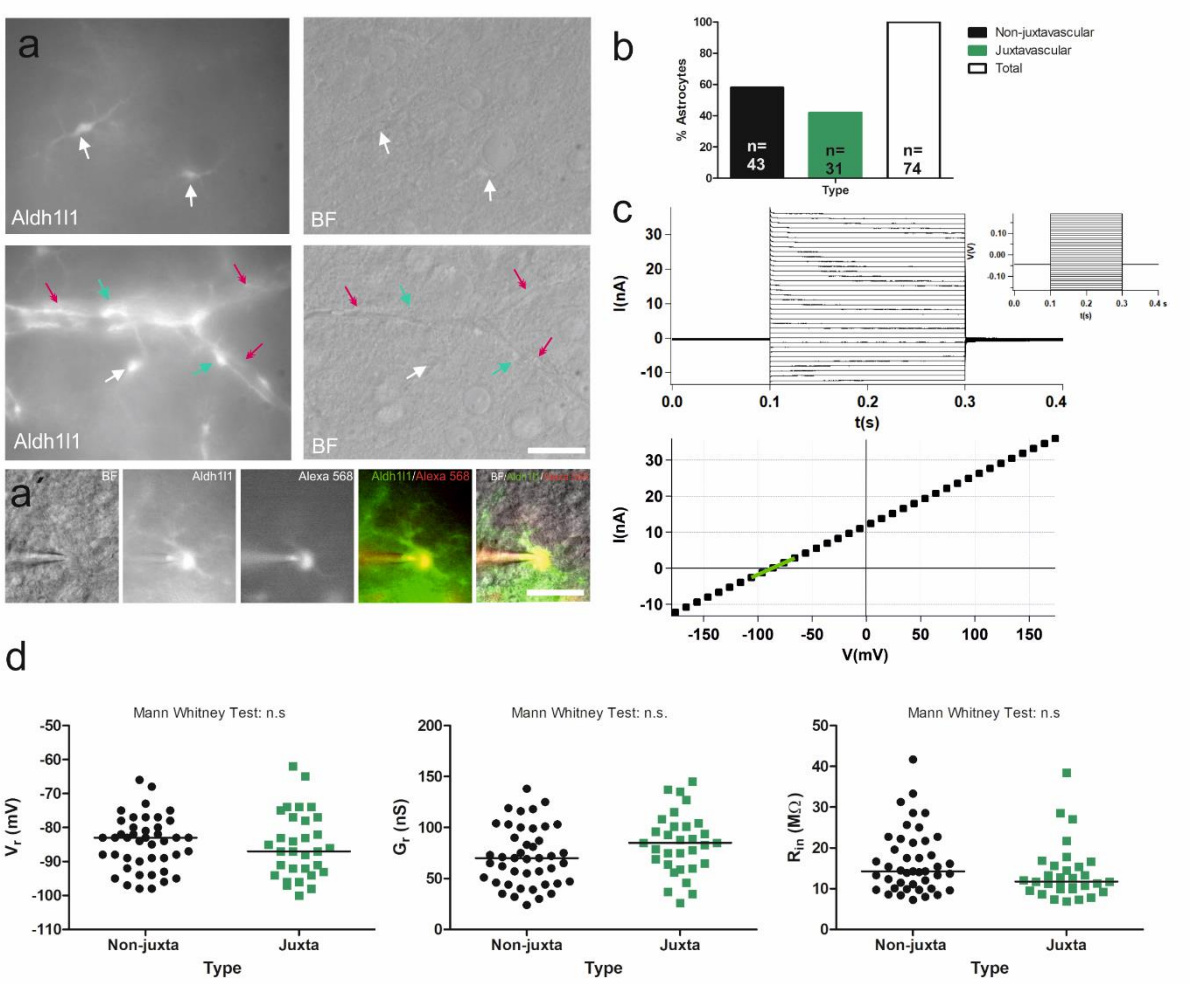

Figure 6: Electrophysiological characterization of non-juxtavascular and juxtavascular astrocytes in the somatosensory cortex

a: Example pictures of fluorescent Aldh1l1-eGFP positive astrocytes (left pictures) and corresponding bright field (BF) images (right pictures) in 200 µm thick somatosensory cortex coronal sections. White arrows mark non-juxtavascular astrocytes. Red arrows point to blood vessels identified either via eGFP fluorescence resulting from astrocytic processes excessively enwrapping them or in the BF picture mode. Cyan arrows point to juxtavascular astrocytes. Scale bar 23µm **a`:** Close up picture of a non-juxtavascular astrocytes (BF picture 1, Aldh1l1-eGFP fluorescence picture 2) patched with a borosilicate glass electrode. The electrode was filled with intracellular solution and Alexa568 fluorescent dye for cell visualisation (Alexa 568 picture 3). Pictures four and five show overlays of the different single channels to proof that the patched cell is really the eGFP positive astrocyte (yellow). Scale bar 45µm. **b:** Distribution of patched astrocytes in the somatosensory cortex of healthy animals. **c:** Current response of an example astrocyte (upper picture) clamped to its V_r and injected with 200 ms long voltage steps ranging from -176 mV to +174 mV in 10 mV increments in voltage-clamp mode (small insert). Lower picture shows the corresponding IV-relationship. G_r of astrocytes can be calculated from a linear fit (green line) performed over five data points, around V_r. **d:** Passive electrophysiological properties of non-juxtavascular (black circles; n = 43) and juxtavascular (green squares; n = 31) astrocytes (total n = 74) of the healthy somatosensory cortex were compared. Left graph shows that the median V_r of non-juxtavascular astrocytes (median = -83 mV) and juxtavascular astrocytes (median = -87 mV) does not differ significantly (Mann-Whitney test: p = 0.6529). Middle graph depicts G_r measured at the steady state and shows no significant difference between non-juxtavascular (median = 70 nS) and juxtavascular (median = 85 nS) astrocytes (Mann-Whitney test: p = 0.0681). R_{in}, shown in the right graph, does also not differ significantly between non-juxtavascular (median = 14.29 MΩ) and juxtavascular (median = 11.76 MΩ) astrocytes (Mann-Whitney test: p = 0.0681).

Astrocytes were clamped to their resting membrane potential (V_r), measured in current-clamp mode and subsequently injected with 200 ms long voltage steps ranging from -176 mV to +174 mV in 10 mV increments (Figure 6c, small insert). From the current response traces the corresponding current-voltage relationship (IV-curve) was calculated at the steady state, as the mean current of each trace over a certain time period, and then plotted against the injected voltages (Figure 6c, bottom). The V_r was taken from the intersection of the IV-curve with the x-axis. For all of the following analyses non-Gaussian distribution was assumed (because not all our results follow Gaussian distribution) and the median of the values was compared. The V_r of somatosensory cortex astrocytes showed a high level of heterogeneity ranging from - 100 mV up to -62 mV, but median V_r of non-juxtavascular astrocytes (black dots) and juxtavascular astrocytes (green squares) did not differ significantly (Figure 6d, left (Mann-Whitney Test: $p = 0.6529$)). Because the IV-curves showed a liner relationship around V_r, the resting membrane conductance (G_r) of astrocytes could be calculated from a linear fit performed over five data points around V_r (Figure 6c, bottom, green line). Since the conductance G is the reciprocal of R, G can be derived from Ohm´s law $R = V/I$ (where R is the resistance in Ohm, I is the current in Ampere and V is the voltage in Volt) hence $G = 1/R$ or $G = I/V$. Because the slope m of the linear fit is defined as $m = \Delta y/\Delta x$ which in our case relates to $m = \Delta I/\Delta V$, this leads to the formula for the conductance namely $G[S] = \Delta I[A]/\Delta V[V]$. The G_r determined at the steady state of astrocytic currents was heterogeneous with values ranging from 24 nS to 145 nS (Figure 6d; middle) with no significant difference between non-juxtavascular astrocytes and juxtavascular astrocytes (Mann-Whitney Test: $p = 0.0681$). As mentioned before, there is a relationship between the input resistance (R_{in}) of a cell and the G_r with $G = 1/R$. Hence the conductance G_r was used to calculate $R_{in} = 1/G_r$, which resulted in heterogeneous R_{in} ranging from 6.62 MΩ to 41.67 MΩ for somatosensory cortex astrocytes (Figure 6d, right) with no significant difference between the non-juxtavascular and juxtavascular astrocytes (Mann-Whitney Test: $p = 0.0681$).

From these results, it was concluded, that somatosensory astrocytes show a high level of heterogeneity regarding their passive electrophysiological properties but no significant difference was observed between non-juxtavascular and juxtavascular astrocytes present in the healthy uninjured brain.

3.1.2 The main current of somatosensory cortex astrocytes is carried by $K_{ir}4.1$ channels

The main current of astrocytes in many brain regions is carried by $K_{ir}4.1$ channels (Mishima et al., 2007; Mishima & Hirase, 2010; Dallérac et al., 2013). Hence, it was studied whether astrocytes residing in the somatosensory cortex vary in their $K_{ir}4.1$ current amplitudes dependent on their location relative to blood vessels (non-juxtavascular or juxtavascular). To test this, electrophysiological recordings on 6 non-juxtavascular and 4 juxtavascular astrocytes of 6 different animals (p24-p38) were performed under control conditions and after the wash-in of the $K_{ir}4.1$ channel blocker $BaCl_2$ (200 µM). V_r and G_r were measured based on steady state IV-relationships and changes were analysed 10 minutes after Ba^{2+} wash-in. Figure 7a shows whole-cell currents of a representative juxtavascular astrocyte under control conditions (upper left), after the wash-in of 200 µM Ba^{2+} (upper right) and the effective $K_{ir}4.1$ (lower left) current pattern, which was obtained by subtracting the current trace where Ba^{2+} was present from the control condition of the same cell. In the lower right graph corresponding IV-relationships of all three conditions are shown. By blocking $K_{ir}4.1$ channels in non-juxtavascular astrocytes, five out of six cells changed to a significantly more positive V_r (Figure 7b left; Wilcoxon matched pairs test: $p = 0.0469$) and three out of four juxtavascular astrocytes showed a similar trend (Figure 7b middle; Wilcoxon matched pairs test: $p = 0.2500$). The median effective change in V_r was not different for non-juxtavascular (median $dV_r = 14$ mV) and juxtavascular astrocytes (median $dV_r = 12$mV) (Figure 7b right; Mann-Whitney test: $p = 0.9273$). Considering G_r in non-juxtavascular astrocytes, changes were very pronounced, with decreases up to 51 nS for one cell (Figure 7c left; Wilcoxon matched pairs test: $p = 0.0313$). The same three out of four juxtavascular astrocytes that showed changes for V_r also decreased in G_r. Despite being rather strong, in some cells even up to 38 nS, changes were not significant but showed a strong trend (Figure 7c middle; Wilcoxon matched pairs test: $p = 0.2500$). Similar to changes in V_r, there was no significant difference in the median change of G_r between non-juxtavascular (median $dG_r = 21$nS) and juxtavascular astrocytes (median $dG_r = 26.5$nS) detectable (Figure 7c right; Mann-Whitney test: $p = 1$). From these findings it was concluded that most of the measured astrocytes in the somatosensory cortex displayed $K_{ir}4.1$ currents that can be blocked with Ba^{2+}.

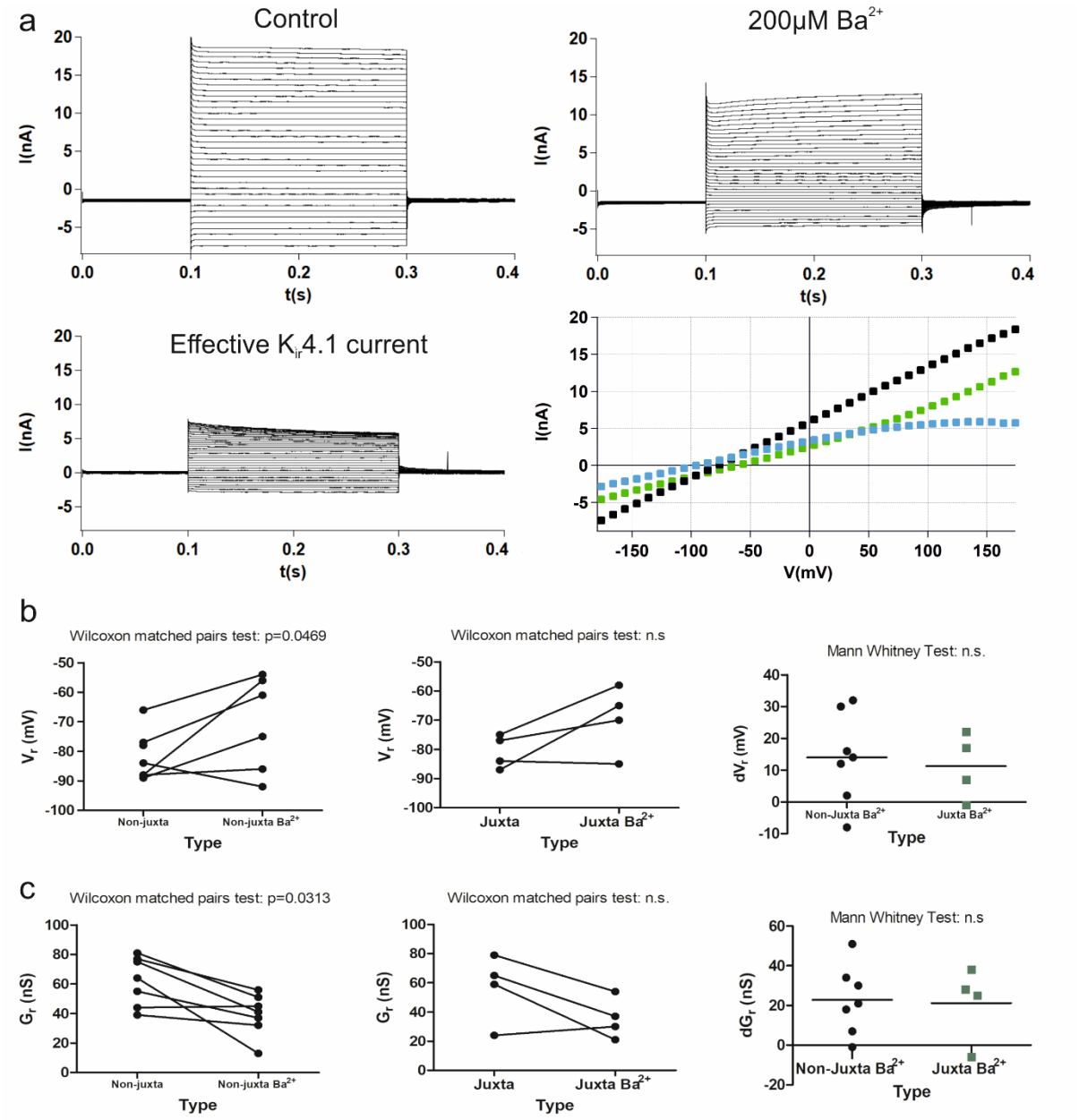

Figure 7: Astrocytic currents in somatosensory cortex are mainly carried by the Ba^{2+} sensitive $K_{ir}4.1$
a: Current responses of a representative juxtavascular astrocyte are shown under control conditions (upper left), and after the wash in of 200 µM Ba^{2+} (upper right). The effective Kir4.1 current (lower left) was obtained by subtracting the current trace with Ba^{2+} from the control ones in the same cell. The graph on the lower right shows the IV-curves at the steady state of the three conditions: Control condition (black), Ba^{2+} blocked condition (green) and effective $K_{ir}4.1$ current (blue). **b:** The V_r of 4 out of 6 non-juxtavascular astrocytes (left; Wilcoxon matched pairs test: p = 0.0469) and 3 out of 4 juxtavascular astrocytes (middle; Wilcoxon matched pairs test: p = 0.2500) became more positive after Ba^{2+} application. Comparison of the effective changes in V_r of non-juxtavascular astrocytes (median dV_r = 14mV) to juxtavascular ones (median dV_r = 12mV) showed no significant difference (right; Mann-Whitney test: p = 0.9273). **c:** The G_r of all non-juxtavascular astrocytes (left; Wilcoxon matched pairs test: p = 0.0313) and 3 out of 4 juxtavascular astrocytes (middle; Wilcoxon matched pairs test: p = 0.2500) decreased significantly after Ba^{2+} application. Analysis of the effective changes in G_r of non- juxtavascular (median dG_r = 21nS) and juxtavascular (median dG_r = 26.5nS) astrocytes revealed no significant difference (right, Mann-Whitney test: p = 1).

3.1.3 Astrocytes in the somatosensory cortex express K_{ir}4.1 channels homogenously

To verify the previous electrophysiological findings, immunohistochemistry against the inwardly rectifying K_{ir}4.1 channels was performed. Figure 8a shows an overview confocal image of a somatosensory cortex slice of an Aldh1l1-eGFP transgenic mouse. To determine the location of astrocytes towards blood vessels DyLight 649 labelled *Lycopersicon esculentum* (Tomato) lectin (TL 649) was used. Tomato lectin is known to be a marker for endothelial cells of the rodent vasculature as well as microglial cells (Mazzetti et al., 2004). It is important to note that no anti-K_{ir}4.1-positive neurons were present throughout all cortical layers. At first glance, there seemed to be a difference between astrocytes in layer I, II and III compared to layer IV, V and VI in the K_{ir}4.1 expression pattern; with the deeper layers showing much higher fluorescence intensity than the upper ones. To determine where this difference originated from close up images of astrocytes in different layers were analysed. All Aldh1l1-eGFP expressing astrocytes (green in overlay) and especially astrocytic processes were extensively labelled with anti-K_{ir}4.1 (red in overlay) with non-juxtavascular (white arrows) and juxtavascular astrocytes (blue arrows) having been equally positive for the anti-K_{ir}4.1 staining (Figure 8b). This leads to the conclusion that the difference in the fluorescence intensity did not originate from heterogeneous expression of K_{ir}4.1 channels but was due to less intensively branched processes in upper layer astrocytes compared to highly branched ones in deeper layers of the somatosensory cortex.

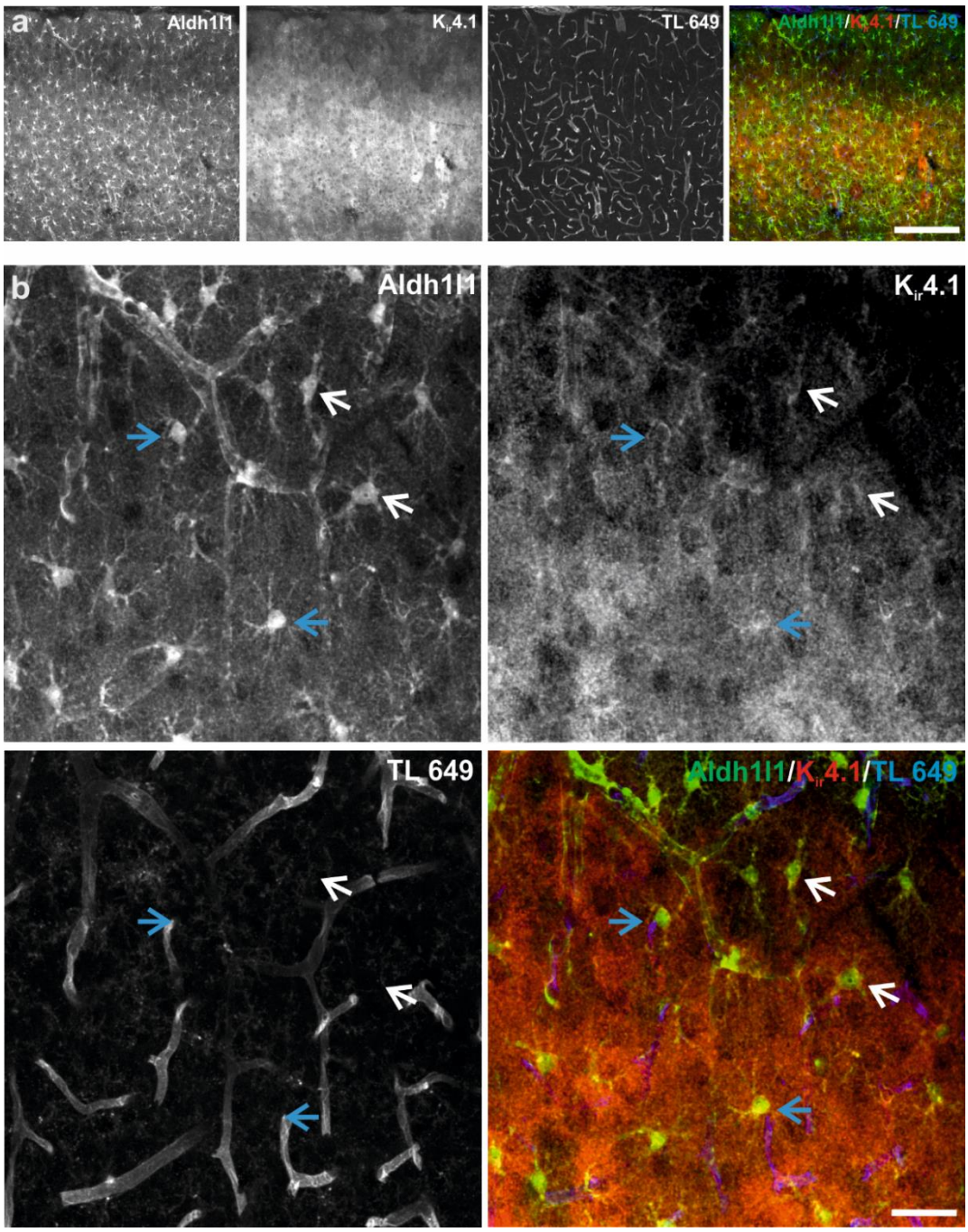

Figure 8: Immunohistochemistry indicates homogeneous expression of K_{ir}4.1 channels in astrocytes of the somatosensory cortex

a: Confocal maximum z-projection (optical section 10-44) of an overview of an adult (p51) Aldh1l1-eGFP transgenic mouse control hemisphere. Three left pictures show from left to right: the Aldh1l1-eGFP expressing astrocytes, the anti-K_{ir}4.1 staining and blood vessels (TL 649). The right image shows an overlay of the three single channels with Aldh1l1-eGFP positive astrocytes (green), the anti-K_{ir}4.1 channel staining (red) and the blood vessels (blue). Scale bar 215µm. **b:** Maximum z-projection (optical section 5-30) of a close up of layer II/III astrocytes in the same slice as in a. White arrows indicate anti-K_{ir}4.1-positive non-juxtavascular astrocytes and blue arrows point to anti-K_{ir}4.1-positive juxtavascular astrocytes. Scale bar 35µm.

To confirm the homogeneous expression of $K_{ir}4.1$ channels, astrocytes of different adult mice (n = 3) were counted in the according cortical layers (Figure 9). Then they were analysed regarding their positivity for anti-$K_{ir}4.1$ and whether they were non-juxtavascular or juxtavascular in nature. The percentage of anti-$K_{ir}4.1$ positive non-juxtavascular (Nj, solid bar) and juxtavascular (J, chequered bar) astrocytes for each animal was plotted in a bar chart (Figure 9b) and the median percentage was determined for each layer. In line with the previous assumption, astrocytes in the somatosensory cortex expressed the inwardly rectifying $K_{ir}4.1$ channel homogenously (no median diverged more than 5 % from a complete homogeneity; see Material and Methods) with no significant difference being present between the medians of non-juxtavascular (Nj median = 100 % for all layers) and juxtavascular astrocytes (Layer I, J median = 98 %; Layers II/III/IV to VI, J median = 100 %) across all cortical layers (Kruskal-Wallis test: p = 0.9175).

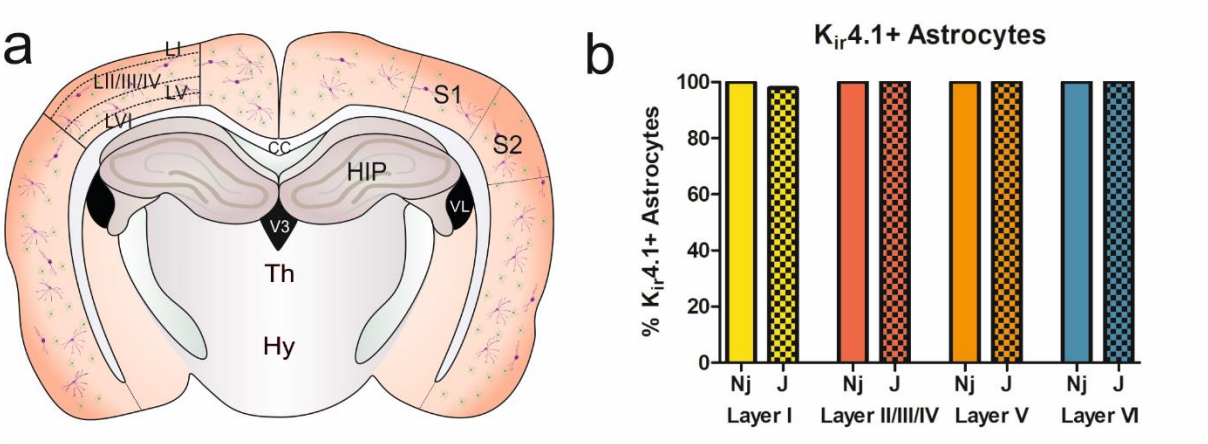

Figure 9: Counting analysis indicates a homogeneous expression of $K_{ir}4.1$ in non-juxtavascular and juxtavascular astrocytes across all layers of the somatosensory cortex in adult mice
a: Schematic of a coronal section of a mouse brain at the level of the somatosensory cortex. In the left hemisphere the different cortical layers are depicted. In the right hemisphere the somatosensory cortex is indicated. Abbreviations: **LI:** Layer I; **LII/III/IV:** Layer II, III and IV; **LV:** Layer V; **LVI:** Layer VI; **S1:** primary somatosensory cortex; **S2:** secondary somatosensory cortex; **CC:** corpus callosum; **HIP:** hippocampus; **VL:** lateral ventricle; **V3:** third ventricle; **Th:** thalamus; **Hy:** hypothalamus. **b:** Counting analysis of anti-$K_{ir}4.1$ positive astrocytes in 3 adult Aldh1l1-eGFP mice (p40-51). Bar chart shows percentage of anti-$K_{ir}4.1$ positive non-juxtavascular (Nj, solid bars) and juxtavascular (J, chequered bars) astrocytes. Median percentages for each astrocyte type were determined. Layer I (yellow): Nj median = 100 %, J median = 98 %. Layer II/III/IV (coral): Nj median = 100 %, J median = 100 %; Layer V (orange): Nj median = 100 %, J median = 100 %; Layer VI (blue): Nj median =100 %, J median = 100 %. The criteria for a homogenous expression pattern was met if the median percentage did not diverge more than 5 % from 100 %. $K_{ir}4.1$ was homogenously expressed in all somatosensory cortex astrocytes (Kruskal-Wallis test: p = 0.9175).

3.1.4 Astrocytes in the somatosensory cortex express $K_{ir}6.2$ channels heterogeneously

The alpha subunits $K_{ir}6.1$ and $K_{ir}6.2$ represent the pore forming part of the ATP-dependent, inwardly rectifying K_{ATP} channel. It has previously been reported that $K_{ir}6.1$ is present in astrocytes in the hippocampus, cerebellum and cortex as well as in Bergman glia (Thomzig et al., 2001), whereas $K_{ir}6.2$ mRNA was present in Müller glia, astrocytes in the cerebellar white matter and in the corpus callosum (Thomzig et al., 2001; Raap et al., 2002; Zhou et al., 2002). In this study, immunohistochemical stainings were performed against the $K_{ir}6.1$ and $K_{ir}6.2$ subunits. In contrast to the literature, the results here showed $K_{ir}6.2$ expression in astrocytes in the somatosensory cortex (Figure 10a) and only little to no $K_{ir}6.1$ expression (data not shown). In layer I less anti- $K_{ir}6.2$ labelling is detectable than in all other deeper cortical layers, where a strong anti-$K_{ir}6.2$ positivity can be seen in astrocytes as well as neurons. The processes of a fraction of cortical Aldh1l1-eGFP astrocytes were intensely labelled with anti-$K_{ir}6.2$, whereas astrocytic somata were labelled very sparsely (Figure 10b, red in overlay). Heterogeneous expression of $K_{ir}6.2$ in both non-juxtavascular (white arrows) and juxtavascular astrocytes (blue arrows) was found throughout the somatosensory cortex (Figure 10b). Moreover, there were astrocytes that lack anti-$K_{ir}6.2$ positivity (asterisk) regardless of the location of their somata (Figure 10b).

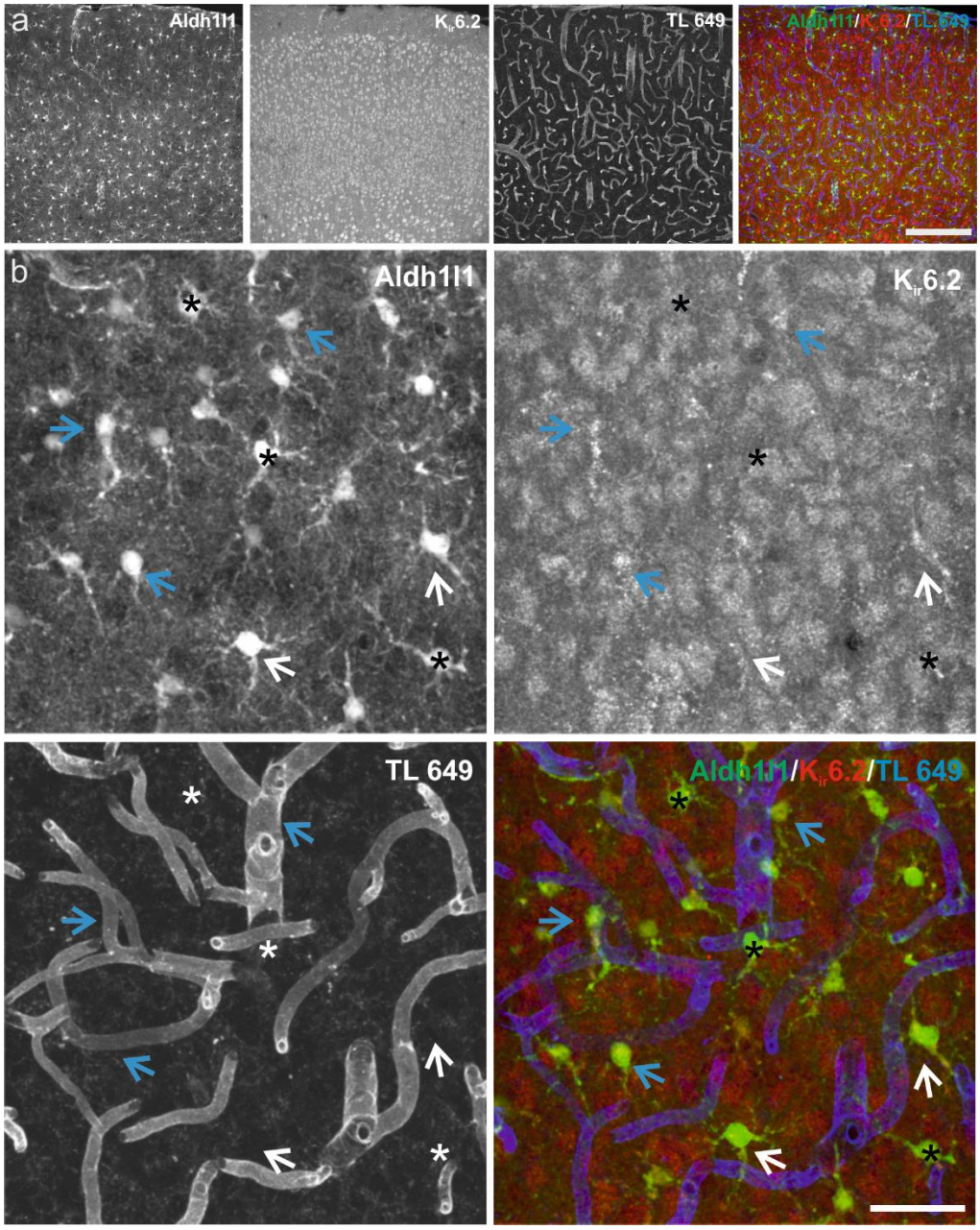

Figure 10: Immunohistochemistry indicates heterogeneous expression of K_{ir}6.2 channels in somatosensory cortex astrocytes

a: Confocal maximum z-projection (all optical sections) of an overview of an adult (p51) Aldh1l1-eGFP transgenic mouse somatosensory cortex control hemisphere. The three left pictures show from left to right: the Aldh1l1-eGFP expressing astrocytes, the anti-K_{ir}6.2 staining and blood vessels (TL 649). The right image shows an overlay of the three single channels with Aldh1l1-eGFP positive astrocytes (green), the anti-K_{ir}6.2 staining (red) and the blood vessels (blue). Scale bar 215µm. **b:** Maximum z-projection (all optical sections) of a close up of layer II/III astrocytes in the same slice as in a. There are non-juxtavascular (white arrows) and juxtavascular (blue arrows) astrocytes positive for anti-K_{ir}6.2. Anti-K_{ir}6.2 negative astrocytes are marked with an asterisk. K_{ir}6.2 is mainly present on astrocytic processes. Heterogeneous expression was observed in cortical astrocytes independent of the astrocytes position towards blood vessels and the cortical layer. Scale bar 26µm.

To further analyse the distribution of $K_{ir}6.2$ channels across non-juxtavascular and juxtavascular astrocytes, cells of 4 adult Aldh1l1-eGFP mice were counted in the according cortical layers (Figure 11a) and analysed for anti-$K_{ir}6.2$ labelling. Analysis was performed the same way as mentioned in paragraph 3.1.3. Heterogeneity in $K_{ir}6.2$ channel expression was detected throughout all layers of the somatosensory cortex (no median higher than 92 %). Nevertheless, despite $K_{ir}6.2$ being heterogeneously expressed, there was no significant difference between different layers as well as between non-juxtavascular (Nj, solid bar) or juxtavascular (J, chequered bar) astrocytes detectable (Figure 11b; Kruskal-Wallis test: $p = 0.8409$). The sparse anti-$K_{ir}6.2$ positivity of layer I (Figure 10a) was not a result of a lower percentage of astrocytes expressing said ion channel in comparison to other layers (Figure 11b), but was rather due to a smaller amount of astrocytes present in layer I as well as the absence of anti-$K_{ir}6.2$ positive neurons (see discussion).

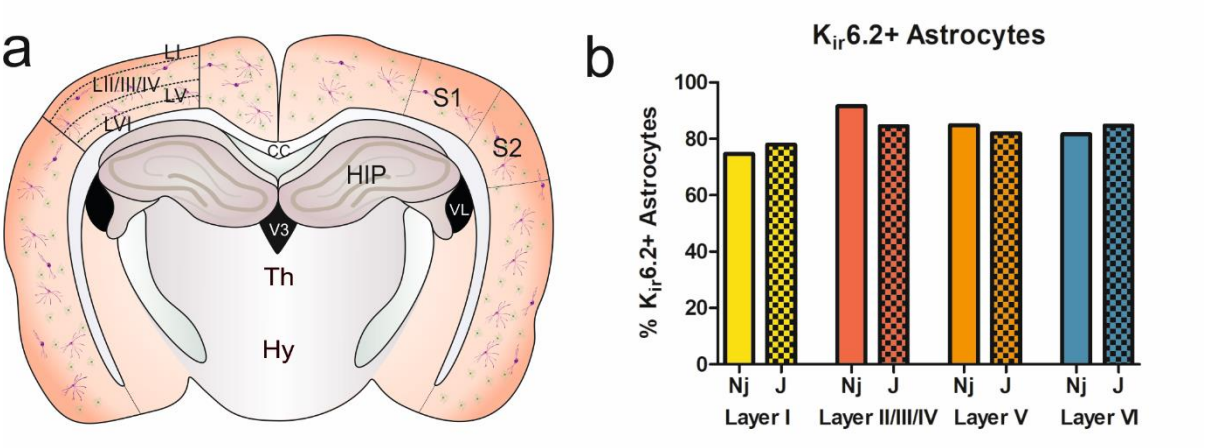

Figure 11: Counting analysis suggests a heterogeneous expression of $K_{ir}6.2$ in non-juxtavascular and juxtavascular astrocytes across all layers of the somatosensory cortex in adult mice
a: Schematic of a coronal section of a mouse brain at the level of the somatosensory cortex. In the left hemisphere the different cortical layers are depicted. In the right hemisphere the somatosensory cortex is indicated. Abbreviations: **LI:** Layer I; **LII/III/IV:** Layer II, III and IV; **LV:** Layer V; **LVI:** Layer VI; **S1:** primary somatosensory cortex; **S2:** secondary somatosensory cortex; **CC:** corpus callosum; **HIP:** hippocampus; **VL:** lateral ventricle; **V3:** third ventricle; **Th:** thalamus; **Hy:** hypothalamus. **b**: Counting analysis of anti-$K_{ir}6.2$ positive astrocytes in 4 adult Aldh1l1-eGFP mice (p36-51). Bar chart shows percentages of anti-$K_{ir}6.2$ positive non-juxtavascular (Nj, solid bars) and juxtavascular (J, chequered bars) astrocytes. Median percentages for each astrocyte type were determined. Layer I (yellow): Nj median = 75 %, J median = 78 %; Layer II/III/IV (coral): Nj median=92%, J median=85%; Layer V (orange): Nj median=85%, J median=82%; Layer VI (blue): Nj median = 82 %, J median = 85 %. The criteria for a homogenous expression pattern was met if the median percentage did not diverge more than 5 % from 100 %. $K_{ir}6.2$ was heterogeneously expressed in somatosensory cortex astrocytes. The heterogeneity was not dependent on the position of astrocytes towards blood vessels or on the cortical layers (Kruskal-Wallis test: $p = 0.8409$).

3.1.5 Astrocytes in the somatosensory cortex express K_v4.3 channels heterogeneously

Because the *Shal* K_v4.3 channel subunit is present in cultured hippocampal astrocytes and is the main underlying source for inactivating A-type currents (I_A) (Bekar, 2004).Therefore, it was of interest to see, whether K_v4.3 is present in somatosensory cortex astrocytes and if so, whether they are homogeneously or heterogeneously distributed between non-juxtavascular and juxtavascular astrocytes. Immunohistochemical stainings against K_v4.3 channels were performed in adult Aldh1l1-eGFP mice (Figure 12). Layer I was way more sparsely labelled, whereas the other layers showed a high amount of K_v4.3 positivity in astrocytes as well as neurons (Figure 12a). Astrocytic processes as well as somata (Figure 12b, green in overlay) were labelled by anti-K_v4.3 (Figure 12b, red in overlay). Both, non-juxtavascular (white arrows) and juxtavascular astrocytes (blue arrows) expressed K_v4.3. In addition, there were also astrocytes that lack K_v4.3 (asterisks). But their absence did not correlate with whether astrocytes had their cell soma directly adjacent to a blood vessel or not. Therefore, the presence of the K_v4.3 subunit appeared to be heterogeneous amongst cortical astrocytes.

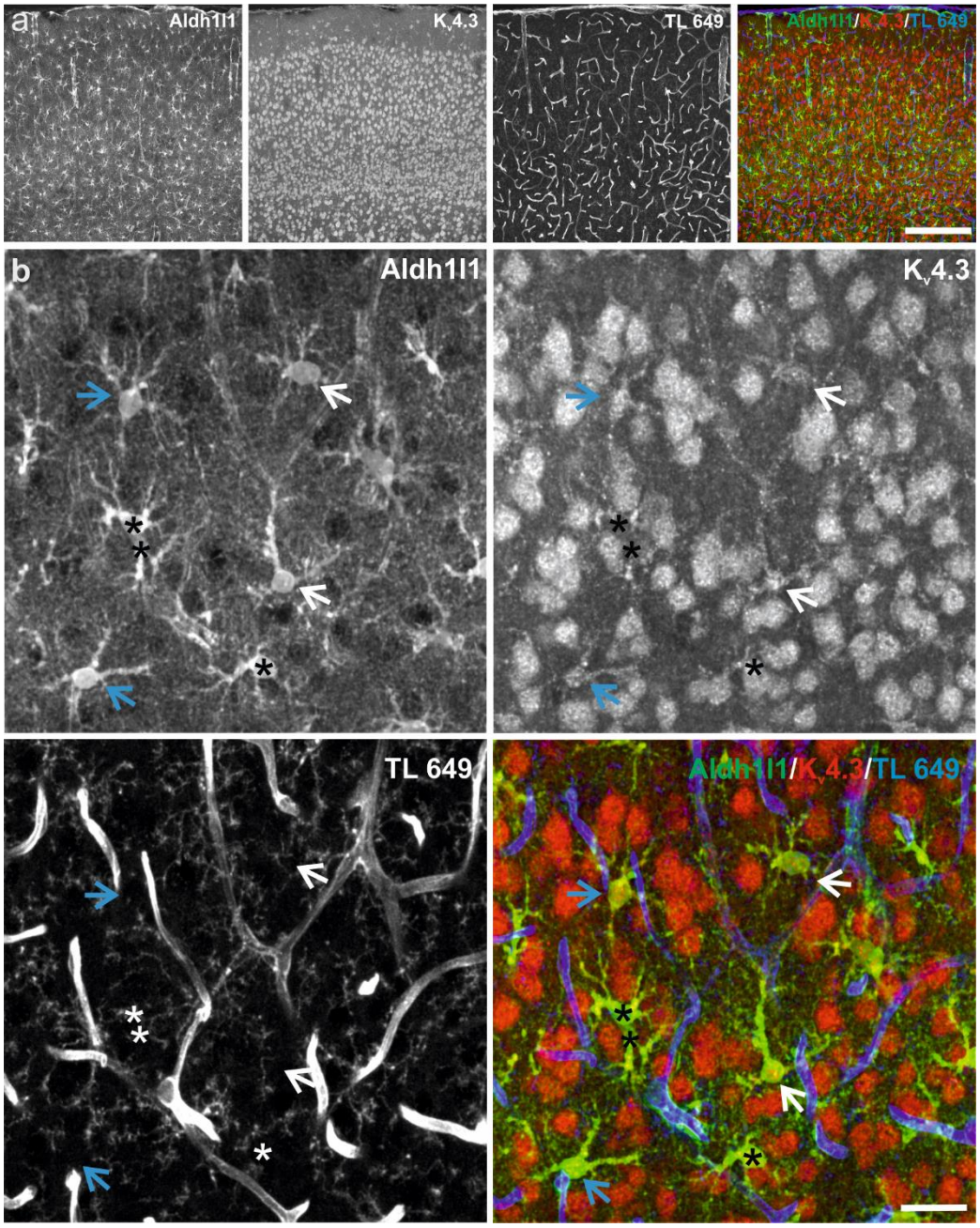

Figure 12: Immunohistochemistry suggests heterogeneous expression of K_v4.3 channels in astrocytes of the somatosensory cortex

a: Overview confocal maximum z-projection (all optical sections) of an adult (p51) Aldh1l1-eGFP transgenic mouse somatosensory cortex control hemisphere. The three left pictures show from left to right: the Aldh1l1-eGFP expressing astrocytes, the anti-K_v4.3 staining and blood vessels (TL 649). The right image shows an overlay of the three single channels with Aldh1l1-eGFP positive astrocytes (green), the K_v4.3 channel staining (red) and the blood vessels (blue). Scale bar 215µm. **b:** Maximum z-projection (optical sections 4-48) of a close up of layer II/III astrocytes in the same slice as in a. There are non-juxtavascular (white arrows) and juxtavascular (blue arrows) astrocytes present that are positive for anit-K_v4.3. Astrocytes that show no anti-K_v4.3 labelling are marked with an asterisk. K_v4.3 was heterogeneously expressed in cortical astrocytes independent of astrocytes position towards blood vessels or location in the cortical layer. Scale bar 26µm.

To obtain a more detailed picture of how K_v4.3 channels were distributed amongst non-juxtavascular and juxtavascular astrocytes, cells of 7 different adult animals were counted in the according cortical layers as shown in Figure 13a and analysed regarding their positivity for anti-K_v4.3. Analysis was performed the same way as mentioned in paragraph 3.1.3. Astrocytes expressed K_v4.3 channels heterogeneously (no median higher than 92 %) with the exception of non-juxtavascular astrocytes in cortical layer VI where 100 % of astrocytes were positive for said ion channel (Figure 13b). Even if K_v4.3 was heterogeneously expressed no significant difference was present between different cortical layers. Moreover, positivity for anti-K_v4.3 could not be related to whether an astrocyte belongs to the non-juxtavascular (Nj, solid bar) or juxtavascular (J, chequered bar) subtype (Kruskal-Wallis test: $p = 0.5925$). The sparse labelling by the anti-K_v4.3 antibody that was observed (Figure 12a) could not be explained by a lower percentage of astrocytes expressing said ion channel but, was rather due to a smaller amount of astrocytes being present in layer I as well as the absence of anti-K_v4.3 positive neurons.

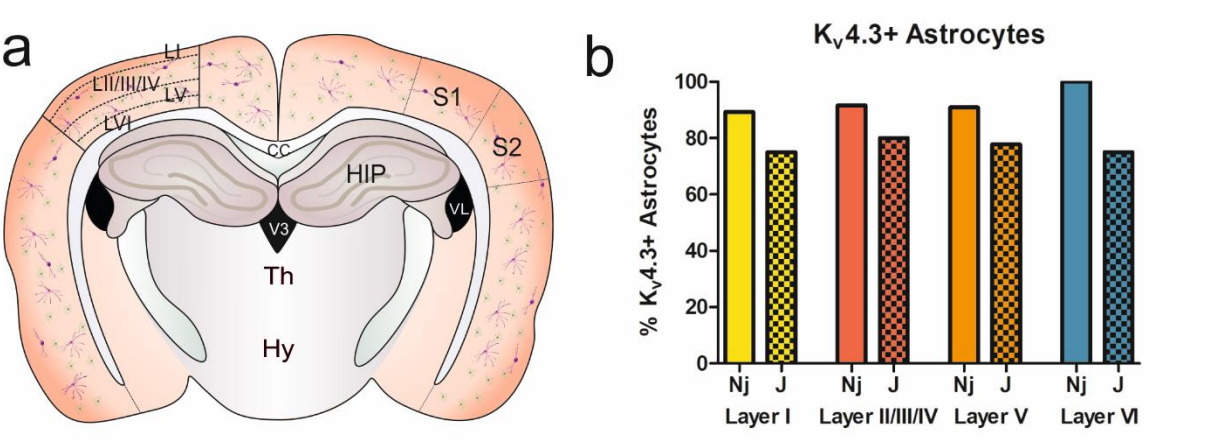

Figure 13: **Counting analysis indicates a heterogeneous expression of K_V4.3 in non-juxtavascular and juxtavascular astrocytes across all layers of the somatosensory cortex in adult mice**
a: Schematic of a coronal section of a mouse brain at the level of the somatosensory cortex. In the left hemisphere the different cortical layers are depicted. In the right hemisphere the somatosensory cortex is indicated. Abbreviations: **LI:** Layer I; **LII/III/IV:** Layer II, III and IV; **LV:** Layer V; **LVI:** Layer VI; **S1:** primary somatosensory cortex; **S2:** secondary somatosensory cortex; **CC:** corpus callosum; **HIP:** hippocampus; **VL:** lateral ventricle; **V3:** third ventricle; **Th:** thalamus; **Hy:** hypothalamus. **b**: Counting analysis of anti-K_V4.3 positive astrocytes in 7 adult Aldh1l1egfp mice (p36-51). Bar chart shows percentages of K_V4.3 positive non-juxtavascular (Nj, solid bars) and juxtavascular (J, chequered bars) astrocytes. Median percentages for each astrocyte type were determined. Layer I (yellow): Nj median = 89 %, J median = 75 %; Layer II/III/IV (coral): Nj median = 92 %, J median =80 %; Layer V (orange): Nj median = 91 %, J median = 78 %; Layer VI (blue): Nj median = 100%, J median = 75 %. The criteria for a homogenous expression pattern would have been met if the median percentage did not diverge more than 5 % from 100 %: K_V4.3 was heterogeneously expressed in somatosensory cortex astrocytes. Heterogeneity was not depending on the position of astrocytes towards blood vessels or on the cortical layers they reside in (Kruskal-Wallis test: p = 0.5925). Error bar shows minimum and maximum range.

3.1.6 Astrocytes can be classified into non-passive and passive types according to their electrophysiological properties

As previously described by several groups (Zhou, 2005; Houades et al., 2008; Kafitz et al., 2008), astrocytes in the barrel cortex and the hippocampus transition during development from mainly non-passive astrocytes to mainly passive, ohmic ones whose currents are predominantly carried by inwardly rectifying ion channels. To see, whether the same predominantly passive current responses were present in the somatosensory cortex of adult Aldh1l1-eGFP mice, cells were clamped to the V_r recorded in current clamp mode and subsequently 200 ms long voltage steps, ranging from -176 mV to +174 mV (Figure 6b, small insert) were injected to obtain the current response (Figure 14a). There were two different types of astrocytes present. The majority of astrocytes showed typical ohmic passive current responses (Figure 14a, c) with linear IV-curves (Figure 14b). The other 26 % of astrocytes showed non-passive current response patterns (Figure 14a, c) with non-linear IV relationships (Figure 14b). It has been shown that these two different types of astrocytes are also present in the developing mouse lateral superior olive (LSO) of the auditory brainstem, with a decrease in the fraction of non-passive cells during development (Stephan & Friauf, 2014). Here, the same electrophysiological experiments as in the somatosensory cortex were performed on astrocytes in the LSO of Aldh1l1-eGFP mice (p15-p30; n=9). At these ages cells are known to be already more likely to be passive (Stephan & Friauf, 2014). Non-passive current patterns could be observed in 34 % of these astrocytes (Figure 14a, c) accompanied by non-linear IV-relationships (Figure 14b) and 66 % of cells showed passive ohmic currents (Figure 14a, c) and associated linear IV-curves (Figure 14b). Somatosensory cortex astrocytes did not differ from LSO astrocytes regarding the ratio of non-passive to passive cells (Figure 14c; Fisher´s-exact test: $p = 0.2800$). When passive properties of somatosensory cortex astrocytes were compared to those in the LSO, all three parameters tested were significantly different (Figure 14d-f). The V_r of LSO astrocytes (Figure 14d; median V_r = -82 mV) was significantly more positive (Mann-Whitney test: $p = 0.0058$) than in cortical ones (median V_r = -85 mV). In addition, G_r and R_{in} differed significantly between the two groups (Figure 14e, f; Mann-Whitney test: $p = 0.0305$), with LSO astrocytes having a much higher G_r (median G_r = 93 nS) and a lower R_{in} (median R_{in} = 10.75 MΩ) than somatosensory cortex astrocytes (median

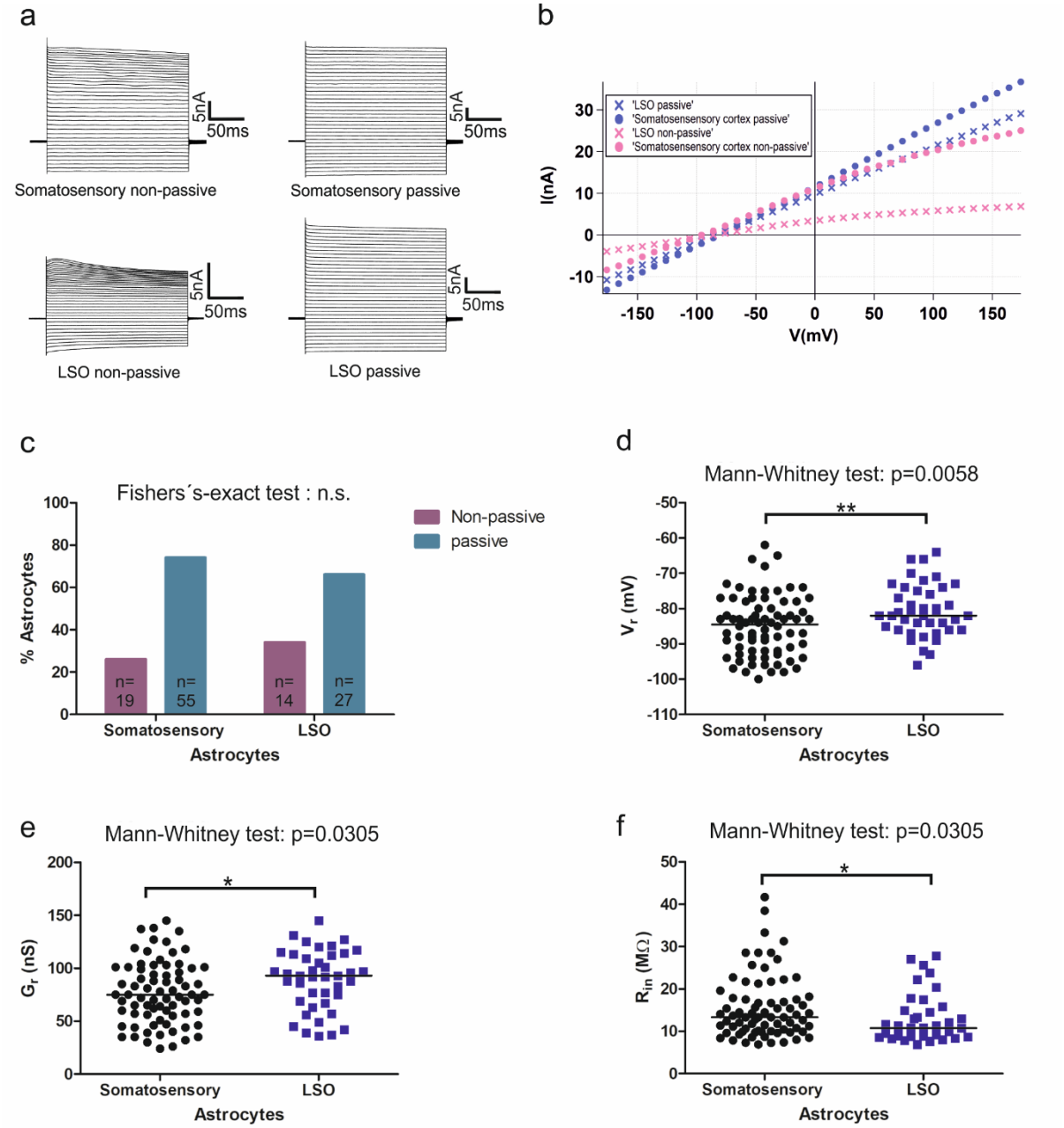

Figure 14: Astrocytes can be classified according to their current response pattern into passive and non-passive

a: Example current responses of non-passive and passive somatosensory astrocytes (upper pictures) as well as for non-passive and passive LSO astrocytes (lower pictures). **b:** Corresponding steady state IV-relationships for the four astrocytes displayed in a. The IV-curves of non-passive cells are displayed in rose, the passive IV-relationships are coded in blue. LSO astrocytes are visualised by crosses, data points for somatosensory cortex astrocytes by circles. **c:** Bar plot for the distribution on a percentage basis of non-passive and passive astrocytes in the somatosensory cortex and the LSO. Non-passive cells are coded in rose and passive cells in blue. A Fisher´s-exact test showed no significant difference in the ratio of non-passive to passive cells for both brain regions ($p = 0.2800$). **d:** Comparing the V_r of somatosensory cortex astrocytes (median $V_r = -84.5$ mV) and LSO astrocytes(median $V_r = -82$mV), showed a significant difference (Mann-Whitney test: $p = 0.0058$). **e:** Regarding G_r somatosensory cortex astrocytes (median $G_r = 75$ nS) differed significantly (Mann-Whitney test: $p = 0.0305$) from LSO astrocytes (median $G_r = 93$ nS). **f:** Comparison of the R_{in} of somatosensory cortex astrocytes (median $R_{in} = 13.33$ MΩ) and LSO astrocytes (median $R_{in} = 10.75$ MΩ) also showed a significant difference (Mann-Whitney test: $p = 0.0305$).

G_r = 75 nS; median R_{in} = 13.33 MΩ). To conclude, astrocytes of the somatosensory cortex were comparable to LSO astrocytes regarding their ratio of non-passive and passive current patterns which is in line with previously published results from the LSO, the barrel cortex as well as the hippocampus (Zhou, 2005; Kafitz et al., 2008; Stephan & Friauf, 2014). However, there was a significant difference between their passive properties, which might be due to different patterns of expressed ion channels, transporters or receptors.

3.1.7 Passive and non-passive current patterns in juxtavascular and non-juxtavascular somatosensory cortex astrocytes

Next it was assessed if the fractioning into non-passive and passive current patterns of astrocytes in the healthy somatosensory cortex was related to whether astrocytes are juxtavascular or non-juxtavascular in nature. When the 74 control astrocytes (43 non-juxtavascular, 31 juxtavascular) from unlesioned brains were sorted according to their current pattern, the majority displayed passive properties (70 % of non-juxtavascular, 81 % juxtavascular astrocytes) (Figure 15a). Testing for differences between the two subgroups, a Fisher´s-exact test showed no significance (p = 0.0996). Next passive properties of non-juxtavascular and juxtavascular astrocytes were analysed when they were sorted according to non-passive and passive current patterns (Figure 15b-d). For all following analysis in this thesis, if more than two groups were compared in one graph, a Kruskal-Wallis test was performed to clarify if there is a difference between all respective groups. If the Kruskal-Wallis test was significant, a Mann-Whitney test was used to perform further testing of groups that were of interest and a Bonferroni correction was used to determine the adequate p value (alpha corrected). Regarding V_r, there was no difference between the two astrocyte subgroups (Figure 15b; Kruskal-Wallis test: p = 0.3571). However, G_r did differ significantly between the subgroups (Figure 15c; Kruskal-Wallis test: p = 0.0004). Non-juxtavascular passive astrocytes had in general a 30 nS higher G_r than the non-juxtavascular non-passive astrocytes (Mann-Whitney test: p = 0.0003; Bonferroni: alpha corrected = 0.025). The same significant difference was found (Kruskal-Wallis test: p = 0.0004) between the median R_{in} of non-juxtavascular passive astrocytes (Figure 15d), which was with 13.33 MΩ significantly lower than in non-juxtavascular non-passive ones (Mann-Whitney test: p = 0.0003; Bonferroni: alpha corrected = 0.025). Despite these significant differences listed above, neither did non-passive

non-juxtavascular astrocytes differ from their juxtavascular counterparts nor did passive astrocytes vary dependent on their localisation (non-juxtavascular vs. juxtavascular) in all analysed parameters. This lead to the conclusion, that the positions of the cell somata with respect to the vasculature did not play a role in whether astrocytes have passive or-non-passive current patterns in the healthy brain.

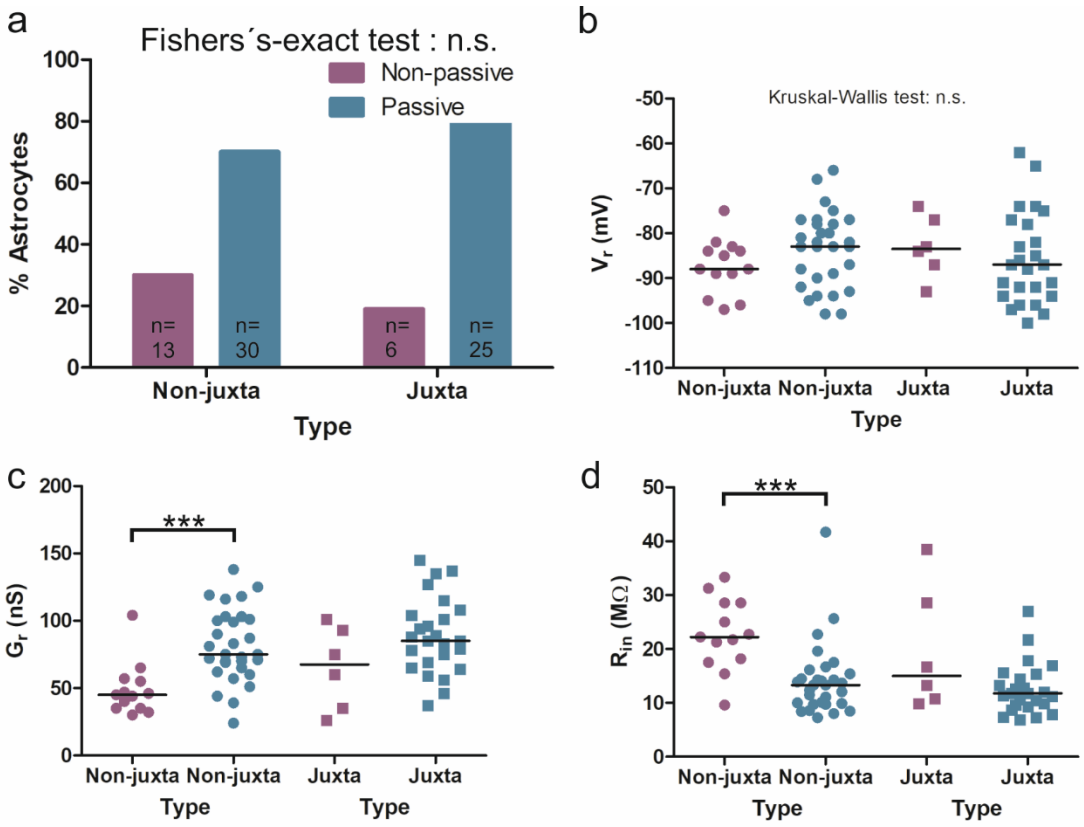

Figure 15: Comparison of non-juxtavascular and juxtavascular astrocytes regarding non-passive and passive current patterns

a: 74 control astrocytes (43 non-juxtavascular, 31 juxtavascular) were sorted according to their current pattern. Non-passive cells are shown in rose; passive ones are coded in blue. 30 % of non-juxtavascular astrocytes displayed non-passive current patterns and 70 % passive ones. 19 % of juxtavascular astrocytes displayed non-passive and 81 % passive current patterns. A Fisher´s-exact test showed no significance ($p = 0.0996$). **b**: Comparison of the V_r of non-passive (rose) and passive (blue) non-juxtavascular (dots) and juxtavascular astrocytes (squares) showed no significant difference (Kruskal-Wallis test: $p = 0.3571$). **c:** Comparison of the G_r of non-passive (rose) and passive (blue) non-juxtavascular (dots) and juxtavascular (squares) astrocytes showed a significant difference (Kruskal-Wallis test: $p = 0.0004$). The median G_r of non-juxtavascular non-passive (45 nS) and non-juxtavascular passive (75 nS) astrocytes differed significantly (Mann-Whitney test: $p = 0.0003$; Bonferroni: alpha corrected = 0.025). **d:** Comparison of the R_{in} of non-passive (rose) and passive (blue) non-juxtavascular (dots) and juxtavascular (squares) astrocytes showed a significant difference (Kruskal-Wallis test: $p = 0.0004$). The median R_{in} of non-juxtavascular non-passive astrocytes (22.22 MΩ) is significantly different from the one of non-juxtavascular passive ones (13.33 MΩ) (Mann-Whitney test: $p = 0.0003$; Bonferroni: alpha corrected = 0.025).

3.1.8 Identification of HCN channels in the healthy somatosensory cortex

It has been shown, that reactive astrocytes after ischemia upregulate the expression of certain sets of HCN cation channels that give rise to so called I_h currents (Honsa et al., 2014). Furthermore, they found that astrocytes in healthy control brains show no signs of HCN channel expression at all. To test whether astrocytes in the somatosensory cortex show HCN currents and whether there is a difference in the expressions of said channels between non-juxtavascular and juxtavascular astrocytes, electrophysiological experiments were performed on 10 astrocytes (3 juxtavascular, 7 non-juxtavascular) from different animals (p26-37; n = 6). The astrocytes were clamped to the cells membrane potential measured in current clamp mode and then subsequently injected with 1 s long voltage steps ranging from -176 mV to -16 mV in 10 mV increments (Figure 16a´) to obtain the current responses (Figure 16a). Consecutively, the astrocytes were incubated with the selective HCN channel blocker ZD7288 (50 μM) for 10 minutes before the recordings were repeated in the same cell (Figure 16b). The mean current for each trace at around the steady state (0.90 s-0.99 s), the corresponding IV-relationship before and after ZD 7288 application as well as the one for the effective current response from the difference trace (Figure 16d) were calculated. A reduction in the slope of the IV-curves after ZD7288 application was observed. However, the subtraction of the ZD7288-blocked current response pattern from the control condition (Figure 16c and d) did not show typical I_h characteristics. Furthermore, as the IV-relation of the difference current was linear this effect is most likely not related to a blockage of HCN channels by ZD7288 but might rather be due to an ion channel rundown (see discussion). This led to the conclusion that functional HCN channels were absent in the recorded cells.

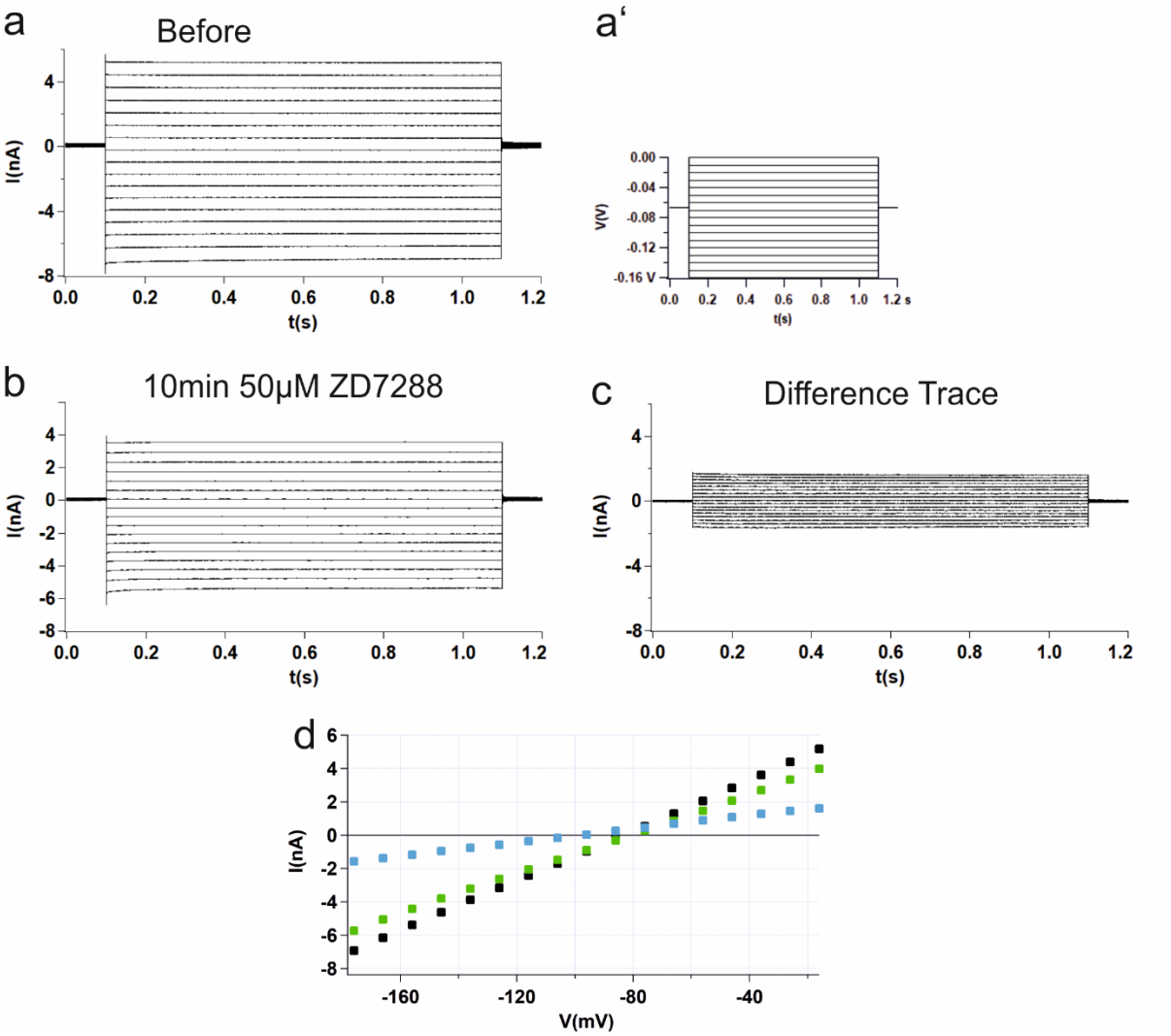

Figure 16: Identification of hyperpolarisation-activated cyclic nucleotide-gated (HCN) cation channels
a: Current responses of a non-juxtavascular example astrocyte. **a':** Small insert shows the stimulus that was used to activate HCN channels. Astrocytes were clamped to the cells V_r measured in current clamp mode and subsequently injected with 1s long voltage steps ranging from -176 mV to -16 mV in 10 mV. **b:** Current response of the same astrocyte after 10 minute incubation with the HCN channel blocker ZD7288 (50 µM). **c:** Effective current obtained by the subtraction of the ZD7288 blocked current responses from the control condition is shown in the difference trace. **d:** The mean current for each trace at around the steady state (0.90s-0.99s) was calculated and the corresponding IV-relationship before (black squared line) and after ZD7288 application (green squared line) as well the effective difference trace (blue squared line) is shown for the example astrocyte.

Immunohistochemical stainings against the HCN1, HCN2 and HCN3 cation channels were performed. Cortical astrocytes were solely positive for the anti-HCN1 channel staining, whereas stainings aimed at the HCN2 (Figure 24a) and HCN3 (data not show) subunits produced negative results in the healthy brain. The processes and somata of cortical Aldh1l1-eGFP astrocytes (Figure 17, green in overlay) were labelled with anti-HCN1 (Figure 17, red in overlay). Non-juxtavascular (white arrows) and juxtavascular astrocytes (blue arrows) that

were positive for HCN1 were found. In addition, there were also astrocytes that lack HCN1 channels (asterisk). But their absence did not correlate with astrocytes having their cell somata directly adjacent to a blood vessel or not. Therefore, the presence of the HCN1 subunit appeared to be heterogeneously amongst cortical astrocytes. Interestingly, this was in contrast to the electrophysiological experiments of this study in which no typical I_h currents were observed (see discussion).

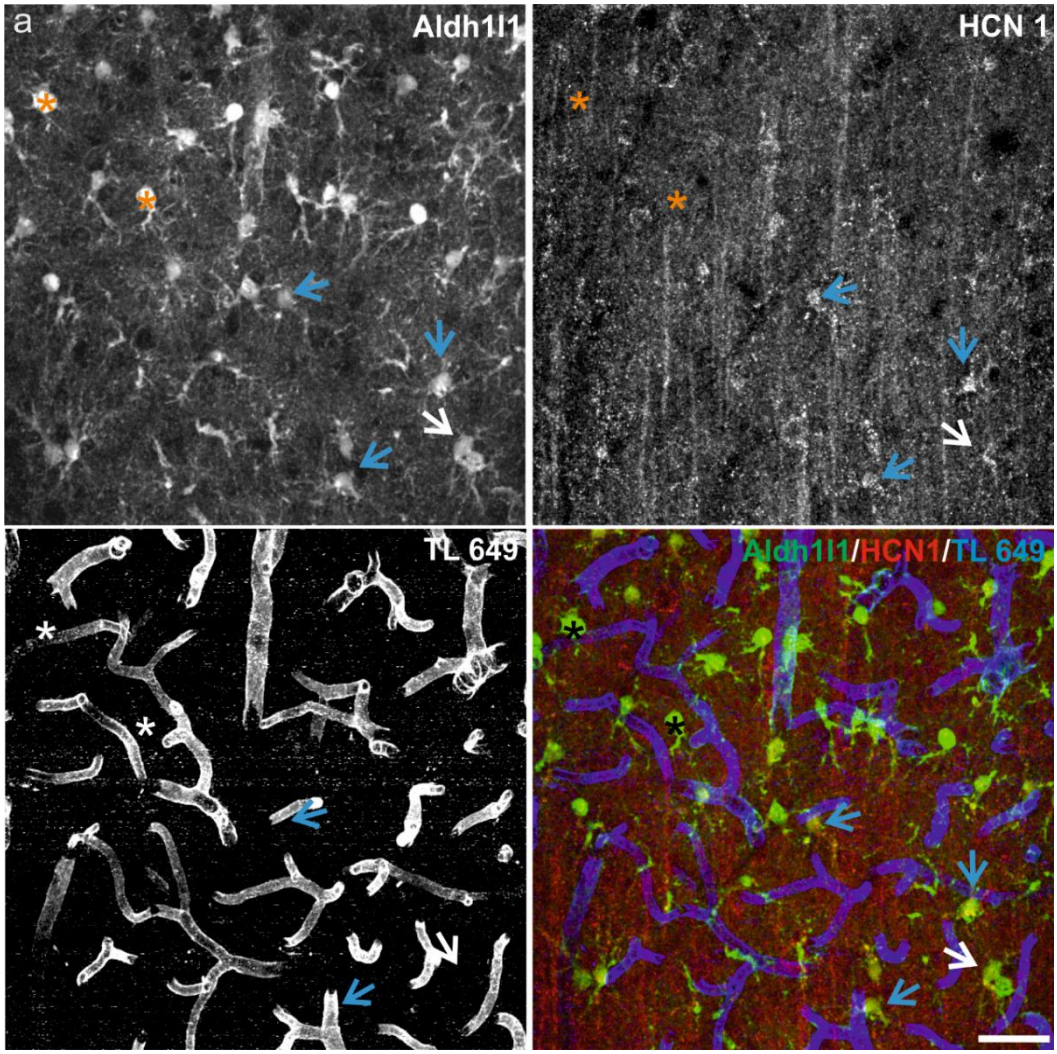

Figure 17: Immunohistochemistry revealed heterogeneous expression of HCN1 channels
Maximum z-projection (all optical sections) of a close up of layer II/III in a somatosensory cortex slice of an adult (p51) Aldh1l1-eGFP mouse. The pictures show: the Aldh1l1-eGFP expressing astrocytes, the anti-HCN1 staining and blood vessels (TL 649).The right lower image shows an overlay of the three single channels with Aldh1l1-eGFP positive astrocytes (green), the HCN1 channel staining (red) and the blood vessels (blue).White arrows indicate non-juxtavascular astrocytes and blue arrows point to juxtavascular ones that are positive for anti-HCN1. Astrocytes that show no HCN1 labelling are marked with an asterisk. HCN1 was heterogeneously expressed in cortical astrocytes but the heterogeneity was not relatable to the astrocytes position towards blood vessels or location in the cortical layer. Scale bar 35µm.

3.2 Characterization of juxtavascular and non-juxtavascular astrocytes in the somatosensory cortex of the lesioned brain

In the healthy brain no differences between non-juxtavascular and juxtavascular astrocytes regarding their passive electrophysiological properties as well as their ion channel expression patterns were observed. The second possibility how ion channels might be involved in the proliferation of astrocytes is their up- or downregulation in a certain subset of astrocytes in response to a traumatic event. Hence, in the second part of this thesis it was assessed whether a stab wound lesion in the brain, which induces astrocytes to become reactive, would lead to a difference in ion channel composition in the two subclasses of reactive astrocytes.

3.2.1 Electrophysiological characterization of juxtavascular and non-juxtavascular astrocytes in the somatosensory cortex of the lesioned brain

To identify potential changes in passive properties of non-juxtavascular and juxtavascular astrocytes induced by a brain lesion, electrophysiological voltage-clamp experiments on somatosensory cortex slices of 7 adult animals (p27-p50) were performed exactly the same way as in paragraph 3.1. The animals were injured with a stab wound lesion in the somatosensory cortex either 1, 3 or 5 days prior to the patch-clamp experiments. For the lesion, a small cranial window was removed from the skull and subsequently a lancet was used to introduce a 0.6 mm deep and 1.0 to 1.5 mm long micro lesion into the parietal cortex parasagittal to the midline (Figure 18a, lesion marked in red). Astrocytes were identified by the green fluorescence of the intracellularly expressed Aldh1l1-eGFP as shown in Figure 18b. To distinguish between non- juxtavascular and juxtavascular astrocytes the blood vessels were visualized by injecting Texas Red® labelled dextran (50 µl) into the tail vein, 10-15 minutes prior to the decapitation of the animals (Figure 18b). Additionally blood vessels were identified by the criteria mentioned in paragraph 3.1. The lesion was easily identifiable with bright field microscopy as seen in Figure 18b and astrocytes surrounding the lesion within a radius of 25 to 275 µm were recorded. In total 33 astrocytes (58 % non-juxtavascular, 42 % juxtavascular) have been analysed in lesioned brains (Figure 18b).

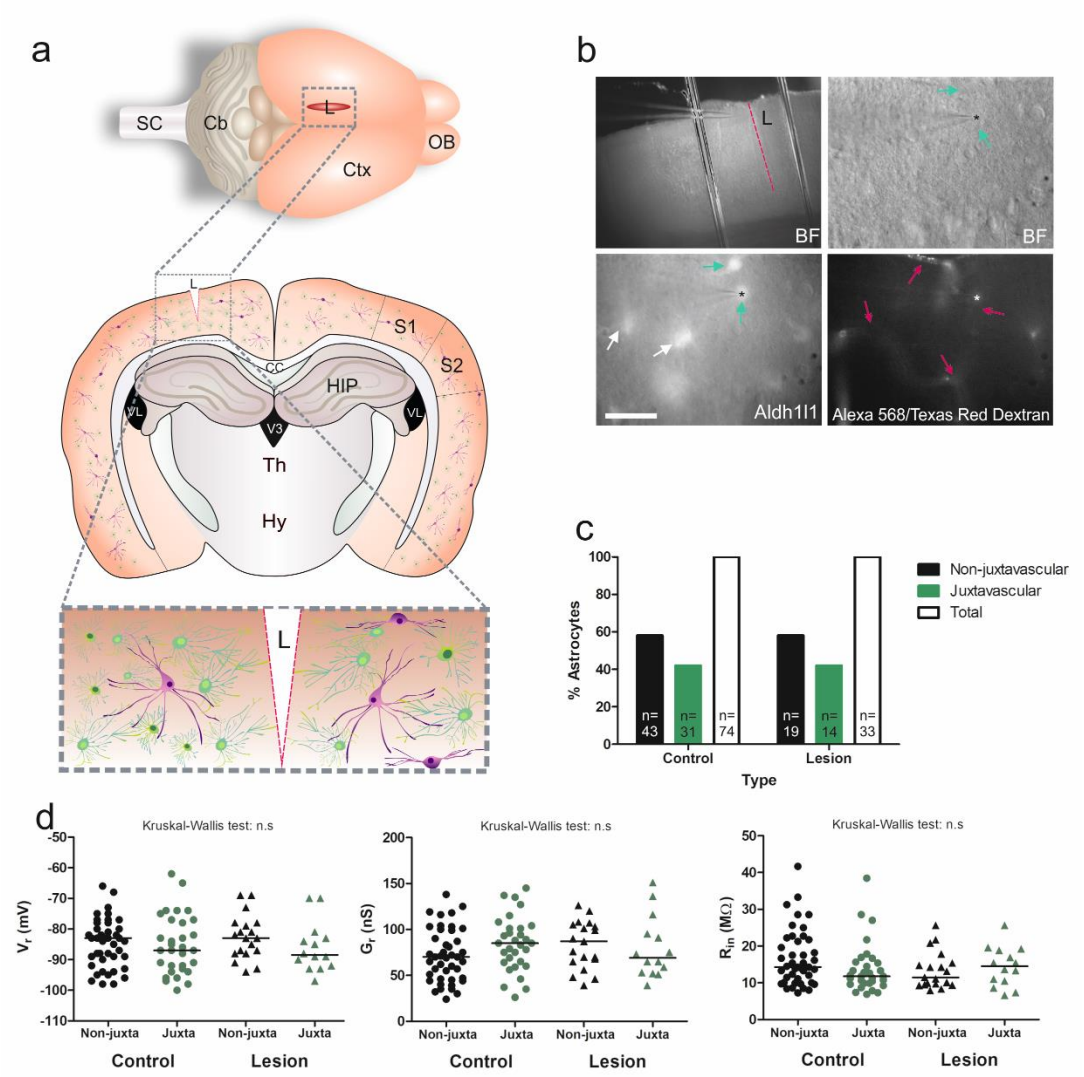

Figure 18: Electrophysiological characterization of juxtavascular and non-juxtavascular astrocytes in the somatosensory cortex after a stab wound lesion

a: Schematic of a mouse brain with a stab wound lesion in the somatosensory cortex (upper picture). The middle picture shows a coronal section through the brain at the level of the lesion. The lower picture depicts a blow up of the lesion and the surrounding cortical tissue. Neurons are shown in lilac, astrocytes in green. Astrocytes surrounding the lesion become reactive (dark green soma, light green nucleus) hypertrophic and polarize towards the lesion. Astrocytes further away from the lesion are not activated (light green soma, dark green nucleus). **SC:** Spinal Cord; **Cb:** Cerebellum; **Ctx:** Cortex; **OB:** Olfactory Bulb; **S1:** Primary Somatosensory Cortex; **S2:** Secondary Somatosensory Cortex; **HIP:** Hippocampus; **VL:** Lateral Ventricle; **V3:** 3rd Ventricle; **Th:** Thalamus; **Hy:** Hypothalamus; **CC:** Corpus Callosum; **L:** Lesion **b:** Coronal section of a lesioned brain at the level of the somatosensory cortex. Left upper picture shows a bright field (BF) overview (scale bar 504 µm) of the lesion (pink dotted line). The other two lines are fibres of the grid. The right BF picture shows the same region magnified (scale bar 29µm). Left lower picture shows the corresponding Aldh1l1-eGFP positive astrocytes. Juxtavascular astrocytes are marked with cyan arrows, non-juxtavascular ones white arrows. Blood vessels are labelled by Texas Red-conjugated dextran (right lower picture red arrows). The patched astrocyte (white asterisk) is filled with Alexa 568 dye delivered through the patch pipette. **c:** In total 33 reactive astrocytes (58 % non-juxtavascular; 42 % juxtavascular) and 74 control cells (58 % non-juxtavascular; 42 % juxtavascular) were analysed. **d:** Comparison of the median V_r of non-juxtavascular (black) and juxtavascular (green) astrocytes of the healthy somatosensory cortex (dots) to astrocytes from lesioned brains (triangles)showed no significant difference (Kruskal-Wallis test: $p = 0.4634$). The same was true or G_r and R_{in} (middle and right graph); (Kruskal-Wallis test: $p = 0.2119$ (for both)).

It has been shown that the peak proliferation of astrocytes surrounding the lesion occurs at 5dpi (Sirko et al., 2015). However, it is possible that changes in ion channel composition and therefore passive electrophysiological properties were already starting prior to induce cell cycle progression. Hence, cells at three different time points post injury (1dpi n = 4, 3dpi n = 4, 5dpi n = 25) were analysed. But, there was no significant difference in the median V_r (Figure 19a; Kruskal-Wallis test: p = 0.8161), G_r (Figure 19b; Kruskal-Wallis test: p = 0.7403) and R_{in} (Figure 19c; Kruskal-Wallis test: p = 0.7403) detected.

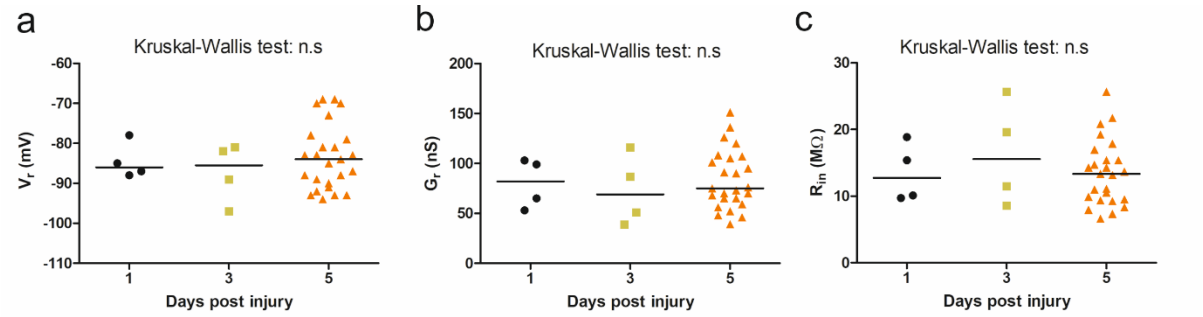

Figure 19: Comparison of passive electrophysiological properties at different time points after a stab wound lesion
Reactive astrocytes were recorded at three different days post injury (1dpi, n = 4; 3dpi, n = 4; 5dpi, n = 25). The comparison shows no significant difference for **a:** V_r (Kruskal-Wallis test: p = 0.8161) **b:** G_r (Kruskal-Wallis test: p = 0.7403) and **c:** R_{in}, (Kruskal-Wallis test: p = 0.7403).

Therefore, patch-clamp recordings were mainly conducted on mice at 5dpi and all reactive astrocytes were pooled together for the following analysis. As juxtavascular astrocytes are more prone to proliferate in response to brain injury, it was determined whether the lesion induced a difference in the passive properties of non-juxtavascular and juxtavascular astrocytes. After a lesion the V_r (Figure 18d, left) of non-juxtavascular (median = -83 mV) and juxtavascular astrocytes (median = -88.5 mV) did not differ significantly within the subclasses of reactive astrocytes, nor when compared to the values of control astrocytes (non-juxtavascular: median = -83 mV; juxtavascular: median = - 87 mV) (Kruskal-Wallis test: p = 0.4634). Regarding the G_r (Figure 18c, middle) of reactive astrocytes the medians of non-juxtavascular cells (median = 87 nS) and juxtavascular ones (median = 69 nS) did not significantly differ. In addition, no significant variations were detected when compared to non-juxtavascular (median = 70 nS) and juxtavascular (median = 85 nS) control astrocytes (Kruskal-Wallis test: p = 0.2119). As expected, the R_{in} (Figure 18c, right) of non-juxtavascular (lesion: median = 11.49 MΩ; control: median = 14.29 MΩ) and juxtavascular (lesion:

median = 14.54 MΩ; control: median = 11.76 MΩ) astrocytes did not vary significantly neither in the lesion nor in comparison to control astrocytes (Kruskal-Wallis test: $p = 0.2119$).

In conclusion, passive electrophysiological properties of somatosensory cortex astrocytes, which became reactive after a stab wound brain lesion, showed a high level of heterogeneity comparable to the situation in unlesioned, healthy control animals. However, this heterogeneity could not be related to whether an astrocyte was non-juxtavascular or juxtavascular in nature. There also was no significant difference in the passive properties of reactive astrocytes compared to non-reactive control ones.

3.2.2 A stab wound lesion in the somatosensory cortex changes the ratio of non-passive to passive astrocytes

Next it was assessed if astrocytes in the lesioned brain also show differences in their passive properties (V_r, G_r, R_{in}) if sorted regarding whether they are non-passive or passive in nature like they did in the healthy brain. 14 juxtavascular and 19 non-juxtavascular astrocytes in the lesioned brain were analysed and compared to the 74 control astrocytes from healthy animals.

After a lesion was introduced into the brain, reactive non-juxtavascular and juxtavascular astrocytes were much more prone to display non-passive current patterns in contrast to control conditions, where most of the astrocytes had passive current patterns (Chi-Square test: $p < 0.0001$). After the stab wound lesion, changes in the ratio of non-passive to passive current patterns could be observed in non-juxtavascular astrocytes, with 53 % of cells showing non-passive current patterns whereas in the control condition only around one third of non-juxtavascular astrocytes (30 %) were non-passive (Figure 20a). Likewise, 64 % of juxtavascular astrocytes were non-passive (Figure 20a) in the lesioned animals. This was in great contrast to astrocytes in the healthy brain, where 81 % of cortical juxtavascular astrocytes showed passive current patterns (Figure 20a). Considering the G_r and the R_{in}, there were clear differences between the groups of astrocytes present (Figure 20c, d; Kruskal-Wallis test: $p < 0.0001$). Non-juxtavascular non-passive and passive astrocytes differed significantly from each other (Mann-Whitney test: $p = 0.0003$; Bonferroni: alpha corrected = 0.0125). In contrast, the V_r of the different subgroups was not significantly different (Figure 20b; Kruskal-Wallis

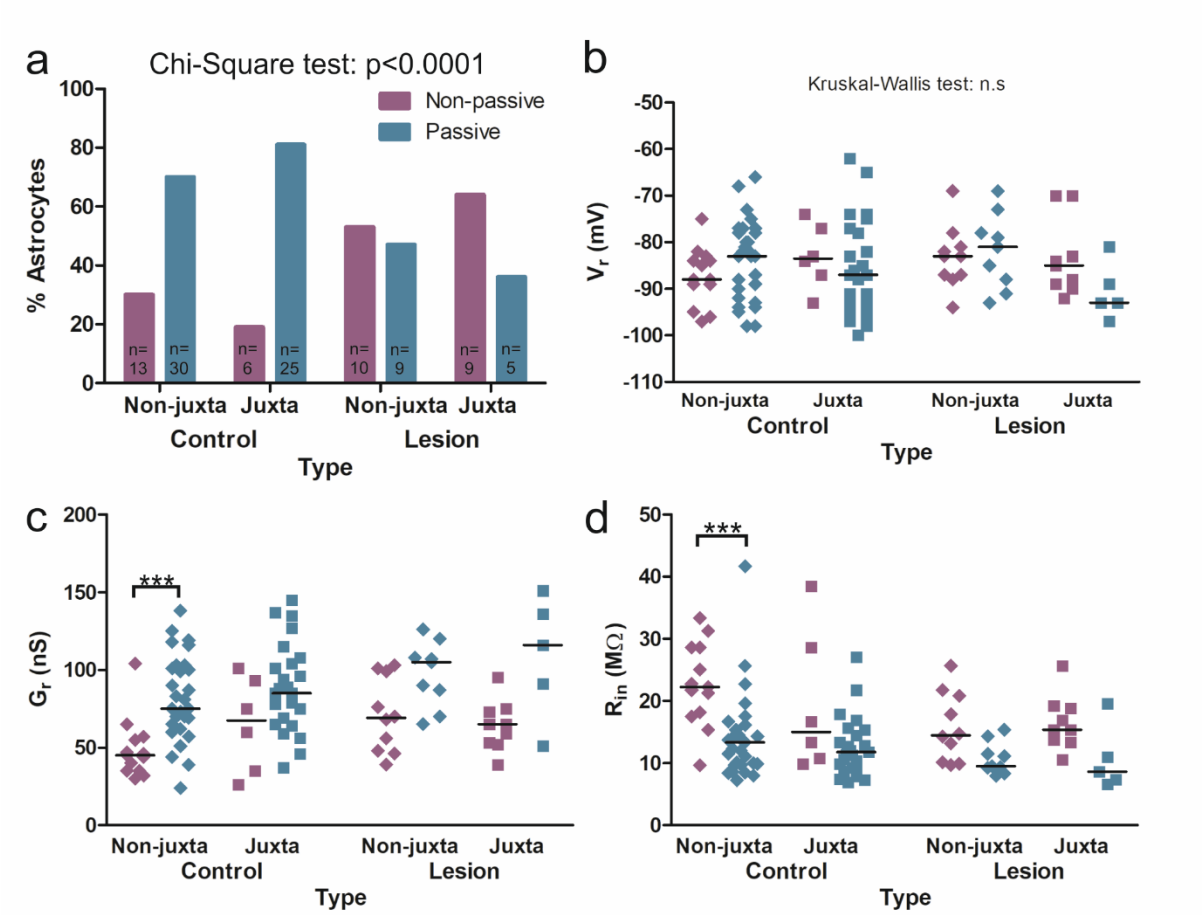

Figure 20: Comparison of non-juxtavascular and juxtavascular astrocytes regarding non-passive and passive current patterns under control conditions and after a stab wound lesion
a: 74 control astrocytes (43 non-juxtavascular, 31 juxtavascular astrocytes) and 33 reactive astrocytes (19 non-juxtavascular, 14 juxtavascular) from lesioned brains were sorted according to their current pattern. Non-passive cells are shown in rose; passive ones are coded in blue. In the healthy brain (control) 30 % of non-juxtavascular astrocytes displayed non-passive and 70 % passive current patterns. 19 % of juxtavascular astrocytes displayed non-passive and 81 % passive current patterns. In lesioned brains 53 % of non-juxtavascular and 64 % of juxtavascular astrocytes had non-passive current patterns. 47 % of reactive non-juxtavascular and 36 % reactive juxtavascular astrocytes displayed passive current patterns. A Chi-square test showed that the subgroups are significantly different ($p < 0.0001$). **b:** Comparison of the V_r of non-passive (rose) and passive (blue) non-juxtavascular (rhombus) and juxtavascular astrocytes (squares) of lesioned and healthy animals showed no significant difference in (Kruskal-Wallis test: $p = 0.3433$). **c:** Comparison of the G_r of non-passive (rose) and passive (blue) non-juxtavascular (rhombus) and juxtavascular (squares) astrocytes of lesioned and healthy animals showed a significant difference (Kruskal-Wallis test: $p < 0.0001$) between non-juxtavascular non-passive and passive control astrocytes (Mann-Whitney test: $p = 0.0003$). **d:** The R_{in} of non-passive (rose) and passive (blue) non-juxtavascular (rhombus) and juxtavascular (squares) astrocytes in lesioned animals and under control conditions was significantly different (Kruskal-Wallis test: $p < 0.0001$ between non-juxtavascular non-passive and passive control astrocytes (Mann-Whitney test: $p = 0.0003$).

test: $p = 0.3433$). Compared to the control condition, in which non-juxtavascular non-passive and passive astrocytes were significantly different in respect to the G_r and the R_{in} (Figure 20c, d), these astrocytes seemed to lose their dissimilarity due to the brain lesion.

Summarizing, astrocytes that became reactive after a stab wound lesion were more prone to display non-passive current patterns than non-reactive astrocytes in the healthy brain.

Since no difference in ion channel expression between non-juxtavascular and juxtavascular astrocytes was found in the healthy brain it was of great interest to consider whether the stab wound lesion induced a difference in ion channel expression in reactive non-juxtavascular and juxtavascular somatosensory cortex astrocytes and if a relationship between proliferation and ion channel expression could be detected.

3.2.3 K_{ir}4.1 channels are downregulated in proliferating astrocytes after stab wound lesion

In paragraph 3.1.3 it has been shown that K_{ir}4.1 channels were homogenously expressed in astrocytes of the healthy somatosensory cortex and there was no difference in the expression pattern between non-juxtavascular and juxtavascular astrocytes. Therefore, the same anti-K_{ir}4.1 antibody that was previously used in the healthy brain was applied after a stab wound lesion was introduced and paired with TL 649 for blood vessels labelling. Additionally, an anti-Ki67 antibody that labels proliferating cells in all phases of the cell cycle except for the M-phase was applied. Figure 21a shows detailed confocal images of a stab wound lesion in the somatosensory cortex of an Aldh1l1-eGFP mouse 5dpi. As TL 649 not only labels the vasculature but also rodent microglia cells (Mazzetti et al., 2004), a high amount of activated microglia can be seen infiltrating the lesion site (Figure 21a). Many non-proliferating reactive astrocytes (both non-juxtavascular and juxtavascular) were positive for anti-K_{ir}4.1 (white arrows) comparable to control conditions. Moreover, proliferating (anti-Ki67 positive) non-juxtavascular and juxtavascular astrocytes were found that were additionally positive for anti-K_{ir}4.1 (dashed double arrows). There were also proliferating non-juxtavascular and juxtavascular astrocytes present, that showed little to no labelling with anti-K_{ir}4.1 (asterisk) even up to the point where it looks like “holes” in the tissue in the anti-K_{ir}4.1 staining (dashed encircling). Comparing these empty spots to the Aldh1l1-eGFP fluorescence clearly showed that these astrocytes were in fact present and occupying their astrocytic domain but had lost their positivity for anti-K_{ir}4.1. Moreover there was evidence that proliferating astrocytes vary in the amount of K_{ir}4.1 expression.

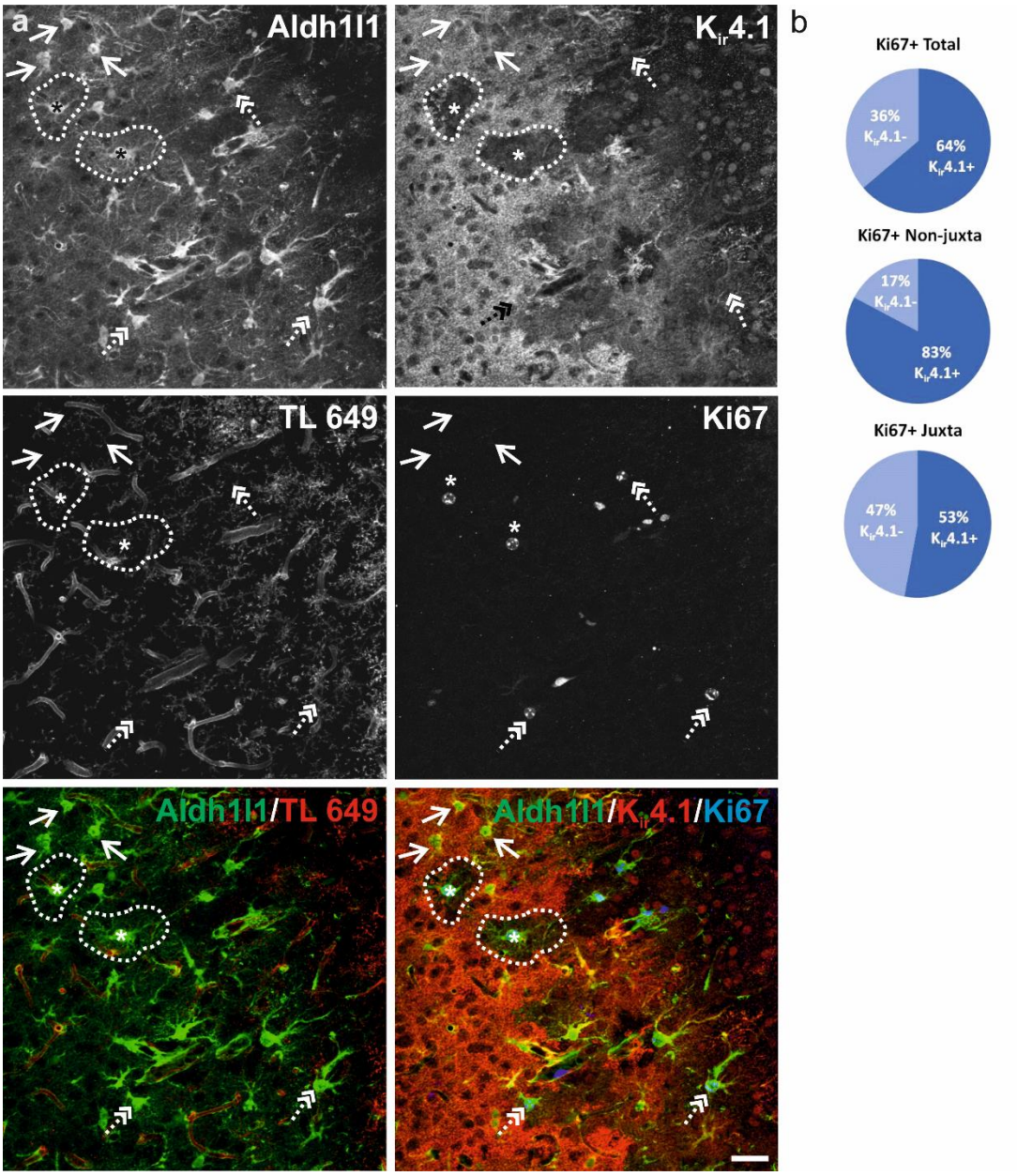

Figure 21: K$_{ir}$4.1 channels are downregulated in a fraction of proliferating reactive astrocytes 5dpi
a: Confocal maximum z-projection (optical sections 1-27) of a lesioned hemisphere 5dpi in an adult (p51) Aldh1l1-eGFP transgenic mouse. The four upper pictures show the Aldh1l1-eGFP expressing astrocytes, the anti-K$_{ir}$4.1 staining, blood vessels and activated microglia (TL 649) and the proliferation marker anti-Ki67. The left lower picture shows an overlay of Aldh1l1-eGFP positive astrocytes (green) and the blood vessels and activated microglial cells (red). The right overlay shows Aldh1l1-eGFP positive astrocytes (green), the anti-K$_{ir}$4.1 staining (red) and the anti-Ki67 positive proliferating nuclei (blue). Arrows indicate non-juxtavascular and juxtavascular non-proliferating astrocytes positive for anti-K$_{ir}$4.1. Dashed double arrows point to non-juxtavascular and juxtavascular astrocytes double positive for anit-K$_{ir}$4.1 and anti-Ki67. Anti-K$_{ir}$4.1 negative but anti-Ki67 positive astrocytes are marked with an asterisk. Dashed circle highlights the astrocytic domain of two anti-K$_{ir}$4.1 negative proliferating astrocytes. Scale bar 38µm. **b:** Proliferating anti-Ki67 positive non-juxtavascular and juxtavascular astrocytes were counted in two lesioned Aldh1l1-eGFP mice (p51) 5dpi. Out of 80 proliferative cells 64 % were positive for anti-K$_{ir}$4.1. Out of 29 proliferative non-juxtavascular astrocytes 83 % were labelled by anti-K$_{ir}$4.1. Out of 51 juxtavascular proliferative astrocytes 53 % remained positive for anti-Kir4.1.

For quantification, proliferating anti-Ki67 positive astrocytes (n = 80) were counted in two lesioned mice 5dpi and contemplated regarding their anti-K_{ir}4.1 positivity as well as their position towards blood vessels. In total 64 % of proliferating (anti-Ki67 positive) astrocytes were positive for anti-K_{ir}4.1 (Figure 21b, upper pie chart). When proliferating astrocytes were sorted according to whether they were non-juxtavascular or juxtavascular in nature, it became clear that the majority (83 %) of proliferating non-juxtavascular astrocytes expressed K_{ir}4.1 (Figure 21b, middle pie chart). Interestingly, only 53 % of proliferating juxtavascular astrocytes were positive for anti-K_{ir}4.1 (Figure 21b, lower pie chart).

Summarizing, a fraction of proliferating (anti-Ki67 positive) astrocytes downregulated K_{ir}4.1 of which the majority were juxtavascular ones

3.2.4 K_{ir}6.2 show the same heterogeneous distribution 5dpi like in control conditions

To determine whether there was a change in K_{ir}6.2 channel expression 5dpi compared to the heterogeneity present under control conditions (see paragraph 3.1.4) immunohistochemical stainings were performed with anti-K_{ir}6.2 antibodies in somatosensory cortex slices of lesioned adult Aldh1l1-eGFP mice (5dpi; Figure 22). The anti-K_{ir}6.2 staining was paired with TL 649 for blood vessels labelling and the proliferation marker anti-Ki67 was used. Like in Figure 21a TL 649 showed extensive labelling of activated microglia infiltrating the lesion site in addition to blood vessel labelling (Figure 22). Comparable to the findings under control conditions the anti-K_{ir}6.2 positivity was present on non-juxtavascular as well as juxtavascular non–proliferating astrocytes (Figure 22, arrows). Moreover, there were also non-proliferating anti-K_{ir}6.2 negative non-juxtavascular and juxtavascular astrocytes (hollow arrows) present surrounding the lesion which was in line with the heterogeneous expression found in control conditions. Proliferating (anti-Ki67 positive) non-juxtavascular and juxtavascular astrocytes that were also labelled by anti-K_{ir}6.2 (dashed double arrows) could be detected. In contrast to control conditions where anti-K_{ir}6.2 was predominantly visible on astrocytic processes, the localisation of K_{ir}6.2 channels seemed to shift to the somata of astrocytes.

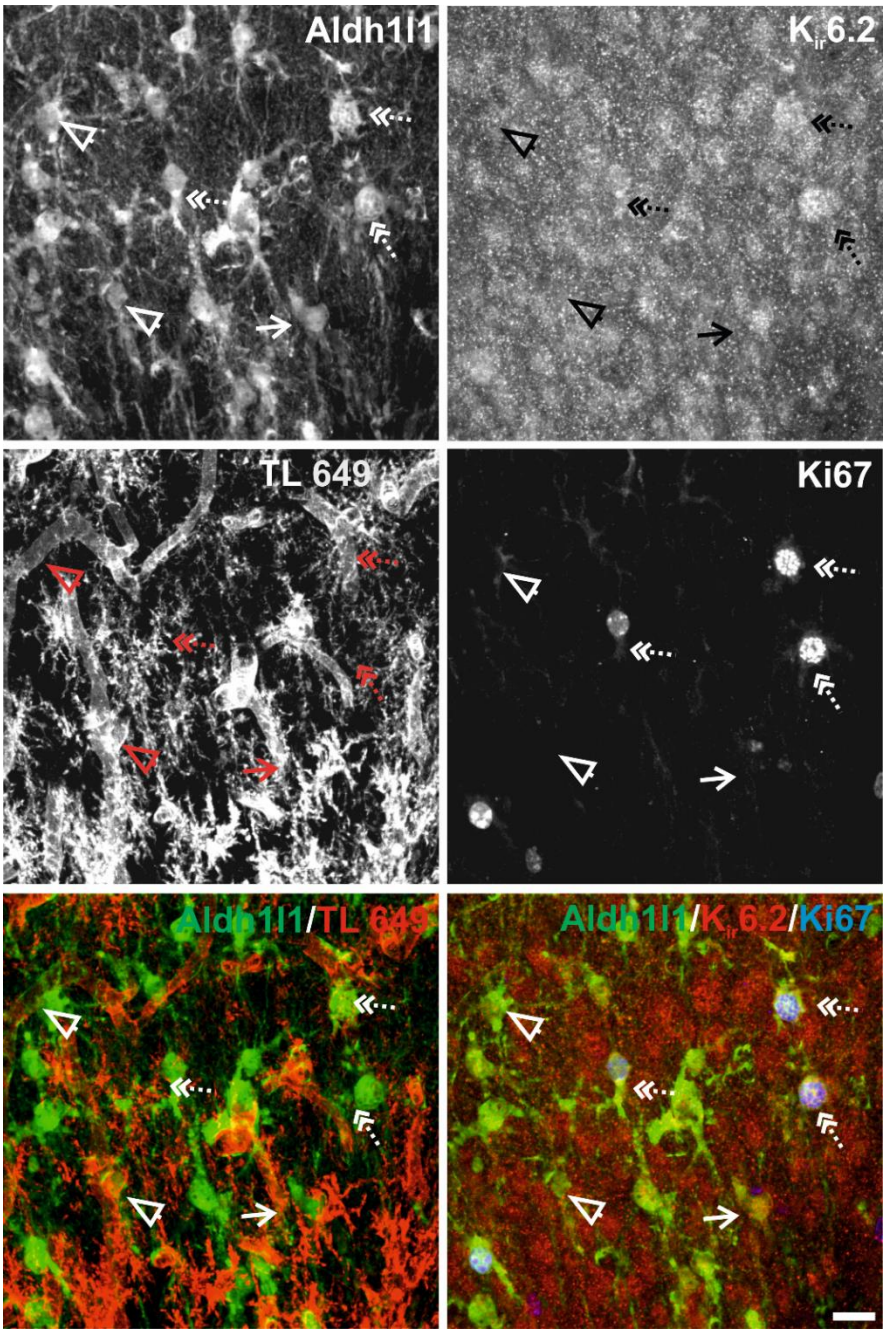

Figure 22: The channel K_{ir}6.2 channel show the same heterogeneous distribution 5dpi as in control conditions

Confocal maximum z-projection (optical sections 5-35) of a lesioned hemisphere 5dpi in an adult (p51) Aldh1l1-eGFP mouse. The four upper pictures show the Aldh1l1-eGFP expressing astrocytes, the anti-K_{ir}6.2 staining, blood vessels and activated microglia (TL 649) and the proliferation marker anti-Ki67. The left lower picture shows an overlay of Aldh1l1-eGFP positive astrocytes (green) and the blood vessels and activated microglial cells (red). The right overlay shows Aldh1l1-eGFP positive astrocytes (green), the anti-K_{ir}6.2 staining (red) and anti-Ki67 positive proliferating nuclei (blue). Arrows indicate non-juxtavascular and juxtavascular non-proliferating astrocytes positive for anti-K_{ir}6.2. Dashed double arrows point to non-juxtavascular and juxtavascular astrocytes double positive for anit-K_{ir}6.2and anti-Ki67. Astrocytes that show no K_{ir}6.2 labelling and are negative for anti-Ki67 are marked by hollow arrows. Scale bar 19µm.

Overall the heterogeneity of $K_{ir}6.2$ in astrocytes was maintained after a stab wound lesion with no difference between non-juxtavascular and juxtavascular astrocytes. Also proliferation seemed to have no impact on $K_{ir}6.2$ expression.

3.2.5 Heterogeneous expression of $K_v4.3$ channels is preserved in lesioned mice 5dpi

In paragraph 3.1.5 it has been shown that $K_v4.3$ ion channels are heterogeneously expressed in astrocytes of the healthy somatosensory cortex. This heterogeneity was independent of the position of astrocytic somata towards the vasculature and the cortical layer they resided in. To determine whether the same was true after a stab wound lesion was inflicted into the somatosensory cortex immunohistochemistry with anti-$K_v4.3$ was performed in combination with TL 649 for blood vessels labelling and the proliferation marker anti-Ki67 on Aldh1l1-eGFP mice 5dpi (Figure 23). Again TL 649 showed extensive labelling of activated microglia infiltrating the lesion site in addition to blood vessel labelling (Figure 23). Comparable to control conditions, non-juxtavascular and juxtavascular non-proliferating astrocytes could be found that were labelled with anti-$K_v4.3$ (Figure 23, arrows) as well as astrocytes that were negative for anti-$K_v4.3$ (hollow arrows). Moreover, there were proliferating anti-Ki67 positive non-juxtavascular and juxtavascular astrocytes present that were positive for anti-$K_v4.3$ (dashed double arrows) as well as proliferating astrocytes that were negative for anti-$K_v4.3$ (asterisk). This was in line with the heterogeneity of $K_v4.3$ seen under control conditions. Interestingly, more intense anti-$K_v4.3$ labelling was observed in some polarized astrocytic processes, which might be due to an upregulation of $K_v4.3$ in certain astrocytes or be the result of hypertrophy in this processes. This observation could neither be related to whether astrocytes were non-juxtavascular or juxtavascular nor to proliferation.

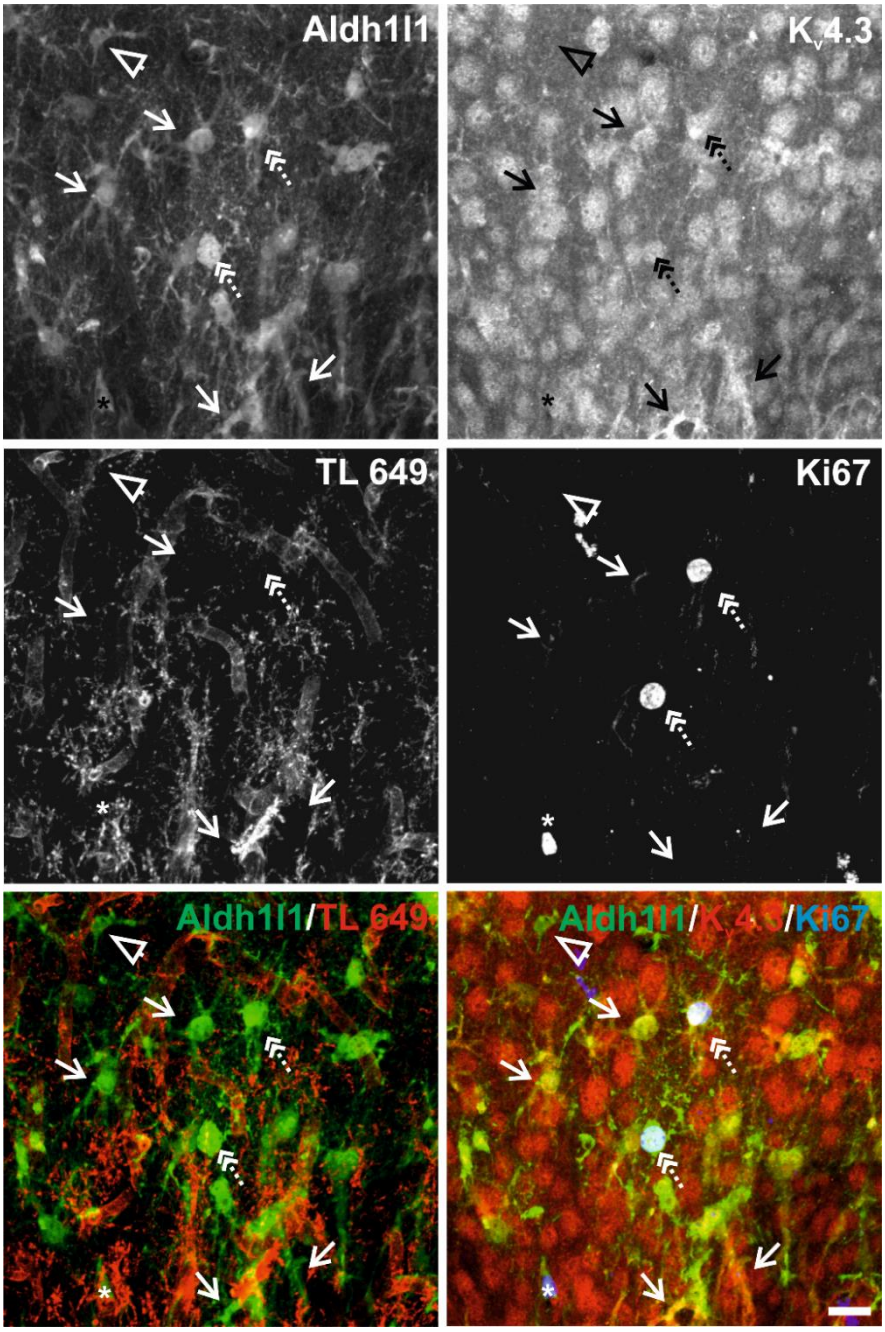

Figure 23: The K_v4.3 channel show the same heterogeneous distribution 5dpi as in control conditions
Confocal maximum z-projection (optical sections 15-51) of a lesioned hemisphere 5dpi in an adult (p51) Aldh1l1-eGFP mouse. The four upper pictures show the Aldh1l1-eGFP expressing astrocytes, the anti-K_v4.3 staining, the blood vessels and activated microglia (TL 649) and the proliferation marker anti-Ki67. The left lower picture shows an overlay of Aldh1l1-eGFP positive astrocytes (green) and blood vessels and activated microglial cells (red). The right overlay shows Aldh1l1-eGFP positive astrocytes (green), the anti-K_v4.3 staining (red) and the anti-Ki67 positive proliferating nuclei (blue). Arrows indicate non-juxtavascular and juxtavascular non-proliferating astrocytes positive for anti-K_v4.3. Dashed double arrows point to non-juxtavascular and juxtavascular astrocytes double positive for anit-K_v4.3 and anti-Ki67. Proliferative astrocytes that are negative for K_v4.3 are marked with an asterisk. Astrocytes that show no K_v4.3 labelling and are negative for anti-Ki67 are marked by hollow arrows. Scale bar 19µm.

3.2.6 HCN2 becomes upregulated in a subset of astrocytes at 5dpi

As already mentioned before, it has been shown that reactive astrocytes upregulate the expression of certain sets of HCN channels that give rise to so called I_h currents weeks after ischemia (Honsa et al., 2014). The previous immunohistochemical findings in this study confirmed the presence of the HCN1 channel in healthy control animals (see paragraph 3.1.8.). Next it was of great interest to see if a stab wound lesion would induce an upregulation in HCN channels already 5dpi. Therefore immunohistochemical stainings for HCN1, HCN2 and HCN3 channel were done on somatosensory cortex slices of lesioned adult Aldh1l1-eGFP mice (5dpi). For the HCN1 channel which was heterogeneously expressed in astrocytes of the healthy brain no changes in the expression pattern was found 5dpi (data not shown). The HCN3 channel was neither expressed in astrocytes under control conditions nor after a stab wound lesion (5dpi; data not shown). Regarding the HCN2 channel which was not detectable in astrocytes in the healthy somatosensory cortex (Figure 24a, hollow arrows) an upregulation of said ion channel in a subset of reactive astrocytes was observed 5dpi (Figure 24b). The HCN2 staining was paired with TL 649 for blood vessels labelling and the proliferation marker anti-Ki67. As above TL 649 showed extensive labelling of activated microglia infiltrating the lesion site in addition to blood vessel labelling. In stark, contrast to control conditions intense upregulation of HCN2 channels was seen in processes of certain reactive, polarizing astrocytes (Figure 24b). Anti-HCN2 labelling was present in processes of non-juxtavascular and juxtavascular non-proliferating astrocytes (arrows). Nevertheless, there were also anti-HCN2 negative non-juxtavascular and juxtavascular astrocytes present (hollow arrows) suggesting a heterogeneous expression of HCN2 channels after a stab wound lesion. Regarding anti-Ki67 positive proliferating astrocytes, anti-HCN2 labelling was also heterogeneous with some proliferating astrocytes expressing HCN2 channels whereas others were negative for anti-HCN2 (asterisks).This did not depend on the location astrocytic somata had relative to blood vessels.

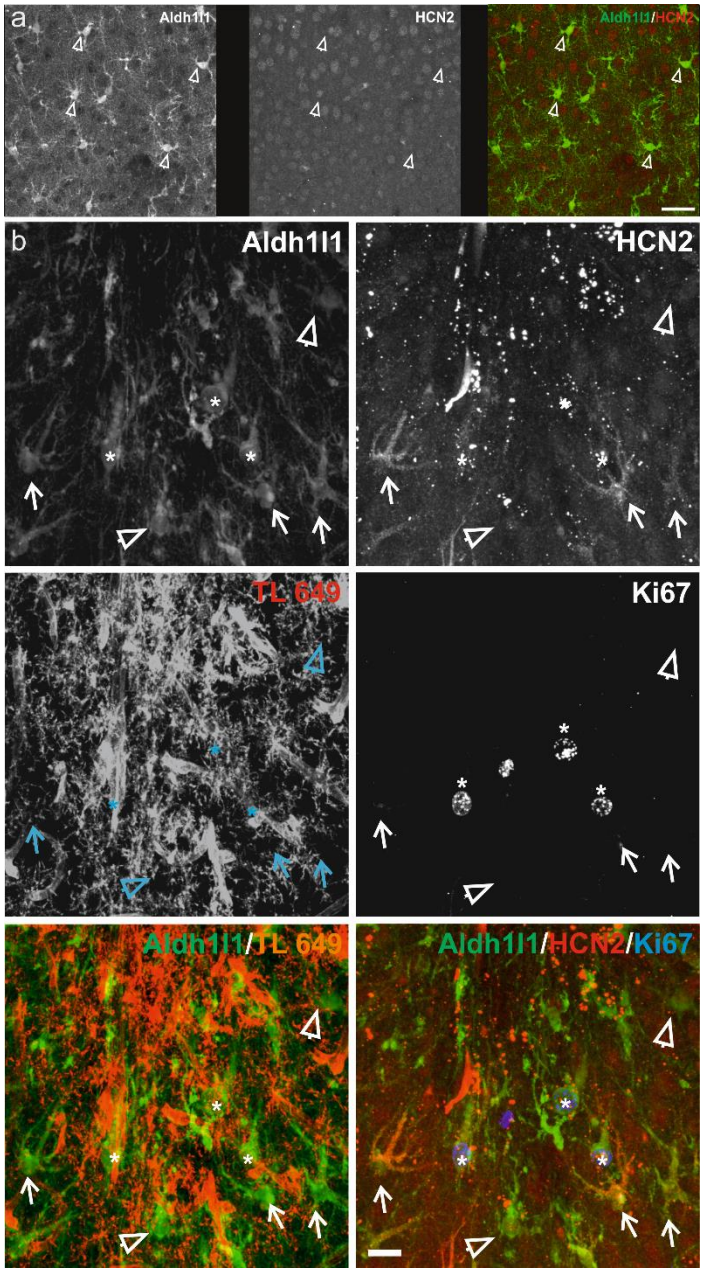

Figure 24: HCN2 channels become upregulated in a subset of reactive astrocytes 5dpi
a: Confocal maximum z-projection (all optical sections) of a control hemisphere in an adult (p51) Aldh1l1-eGFP mouse. From left to right the Aldh1l1-eGFP expressing astrocytes and the anti-HCN2 staining are shown. The right image shows an overlay of the two single channels with Aldh1l1-eGFP positive astrocytes (green) and anti-HCN2 (red). Astrocytes showed no sign of anti-HCN2 positivity indicated by hollow arrows. Anti-HCN2 positive neurons were present. Scale bar 41µm. **b:** Maximum z-projection (optical sections 10-33) of a close up of astrocytes surrounding the lesion in an adult (p51) Aldh1l1-eGFP mouse at 5dpi. The four upper pictures show Aldh1l1-eGFP expressing astrocytes, the anti-HCN2 staining, blood vessels and activated microglia (TL 649) and the proliferation marker anti-Ki67. Left lower picture shows an overlay of Aldh1l1-eGFP positive astrocytes (green) and blood vessels and activated microglial cells (red). Right overlay shows Aldh1l1-eGFP positive astrocytes (green), the anti-HCN2 staining (red) and the anti-Ki67 positive proliferating nuclei (blue). Arrows indicate non-juxtavascular and juxtavascular non-proliferating astrocytes labelled by anti-HCN2. Proliferative astrocytes that are negative for anti-HCN2 are marked with an asterisk. Astrocytes that show no anti-HCN2 labelling and are negative for anti-Ki67 are marked with hollow arrows. Scale bar 19µm.

4 Discussion

The aim of this doctoral thesis was to characterize non-juxtavascular and juxtavascular astrocytes regarding their ion channel expression pattern and electrophysiological properties to analyse if there are differences present between the two astrocyte subsets that might be responsible for their differential reaction to traumatic events. This discussion will elaborate the findings in the healthy somatosensory cortex, which show that the two subgroups are not inherently different regarding their ion channel expression pattern. Moreover, the results gathered in the two astrocyte subgroups after a stab wound lesion was inflicted will be elaborated and compared to the healthy control brain. Astrocytes transition from mainly passive current response patterns, which are present in non-reactive healthy somatosensory cortex astrocytes, to non-passive current response patterns, when they become reactive in response to traumatic brain injury. Moreover, the shift in ion channel expression patterns in response to traumatic brain injury will be elucidated and critically examined in the context of proliferation.

4.1 Passive electrophysiological properties of non-juxtavascular and juxtavascular astrocytes before and after a lesion

In this study, the passive electrophysiological properties V_r (resting membrane potential), G_r (resting membrane conductance) and R_{in} (input resistance) were used to define whether there are differences present between non-juxtavascular and juxtavascular astrocytes. In the healthy brain the two astrocyte subtypes did not differ significantly regarding any of these passive properties (Figure 6d). However, great heterogeneity in V_r, G_r and R_{in} could be observed between single astrocytes of both groups (Figure 6d). The V_r lay between -100 mV and - 62 mV with the median of both subtypes being more negative than - 80mV. This suggests a dominant role of inwardly rectifying K^+ channels of the $K_{ir}4.1$ type in the majority of somatosensory cortex astrocytes as these channels maintain a V_r close to the K^+ equilibrium potential (E_K) of around -80 mV. (Mishima et al., 2007; Seifert et al., 2009; Mishima & Hirase, 2010; Dallérac et al., 2013; Verkhratsky & Nedergaard, 2015, 2018). This is well known from Bergman glia as well as astrocytes in the neocortex, hippocampus, the medial nucleus of the trapezoid body (MNTB) and the lateral superior olive (LSO) (Clark & Barbour, 1997; Matthias et al., 2003; Zhou, 2005; Houades et al., 2008; Kafitz et al., 2008; Müller et al., 2009; Seifert

et al., 2009; Reyes-Haro et al., 2010; Uwechue et al., 2012; Stephan & Friauf, 2014). Even if the median V_r in somatosensory cortex astrocytes was hyperpolarised, the great heterogeneity between the cells is not completely in line with the very negative astrocytic V_rs that are reported for most astrocytes. However, in contrast to other studies, in which astrocytes with depolarised membrane potentials are excluded, here it was decided to include all astrocytes that showed stable recordings over time. This prevented the exclusion of astrocytes with a more depolarized V_r. McKhann et al. (1997) critically discussed studies that excluded astrocytes with a depolarized V_r and were able to show that cultured neocortical rat astrocytes, as well as astrocytes in hippocampal slices of rats showed great heterogeneity in V_r independent of external and developmental factors. They propose that variations in V_r stem from dynamic changes in cell coupling that help and facilitate spatial K^+ buffering (McKhann et al., 1997). Studies in the rodent optic nerve also show heterogeneous and depolarized resting membrane potentials in mature astrocytes that seem to be caused by protein kinase A (PKA) and cAMP (Bolton et al., 2006).

G_r and its inverse R_{in} were used as other passive electrophysiological parameters to compare non-juxtavascular and juxtavascular astrocytes. The same as for V_r, also G_r and R_{in} did not differ between non-juxtavascular and juxtavascular astrocytes and showed great heterogeneity amongst single astrocytes (Figure 6d). Both astrocyte subgroups had a very low R_{in} (Figure 6d), which is in line with literature (Zhou, 2005; Kafitz et al., 2008; Seifert et al., 2009; Ma et al., 2014; Stephan & Friauf, 2014). The underlying cause of the high G_r and very low R_{in} is the high amount of K_{ir}4.1 channels present in astrocytic membranes (Mishima et al., 2007; Mishima & Hirase, 2010; Dallérac et al., 2013). The heterogeneity observed in my study, might be attributed to the various functions these cells have to perform, as well as to different ion channel and transmitter receptor expression, a variance in morphology and the different cortical layers they are residing in (Matyash & Kettenmann, 2010). Furthermore, the heterogeneity in gap-junctional coupling between astrocytes, which leads to isopotentiality in astrocytic networks, has to be considered (Ma et al., 2016). It has also been shown by clonal *Star Track* analysis in mice, that the clonal identity of an astrocyte defines heterogeneity in cortical astrocytes. For example astrocytes of different lineage origin are arranged in specific cortical domains (García-Marqués & López-Mascaraque, 2013). It might be possible, that

astrocytes of a specific clonal origin also possess special electrophysiological features that delineate them from other clones.

After a stab wound lesion, V_r, G_r and R_{in} did not differ significantly between non-juxtavascular and juxtavascular reactive astrocytes. Moreover, they were similar compared to the ones from healthy control conditions (Figure 18d). It has been shown that reactive astrocytes in the hippocampus of rats have a depolarized V_r already 3 days after an ischemic event caused by a downregulation of $K_{ir}4.1$ ion channels in these cells (Pivonkova et al., 2010). This downregulation would also result in smaller G_r and higher R_{in} values which was not observed here. Another study showed that 5 weeks after global cerebral ischemia in rats, the V_r of astrocytes is depolarized accompanied by an increase in the cells´ R_{in} (Honsa et al., 2014). In mice that suffer from focal cerebral ischemia, V_r was also depolarized, while R_{in} decreased significantly (Honsa et al., 2014). However, it might be possible, that $K_{ir}4.1$ channels are not the only K^+ conducting channels that contribute to the negative V_r of astrocytes and that other ion channels are able to mask the effect of $K_{ir}4.1$ loss (Ferroni et al., 2003; Kucheryavykh et al., 2006; Djukic et al., 2007; Kucheryavykh et al., 2009). Also, it is important to keep in mind that the previously discussed results stem from experiments where astrocytes become reactive due to an ischemic event, while here astrocyte reactivity was induced by a stab wound lesion. It is known that astrocytes react differently depending on the underlying cause of an injury as well as the severity of the insult (Sofroniew & Vinters, 2010). Moreover, scratch wound assays in rat spinal cord astrocyte cultures trigger proliferation of astrocytes, accompanied by a downregulation of $K_{ir}4.1$ currents as well as an upregulation of outwardly rectifying currents resulting in a more depolarized V_r compared to non-proliferating astrocytes (MacFarlane & Sontheimer, 1997). However, spinal cord astrocytes and astrocytes in the somatosensory cortex might react differently. As mentioned above, astrocytes of different lineage origin are arranged in specific cortical domains (García-Marqués & López-Mascaraque, 2013). It has been shown via clonal *Star Track* analysis that astrocytes of different clonal origin react differently to mechanical cortical injury in mice. Even astrocytes with the same clonal background show dissimilar responses. This suggests that the astrocytic response to injury is depending on intrinsic as well as extrinsic factors (Martín-López et al., 2013).

Most importantly, here (for electrophysiological recordings), I did not differentiate between proliferating and non-proliferating reactive astrocytes. Astrocytes were sorted according to their location towards the vasculature, meaning that reactive non-proliferating non-juxtavascular and juxtavascular astrocytes were mixed with proliferating ones. In future experiments it would be of great interest to compare reactive proliferating astrocytes to their reactive non-proliferating counterparts. This would especially be important, because as previously elaborated in the introduction, a negative V_r is linked to the incapability of a cell to enter the cell cycle while a depolarized V_r promotes cell cycle progression and hence proliferation (Blackiston et al., 2009).

4.2 Homogeneous K_{ir}4.1 expression is lost in a subset of astrocytes that proliferate after a stab wound lesion

As discussed in the previous paragraph, it might be possible that not in all of the astrocytes that were recorded in somatosensory cortex of Aldh1l1-eGFP mice, K_{ir}4.1 channels are the dominating K^+ conducting channels. This could explain why non-juxtavascular and juxtavascular astrocytes in the somatosensory cortex did not differ significantly regarding their passive properties but showed great all over heterogeneity.

Therefore, I performed Ba^{2+} (200 µM) blocking experiments on both astrocyte subtypes to show whether K_{ir}4.1 channels are the dominating ion channels in cortical astrocytes, as well as to clarify if there are differences in K_{ir}4.1 expression between the two respective groups in the healthy brain (Figure 7). Ba^{2+} interacts with K_{ir}4.1 channels in the deep binding site of the pore, where only a single ion is capable of blocking the whole channel (Standen & Stanfield, 1978; Shieh et al., 1998). The majority of non-juxtavascular and juxtavascular astrocytes were sensitive to Ba^{2+} showing decreased K_{ir}4.1 currents accompanied by a tendency towards a more positive V_r (Figure 7b) and a decrease in G_r (Figure 7c). These findings were reinforced by immunohistochemistry performed on healthy control somatosensory cortex slices. I found, that mature astrocytes in somatosensory cortex express the inwardly rectifying K_{ir}4.1 ion channel homogenously independent of their somal position towards blood vessels and across all cortical layers (Figure 8 and 9). This is in accordance with literature, where it has been shown that K_{ir}4.1 ion channels are the dominating channel type defining the membrane conductance of astrocytes in the hippocampus, cerebellum and in the ventral horn of the spinal cord of

rodents (Steinhäuser et al., 1992; Müller et al., 1994; Chvátal et al., 1995; Pastor et al., 1995; Olsen et al., 2007; Seifert et al., 2009). Moreover, especially astrocytic processes are excessively labelled by anti-K_{ir}4.1 showing that non-juxtavascular and juxtavascular astrocytes analysed here represent mature astrocytes. It is known that there is a developmentally regulated shift from somatic expression of said ion channel towards the processes between postnatal day 0 to 60 in rats (Moroni et al., 2015), which is also accompanied by an increase in K_{ir}4.1 channel density in mice (Seifert et al., 2009). However, other studies also suggest important roles of two-pore-domain potassium channels of the TWIK-1 and TREK-1 subtype for the passive conductance of mature astrocytes at least in the hippocampus of rodents (Seifert et al., 2009; Zhou et al., 2009). K_{ir}4.1 channel expression is known to be positively correlated with end-differentiated cells and therefore seems to influence the proliferative potential (Sontheimer et al., 1989; Barres et al., 1990; MacFarlane & Sontheimer, 1997, 2000; Olsen & Sontheimer, 2004). The results discussed above clearly indicate that if a difference in K_{ir}4.1 expression between non-juxtavascular and juxtavascular astrocytes would be involved in their distinct proliferative behaviour after brain injury, this must occur after the traumatic event has happened.

Five days after a stab wound lesion was introduced into the brain the homogeneous expression of K_{ir}4.1 channels, present under control conditions, was disrupted. 36 % of all proliferating reactive astrocytes completely downregulated K_{ir}4.1 channel expression (Figure 21b and Figure 25b, c). Only 17 % of proliferating non-juxtavascular astrocytes lost their K_{ir}4.1 positivity while 47 % of proliferating juxtavascular astrocytes completely lacked K_{ir}4.1 (Figure 21b). In rat spinal cord cultures proliferating BrdU+ astrocytes are known to show a reduction in V_r, G_r as well as an increase in R_{in} attributed to K_{ir}4.1 downregulation, suggesting that this change is crucial for cell proliferation (MacFarlane & Sontheimer, 1997). The results in my study are in line with these findings leading to the conclusion that also in cortical astrocytes the reduction of K_{ir}4.1 seems to be essential for cell proliferation (Figure 25). Also other studies have previously described a downregulation of K_{ir}4.1 ion channels in reactive astrocytes. Seven days after crush spinal cord injury in adult rats, K_{ir}4.1 protein expression was found to be downregulated by up to 80 % in reactive astrocytes surrounding the lesion site; a change that persists up to four weeks post injury (Olsen et al., 2010). Additionally, RT-PCR and immunoblot results proved that in the pericontusional ipsilateral cerebral cortex in mice K_{ir}4.1

channels were downregulated as a function of time after injury (Gupta & Prasad, 2013). In both studies, in addition to a decrease in $K_{ir}4.1$ expression, a downregulation of the glutamate transporter GLT-1 was found (Olsen et al., 2010; Gupta & Prasad, 2013). As $K_{ir}4.1$ ion channels and the GLT-1 transporter are known to work together to prevent excitotoxicity in the CNS, the authors suggested that this downregulation would have detrimental effects after a lesion. It has also been reported that already 3 days after an ischemic event reactive astrocytes in the hippocampus of rats downregulated $K_{ir}4.1$ channels accompanied by depolarisation in these cells (Pivonkova et al., 2010).

Proliferating astrocytes that still expressed $K_{ir}4.1$ in their membrane, varied strongly in their intensity for anti- $K_{ir}4.1$ positivity (Figure 21a and Figure 25). One might speculate that these astrocytes were in a different phase of the cell cycle, where $K_{ir}4.1$ downregulation was still in progress. While cells are known to still be hyperpolarised at the transition from G1- into the S-phase, depolarisation is crucial during the S-phase and the transition from S-phase to the G2-phase (Blackiston et al., 2009; Urrego et al., 2014). As Ki67 labels all active phases of the cell cycle (G1-, S- and G2-phase) (Kim et al., 2017; Gerdes et al., 2018), $K_{ir}4.1$ positive cells might be in the early phases of the cell cycle and hence at the start of $K_{ir}4.1$ downregulation. Thus, it would be of interest for follow up experiments, to use proliferation markers that label later stages of the cell cycle in which the membrane is known to be depolarised the most (Blackiston et al., 2009; Urrego et al., 2014). This could help to determine whether all proliferative astrocytes completely downregulate their $K_{ir}4.1$ expression at some point. One candidate marker would be anti-PHH3 (phospho-histone 3) that labels the mitosis phase (Kim et al., 2017). Also cyclins and their primary CDK partners would be a good target. Cyclin A, which activates its partner CDK2 as well as CDC2 to initiate the transition from the S- to G2-phase and peaks during the G2- an M-phase, would be a promising candidate. Moreover, cyclin B1 also activates CDC2 and initiates the transition from the G2- into M-phase while peaking during the late G2- and early M-phase, and thus would be an appropriate marker (Darzynkiewicz et al., 1996).

As $K_{ir}4.1^{-/-}$ mouse models exist and have been used to prove the importance of $K_{ir}4.1$ channels in mature, non-reactive astrocytes it would be of interest to use $K_{ir}4.1$ deficient mice for further experiments (Kofuji et al., 2000; Kofuji et al., 2002; Neusch, 2006; Seifert et al., 2009). First,

one would be able to determine whether non-reactive astrocytes in the CNS of these animals already proliferate without an injury, just due to a depolarized V_r and the lack of $K_{ir}4.1$ channels. Second, it would be interesting to resolve whether proliferation of reactive astrocytes in these animals would be enhanced in response to traumatic injury.

This could be of great importance, as it has been shown that enhanced proliferation of astrocytes surrounding a lesion initiated by a lack of monocyte invasion led to a decrease in astrocyte reactivity accompanied by a reduction of the glia scar with less extracellular matrix deposition. This resulted in higher neuronal coverage surrounding the smaller lesion site (Frik et al., 2018). Thus, one might speculate that if proliferation could be enhanced by blocking or knocking down astrocytic $K_{ir}4.1$ channel functions, regeneration and protection of the tissue surrounding the lesion could be enhanced. Hence, astrocytic $K_{ir}4.1$ channels might be a target in improving the outcome of stroke, contusion and traumatic brain injuries.

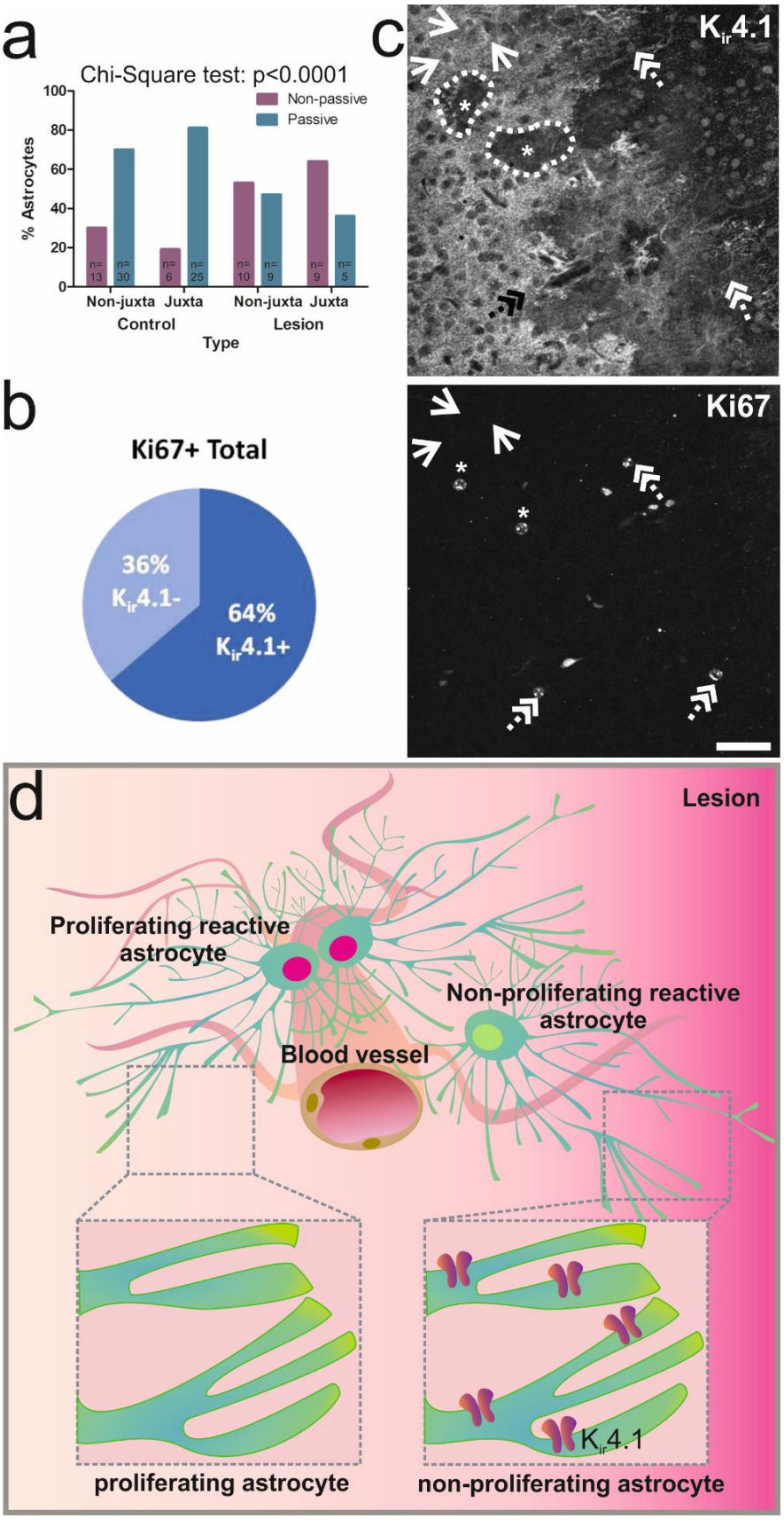
a
Chi-Square test: p<0.0001
Non-passive
Passive
% Astrocytes
100
80
60
40
20
0
n= 13
n= 30
n= 6
n= 25
n= 10
n= 9
n= 9
n= 5
Non-juxta
Juxta
Non-juxta
Juxta
Control
Lesion
Type
b
Ki67+ Total
36%
Kir4.1-
64%
Kir4.1+
c
Kir4.1
Ki67
d
Lesion
Proliferating reactive astrocyte
Non-proliferating reactive astrocyte
Blood vessel
Kir4.1
proliferating astrocyte
non-proliferating astrocyte

Figure 25: K_{ir}4.1 channels become downregulated in a subset of proliferating astrocytes after TBI
a: 74 control astrocytes (43 non-juxtavascular and 31 juxtavascular astrocytes) and 33 reactive astrocytes (19 non-juxtavascular and 14 juxtavascular) from lesioned brains were sorted according to their current pattern. Under control conditions, only 30 % of non-juxtavascular and 19 % of juxtavascular astrocytes display non-passive current patterns. In the lesioned brains 53 % of non-juxtavascular and 64 % of juxtavascular astrocytes have non-passive current patterns. A Chi-square test shows that the subgroups are significantly different ($p < 0.0001$). **b:** Proliferating anti-Ki67 positive non-juxtavascular and juxtavascular astrocytes were counted in two adult lesioned Aldh1l1-eGFP mice 5dpi. Out of the 80 proliferative cells 64 % were positive for anti-K_{ir}4.1 **c:** Confocal maximum z-projection (optical sections 1-27) of an adult (p51) Aldh1l1-eGFP transgenic mouse lesioned hemisphere 5dpi. The upper picture shows the anti-K_{ir}4.1 staining, the lower one the proliferation marker anti-Ki67. Arrows indicate non-proliferating astrocytes labelled by anti-K_{ir}4.1. Dashed double arrows point to astrocytes double positive for anit-K_{ir}4.1 and anti-Ki67. Astrocytes that show no K_{ir}4.1 labelling but are proliferative are marked with an asterisk. The dashed circle indicates the astrocytic domain of two proliferating astrocytes that are negative for anti-K_{ir}4.1. Scale bar 57µm. **d:** Schematic of the lesioned cortex. Reactive proliferating astrocytes (dark green, pink nucleus) downregulate K_{ir}4.1 channels. Reactive non-proliferating astrocytes (dark green, green nucleus) do not downregulate K_{ir}4.1.

4.3 Astrocyte reactivity results in a shift towards non-passive current responses especially in juxtavascular astrocytes

I found two different types (non-passive and passive) of current responses in mature somatosensory astrocytes in Aldh1l1-eGFP mice. Typical Ohmic passive current patterns (Figure 14a) with linear IV-curves (Figure 14b) were dominant in the healthy brain. Nevertheless, 26 % of astrocytes show non-passive current response patterns (Figure 14a, c) with non-linear IV-relationships (Figure 14b). Astrocytes in the barrel cortex, the brainstem and the hippocampus of rodents are known to transition during development from mainly non-passive outwardly rectifying astrocytes to mainly passive ones, whose currents are predominantly carried by inwardly rectifying ion channels (Zhou, 2005; Houades et al., 2008; Kafitz et al., 2008; Stephan & Friauf, 2014). Additionally, many other K^+ channels are known to be present in astrocytic membranes which together with the K_{ir}4.1 ion channels are the underlying cause for mainly passive current patterns that result in linear IV-relationships (Pastor et al., 1995; Isokawa & McKhann, 2005; Fazel et al., 2006; Djukic et al., 2007; Adermark & Lovinger, 2008; Du et al., 2015).

The presence of non-passive current patterns in astrocytes of healthy animals that were seen in this study might be explained by their age (postnatal day 24 to 48). It has been shown that in rodent astrocytes there is a continuous increase in K_{ir}4.1 expression until postnatal day 60 (Zhou, 2005; Houades et al., 2008; Kafitz et al., 2008; Seifert et al., 2009; Stephan & Friauf,

2014; Moroni et al., 2015). At embryonic stage E20, $K_{ir}4.1$ is nearly undetectable in astrocytes in the hippocampus and somatosensory cortex of rats. During development $K_{ir}4.1$ is upregulated to the point, where it is the dominating ion channel at around p60 (Moroni et al., 2015). In addition, electrophysiological recordings have shown that the activity of $K_{ir}4.1$ channels increases enormously over the course of the first postnatal weeks accompanied by a change in astrocyte morphology and passive electrophysiological properties in rats and mice (Bordey & Sontheimer, 1997; Seifert et al., 2009). Hence, it might have been possible that not in all of the somatosensory cortex astrocytes recorded in this study, $K_{ir}4.1$ channels were the dominating K^+ conducting channels. Even though I found homogeneous expression of $K_{ir}4.1$ channels in healthy somatosensory cortex astrocytes (Figure 8 and 9) it might be possible that in some astrocytes $K_{ir}4.1$ expression was indeed present but still relatively low and hence did not constitute the dominating current. I obtained similar results for astrocytes in the lateral superior olive in Aldh1l1-eGFP mice. Passive astrocytes with non-linear IV-relationships were already dominating (66 %) between the ages p15-p30 (Figure 14c). Somatosensory cortex astrocytes differed from those in the lateral superior olive regarding their passive properties (V_r, G_r, R_{in}) (Figure 14d, e, f). However, these discrepancies might be explained by the fact that on average, younger animals have been used in LSO recordings than in somatosensory cortex ones, and hence the transition towards higher levels of $K_{ir}4.1$ channel expression was not as advanced as in somatosensory cortex astrocytes. It also has to be considered that different types of ion channels, transporters and transmitter receptors might be present in LSO astrocytes that cater to the special needs of LSO neurons that receive excitatory as well as inhibitory inputs to process interaural level differences (Grothe et al., 2010).

In young rodent astrocytes, the dominant currents are known to be delayed rectifying (I_d) and transient (I_A) currents caused by voltage-activated K^+ channel (K_v) subfamilies (Bordey & Sontheimer, 1997; Seifert et al., 2009). K_v channel expression and the according I_d and I_A currents are known to be associated with immature astrocytes that are either still mitotic or have proliferative potential, whereas $K_{ir}4.1$ channel expression is strongly linked to end-differentiated non-proliferative astrocytes (Sontheimer, 1994; Roy & Sontheimer, 1995; Bordey & Sontheimer, 1997; MacFarlane & Sontheimer, 1997, 2000; Higashimori & Sontheimer, 2007). Hence, I studied whether the non-passive current patterns already correlated with juxtavascular astrocytes in the healthy brain. Surprisingly, it was the opposite.

19 % of cortical juxtavascular astrocytes showed non-passive and 81 % passive current patterns while 30 % of non-juxtavascular astrocytes displayed non-passive and 70 % passive ones (Figure 15a). Even though I found that $K_{ir}4.1$ was homogenously expressed in non-reactive somatosensory cortex astrocytes, one might speculate, that the underlying cause for such dominance in passive current patterns of juxtavascular astrocytes might be due to higher amounts of $K_{ir}4.1$ expression. Maybe the close association of juxtavascular astrocytes with the vasculature is linked to increased amounts of $K_{ir}4.1$ channels in the membrane of these cells, as it has previously been shown in rats that $K_{ir}4.1$ channels are preferably located on astrocytic endfeet, that are in contact with either blood vessels or synapses (Higashi et al., 2001). Analysing passive electrophysiological properties of non-juxtavascular and juxtavascular astrocytes when sorted according to non-passive and passive current patterns revealed a 30 nS higher G_r accompanied by a 13 MΩ lower R_{in} in non-juxtavascular passive astrocytes than in non-juxtavascular non-passive astrocytes (Figure 15c, d). This difference might be attributed to the high G_r of $K_{ir}4.1$ channels (Bordey & Sontheimer, 1997; Seifert et al., 2009) that might be more extensively expressed in these passive cells.

After the stab wound lesion, the ratio of non-passive to passive current patterns in reactive astrocytes changed drastically. 53 % of reactive non-juxtavascular astrocytes displayed non-passive current patterns while in the control condition only around 30 % did so (Figure 25a). In reactive juxtavascular astrocytes even a bigger portion, namely 64 % of cells, showed a non-passive current response pattern while under control conditions only 19 % behaved like this (Figure 25a). This transition from mainly passive current response patterns towards non-passive ones in reactive astrocytes can be explained by my findings that $K_{ir}4.1$ was downregulated in proliferating astrocytes. Also, that a higher proportion of juxtavascular astrocytes displayed non-passive current patterns compared to non-juxtavascular ones was in line with the much higher amount of proliferating juxtavascular astrocytes that completely lacked $K_{ir}4.1$. These findings suggest, that reactive astrocytes transition from typical mature astrocytes with passive current responses back towards a state where they much more represent immature astrocytes with non-passive current patterns. As previously mentioned it is known from literature that non-passive current patterns present in immature astrocytes are related to a dominance of delayed rectifying (I_d) and transient (I_A) currents, caused by the presence of K_v channels and only little to no expression of $K_{ir}4.1$ channels (Bordey & Sontheimer, 1997;

Seifert et al., 2009). Hence, the shift towards non-passive current patterns would likely be accompanied by a more positive V_r, as well as a decrease in G_r and an increase in R_{in}. The results shown here, are only partly in line with these assumptions. As mentioned, the V_r of the different subgroups of reactive astrocytes did not differ (Figure 20b). G_r and R_{in} of non-juxtavascular non-passive and passive astrocytes did change in comparison to control conditions by losing their significant dissimilarity (Figure 20c, d). Opposite to what one would expect, R_{in} decreased in reactive non-juxtavascular non-passive astrocytes accompanied by an increase in G_r. This discrepancy might be explained by an upregulation of other ion channels in these astrocytes. For example, HCN channels that are known to be expressed in reactive astrocytes in rodents (Rusnakova et al., 2013; Honsa et al., 2014) might influence astrocytic G_r and R_{in} and are also known to contribute to a hyperpolarised V_r. The upregulation of HCN channels in reactive astrocytes will be discussed in detail in paragraph 4.6. In addition, cultured rat astrocytes in *in-vitro* ischemia models are known to upregulate two-pore-domain potassium channels of the TREK2 subtype (Kucheryavykh et al., 2009).

For future studies it would be of interest to segregate reactive astrocytes not only into non-juxtavascular and juxtavascular, but also focus on whether an astrocyte is proliferative or not. Here also reactive astrocytes were taken into account that were clearly non-proliferative and as already discussed in the last paragraph, ion channel expression patterns were different in reactive non-proliferating astrocytes compared to proliferating ones.

4.4 $K_{ir}6.2$ channels are heterogeneously expressed in astrocytes before and after a lesion

The $K_{ir}6$ channel subfamily forms ATP-sensitive K^+ channels (K_{ATP}) that are involved in metabolic processes in many cell types (Hille, 1992). They are known to be present in rat astrocytes and speculated to play a role in the cells´ protection after metabolic stress as well as the regulation of gap-junctional permeability (Thomzig et al., 2001; Wu et al., 2011). Therefore, they are perfect candidates to be involved in astrocytic behaviour following an injury.

In the healthy, unlesioned somatosensory cortex, immunohistochemical stainings showed, that $K_{ir}6.2$ is widely expressed in somatosensory cortex astrocytes. In contrast, only little to no $K_{ir}6.1$

expression was found. K_{ir}6.2 labelling was detectable throughout all cortical layers in astrocytes, as well as in neurons. Especially astrocytic processes of a fraction of cortical astrocytes were intensely positive for the K_{ir}6.2 antibody, whereas astrocytic somata were very sparsely labelled. I found heterogeneous expression of K_{ir}6.2 in cortical astrocytes, however, heterogeneity did not relate to whether an astrocytes was non-juxtavascular or juxtavascular (Figure 10 and Figure 11). In agreement with my findings, K_{ir}6.2 mRNA is known to be present in other astrocyte types like Müller glia in the retina, astrocytes in the cerebellar white matter and the corpus callosum of rats and guinea-pigs (Thomzig et al., 2001; Raap et al., 2002; Zhou et al., 2002). In contrast, it has been shown by means of immunohistochemistry that only the K_{ir}6.1 subunit and not K_{ir}6.2 is present in rat cortical astrocytes (Thomzig et al., 2001).

After a stab wound lesion was introduced into the brain, the heterogeneity in K_{ir}6.2 expression was maintained up to 5dpi and non-juxtavascular and juxtavascular astrocytes did still not differ. Also proliferation did not impact K_{ir}6.2 expression. Interestingly, a shift from K_{ir}6.2 channels mainly being present on astrocytic processes under control conditions towards more somal regions in reactive astrocytes could be observed (Figure 22). This shift might protect astrocytes from metabolic stress after traumatic events. As astrocytic processes polarize towards a lesion and astrocytic domains are broken up after an injury this could lead to the reorganisation of K_{ir}6.2 (Wilhelmsson et al., 2006; Sofroniew, 2009; Sofroniew & Vinters, 2010). As the expression of K_{ir}6.2 in cortical astrocytes is controversial, nothing is known about an up or downregulation of said ion channel in reactive astrocytes yet. Hence it might be of interest to verify K_{ir}6.2 expression in somatosensory cortex astrocytes by in situ hybridization as well as single-cell RT-PCR to verify gene expression in single astrocytes (Toledo-Rodriguez & Markram, 2014) and compare them before and after a lesion.

4.5 K_v4.3 channels are upregulated in polarized processes of reactive astrocytes

In cultured rat hippocampal astrocytes, pharmacological experiments showed that 70 % of A-type currents in these cells are generated by the K_v4 channel subfamily and the main subtype present is the *Shal* K_v4.3 channel subunit (Bekar, 2004). K_v4 channel subfamilies are also known to play an important role in regulation of cell proliferation and to influence cell cycle progression (Blackiston et al., 2009; Urrego et al., 2014).

Here I showed by means of immunohistochemistry, that K_v4.3 labels processes of cortical astrocytes as well as astrocytic somata. Both non-juxtavascular and juxtavascular astrocytes expressed K_v4.3 heterogeneously throughout all layers of the healthy somatosensory cortex. One exception are non-juxtavascular astrocytes in cortical layer VI that are 100 % K_v4.3 positive (Figure 12 and Figure 13). An explanation might be the type of progenitor cell these astrocytes are derived from. It is known that progenitor cells residing in the marginal zone of the embryonic and neonatal cortex of mice give rise to astrocytes residing in cortical layer I-IV, while astrocytes in deeper cortical layers are generated by a different subset of progenitor cells (Costa et al., 2007; Breunig et al., 2012; Schitine et al., 2015). In addition, the clonal identity of an astrocyte, which defines heterogeneity in these cells in the cortex, and the subsequent arrangement of astrocytes in specific cortical domains might influence K_v4.3 heterogeneity (García-Marqués & López-Mascaraque, 2013). The heterogeneously expressed K_v4.3 is probably at least one of the ion channels present in astrocytes that display non-passive current patterns observed in the electrophysiological experiments of this study.

Five days after a stab wound lesion reactive non-juxtavascular and juxtavascular astrocytes retained their heterogeneity regarding K_v4.3 channel expression. Heterogeneous expression was also observed in proliferating astrocytes. Nevertheless, more intense anti-K_v4.3 labelling was present in hypertrophic, polarized astrocytic processes (Figure 23). A potential explanation might be an optical effect, as swollen processes are bigger and therefore labelling could appear more intense even if there is no upregulation of the ion channel in reality. However, if the more intense labelling of astrocytic processes would be due to swelling, this effect would have to be observed for all ion channel stainings performed in my study. But polarization and hypertrophy did not influence the intensity of the anti-K_{ir}4.1, anti-K_{ir}6.2 and anti-HCN2 channel labelling (Figure 21, 22, 24) suggesting that an upregulation of K_v4.3 was happening indeed. Astrocyte proliferation is often preceded by polarization of astrocytic processes towards the lesion site (Bardehle et al., 2013). This further reinforces the upregulation of K_v4.3 observed here. Because it is known that delayed rectifying (I_d) and transient (I_A) currents, caused by the presence of K_v channels, are dominant in young and immature astrocytes that are either still mitotic or have the potential to proliferate (Bordey & Sontheimer, 1997; Seifert et al., 2009). K_v4.3 upregulation on astrocytic processes might be important for subsequent proliferation of a subset of these polarized astrocytes. Moreover, it is known that I_d and I_A currents are also

dominating in reactive proliferating astrocytes in rat spinal cord cultures (MacFarlane & Sontheimer, 1997). The upregulation of $K_v4.3$ channels in polarized reactive astrocytes, together with the downregulation of $K_{ir}4.1$, might be the origin of the high increase of non-passive current patterns observed in reactive astrocytes by means of electrophysiology (Figure 20 and 25a).

Even though $K_v4.3$ channels are present in astrocytes and upregulated in reactive ones after injury, I found no functional I_A currents in electrophysiological recordings performed in this study. However, this might be explained by the small amplitude of these currents and thus they are masked by the much larger and dominating $K_{ir}4.1$ currents in astrocytes (Bekar, 2004; Seifert et al., 2009). Hence for future experiments one should consider to perform electrophysiological recordings combined with pharmacological blocking of $K_{ir}4.1$ channels on non-reactive and reactive, non-juxtavascular and juxtavascular astrocytes to verify the presence of I_A currents evoked by $K_v4.3$. In addition, it would be interesting to see if I_A current amplitudes are bigger in proliferating cells than in non-proliferating ones.

4.6 HCN channel expression patterns in astrocytes are altered after a stab wound lesion

It has been shown that HCN channels are involved in the cell cycle progression of embryonic stem cells. Blocking of these channels with ZD7288 decreased the amounts of cells in G0-state and G1-phase and increased the amount of embryonic stem cells in the S-phase (Lau et al., 2011). Transcripts of HCN channels are present in primary astrocyte cultures and post-ischemic astrocytes of rats and mice and might therefore play a role in cation influx in these cells (Rusnakova et al., 2013; Honsa et al., 2014). In my study, electrophysiological whole-cell patch-clamp experiments performed on healthy somatosensory cortex astrocytes showed a reduction in the slope of the IV-relationship after ZD7288 application (Figure 16). It is important to note that the reduction in the slope of the IV-curves that was observed after HCN channel blocker (ZD7288) application is a linear reduction (Figure 16d). HCN current-voltage relationships are nearly linear quite similar to the ones for K_{ir} channels, but their reversal potential lies at around -20 mV (Hille, 1992). The IV of the difference current (subtraction of the blocked current response pattern from the control condition) (Difference Trace; Figure 16c and d) also showed a linearity. However, the reversal potential of the difference current was

very negative (below -80 mV) and resembles the one caused by $K_{ir}4.1$ channels and not HCN channels, which lies at around - 20mV (Hille, 1992). Moreover, the reversal potential before and after the application of the HCN channel blocker remained similar. This suggests no or only little involvement of HCN channels in the measured currents. Hence the current reduction I observed here might most probably be due to a run-down of $K_{ir}4.1$ channels over the course of the recording period. Another possibility might be a slightly higher input resistance caused by eventual clogging of the electrode after the long recording. However, immunohistochemical stainings in my study showed that cortical astrocytes were positive for anti-HCN1 in the healthy somatosensory cortex (Figure 17), while HCN2 (Figure 24a) and HCN3 (data not shown) were not present at all. Moreover, the expression of HCN1 is heterogeneous but not linked to whether an astrocyte is non-juxtavascular or juxtavascular in nature (Figure 17). One explanation for the absence of functional HCN1 currents in electrophysiological recordings of this study might be the extremely high amount of $K_{ir}4.1$ currents and their run-down that might mask the much smaller HCN currents. As it has been discussed in previous paragraphs $K_{ir}4.1$ current amplitudes are very high. Therefore, it might be of interest to repeat the HCN channel blocking experiments under the presence of the $K_{ir}4.1$ channel blockers. Ba^{2+} would be the best choice because in comparison to other $K_{ir}4.1$ channel blockers like Cs^{+} and Rb^{+}, it does not strongly block HCN currents (Hille, 1992). However this might be difficult as Ba^{2+} often times impacts the longevity of the cell and the wash-in of the HCN channel blocker (ZD7288) takes time. Additionally, ZD7288 also activates and inhibits several other types of ion channels like low-threshold Ca^{2+} channels, $Na_v1.4$ channels and NMDA-evoked currents that might also be present in astrocytes (Felix et al., 2003; Klar et al., 2003; Wu et al., 2012; Han et al., 2013). Therefore, it is possible that the application of ZD7288 simultaneously activates or inhibits other channels, which could mask the effect of the HCN channel blocking. The presence of HCN1 in cortical astrocytes observed here is only partially in line with literature. Even though HCN1-4 channel mRNA is present in astrocytes of the healthy rodent brain in small amounts (Rusnakova et al., 2013), another study has shown that HCN1 channels were only present in polydendrocytes but not in other glia cells in the rodent cortex (Honsa et al., 2014). However, the results from my study are strongly supported by the aforementioned presence of small amounts of HCN1 channel mRNA expression seen in single cell RT-qPCR experiments (Rusnakova et al., 2013; Honsa et al., 2014). One additional consideration has to be made for

why no HCN currents were detectable in electrophysiological recordings in my study. This might be the result of to the heterogeneous expression which I found for HCN1 channels in the somatosensory cortex and the very minimal percentage of HCN1-4 channel transcripts known to be present in the healthy rodent brain (Rusnakova et al., 2013; Honsa et al., 2014). It is possible that the number of studied astrocytes was simply too small to have the chance of recording from an astrocyte with functional HCN channels.

As already mentioned, reactive astrocytes are known to upregulate the expression of certain sets of HCN channels weeks after ischemia in rats and mice and transcripts of these channels are already upregulated earlier (Rusnakova et al., 2013; Honsa et al., 2014). After a stab wound lesion in the somatosensory cortex, up to 5dpi no changes in HCN1 channel expression were found compared to control conditions. The same was true for HCN3 channels which were not expressed in astrocytes in the healthy brain and still absent five days after a stab wound lesion was inflicted (data not shown). Nevertheless, it is possible that HCN1 and HCN3 channels might still upregulate at later stages which I did not study. HCN2 channels, which were absent in astrocytes in the healthy somatosensory cortex (Figure 24a), were extensively upregulated on processes of a subset of reactive polarizing astrocytes already at 5dpi (Figure 24b). The upregulation was independent of non-juxtavascular and juxtavascular positions of astrocytic somata and proliferative behaviour of these astrocytes. This is in line with the findings in the ischemic brain of mice and rats where reactive astrocytes are known to upregulate HCN2 channels as well (Rusnakova et al., 2013; Honsa et al., 2014). However, after a stab wound lesion, the HCN2 upregulation seems to happen much faster. The earlier presence of HCN2 channels shown in my study might be related to the severity of the injury that results in severe reactive astrogliosis in combination with proliferation and scar formation early on. Astrocyte reactivity peaks later under ischemic conditions (Anderova et al., 2011). It is known that HCN channels play a role in proliferation in embryonic stem cells (Lau et al., 2011). In my study, HCN2 channel expression was upregulated not only in proliferating but also in non-proliferating astrocytes. This suggests that HCN2 channel upregulation might not exclusively play a role in the proliferation of reactive astrocytes. As the upregulation of HCN2 occurs mainly on hypertrophic polarized processes of reactive astrocytes, it might be important for the homeostasis of sodium in the lesioned brain or to prevent seizures by supporting the Na^+/K^+ ATPase-dependent ionic homeostasis (Sontheimer et al., 1994; Ouwerkerk et al., 2003;

Thulborn et al., 2005; Black et al., 2010; Honsa et al., 2014). Moreover, HCN2 upregulation might prevent glutamate excitotoxicity by influencing glutamate release at presynaptic terminals (Neitz et al., 2011; Honsa et al., 2014). Moreover, it might together with the downregulation of $K_{ir}4.1$ channels and the upregulation of $K_v4.3$, be involved in the shift towards non-passive current patterns in reactive astrocytes that I observed after the stab wound lesion (Figure 20 and 25a). Additionally, the combination of the upregulation of HCN2 and Kv4.3 channels might also explain why I did not observe an overall reduction in G_r and an increase in R_{in} in reactive astrocytes after a stab wound lesion compared to the control condition (Figure 18). The upregulation of these channels might compensate for the reduction in G_r and increase in R_{in} that is caused by the loss of $K_{ir}4.1$ channels.

4.7 Final conclusion

The findings of my study show that non-juxtavascular and juxtavascular astrocytes do not inherently differ regarding their expression patterns of major K^+ channels studied here. Accordingly, no dissimilarities in passive electrophysiological properties were detectable between the two astrocyte subgroups. Most of the astrocytes in the somatosensory cortex of mice were typical mature astrocytes with passive current response patterns and linear IV-relationships mainly caused by $K_{ir}4.1$ activity. The stab wound lesion and the subsequently following reactive astrogliosis triggered a shift especially in juxtavascular astrocytes towards non-passive current patterns. This suggests that these reactive astrocytes might resemble immature astrocytes that are known to still have proliferative potential. Especially the downregulation of $K_{ir}4.1$ in proliferating reactive astrocytes as well as the upregulation of $K_v4.3$ channels on polarized astrocytic processes seem to be the underlying causes for the aforementioned shift. Hence, I propose an important role of these two K^+ channel subtypes in the astrocytes´ proliferative response to traumatic brain injury. Moreover, HCN2 channels, which were absent in astrocytes in the healthy somatosensory cortex were extensively upregulated on processes of a subset of reactive polarizing astrocytes independently of non-juxtavascular and juxtavascular positions of astrocytic somata and proliferative behaviour of these astrocytes which might be important for sodium homeostasis and the prevention of glutamate excitotoxicity. Furthermore, the upregulation of HCN2 channels might also contribute to the shift towards non-passive current patterns.

These findings might be of great interest for therapeutic approaches since there is increasing evidence, that astrocyte proliferation positively affects healing processes and axon regeneration after traumatic brain injury. Moreover, an increase in astrocyte numbers due to proliferation of reactive astrocytes is known to limit monocyte invasion into the brain, which minimizes scar formation. Therefore manipulating ion channels in astrocytes to promote astrocyte proliferation could be beneficial to ameliorate the patients' outcome and rehabilitation after different detrimental occurrences like stroke, brain contusions and lesions.

5 Bibliography

Aaku-Saraste E., Hellwig A., & Huttner W. B. (1996). "Loss of occludin and functional tight junctions, but not ZO-1, during neural tube closure - Remodeling of the neuroepithelium prior to neurogenesis." Developmental Biology 180(2): 664-679

Abbott N. J., Rönnbäck L., & Hansson E. (2006). "Astrocyte-endothelial interactions at the blood-brain barrier." Nature Reviews Neuroscience 7(1): 41-53

Abbott N. J., Patabendige A. A. K., Dolman D. E. M., Yusof S. R., & Begley D. J. (2010). "Structure and function of the blood–brain barrier." Neurobiology of Disease 37(1): 13-25

Adermark L., & Lovinger D. M. (2008). "Electrophysiological properties and gap junction coupling of striatal astrocytes." Neurochemistry International 52(7): 1365-1372

Afifi A. K. (1991). "The Fine Structure of the Nervous System." Neurology 41(9): 1535

Aguirre A. (2004). "Postnatal Neurogenesis and Gliogenesis in the Olfactory Bulb from NG2-Expressing Progenitors of the Subventricular Zone." Journal of Neuroscience 24(46): 10530-10541

Aguirre A., Chittajallu R., Belachew S., & Gallo V. (2004). "NG2-expressing cells in the subventricular zone are type C-like cells and contribute to interneuron generation in the postnatal hippocampus." Journal of Cell Biology 165(4): 575-589

Aguirre A., Dupree J. L., Mangin J. M., & Gallo V. (2007). "A functional role for EGFR signaling in myelination and remyelination." Nature Neuroscience 10(8): 990-1002

Allen N. J., & Barres B. A. (2009). "Neuroscience: Glia - more than just brain glue." Nature 457(7230): 675-677

Almolda B., Gonzalez B., & Castellano B. (2011). "Antigen presentation in EAE: role of microglia, macrophages and dendritic cells." Frontiers in bioscience : a journal and virtual library 16(August 2015): 1157-1171

Alvarez J. I., Dodelet-Devillers A., Kebir H., Ifergan I., Fabre P. J., Terouz S., Sabbagh M., Wosik K., Bourbonnière L., Bernard M., van Horssen J., de Vries H. E., Charron F., & Prat A. (2011). "The Hedgehog Pathway Promotes Blood-Brain Barrier Integrity and CNS Immune Quiescence." Science 334(6063): 1727-1731

Alvarez J. I., Katayama T., & Prat A. (2013). "Glial influence on the blood brain barrier." GLIA 61(12): 1939-1958

Amigorena S., Choquet D., Teillaud J. L., Korn H., & Fridman W. H. (1990). "Ion channel blockers inhibit B cell activation at a precise stage of the G1 phase of the cell cycle. Possible involvement of K+ channels." Journal of immunology (Baltimore, Md. : 1950) 144(6): 2038-2045

Amiry-Moghaddam M., & Ottersen O. P. (2003). "The molecular basis of water transport in the brain." Nature Reviews Neuroscience 4(12): 991-1001

Anderova M., Vorisek I., Pivonkova H., Benesova J., Vargova L., Cicanic M., Chvatal A., & Sykova E. (2011). "Cell death/proliferation and alterations in glial morphology contribute to changes in diffusivity in the rat hippocampus after hypoxia-ischemia." Journal of Cerebral Blood Flow and Metabolism 31(3): 894-907

Andrews M. R., Czvitkovich S., Dassie E., Vogelaar C. F., Faissner A., Blits B., Gage F. H., ffrench-Constant C., & Fawcett J. W. (2009). " 9 Integrin Promotes Neurite Outgrowth on Tenascin-C and Enhances Sensory Axon Regeneration." Journal of Neuroscience 29(17): 5546-5557

Angelova D. M., & Brown D. R. (2018). "Model senescent microglia induce disease related changes in α-synuclein expression and activity." Biomolecules 8(3): 1-25

Arcangeli A., Bianchi L., Becchetti A., Faravelli L., Coronnello M., Mini E., Olivotto M., & Wanke E. (1995). "A novel inward-rectifying K+ current with a cell-cycle dependence governs the resting potential of mammalian neuroblastoma cells." The Journal of Physiology 489(2): 455-471

Argaw A. T., Gurfein B. T., Zhang Y., Zameer A., & John G. R. (2009). "VEGF-mediated disruption of endothelial CLN-5 promotes blood-brain barrier breakdown." Proceedings of the National Academy of Sciences 106(6): 1977-1982

Argaw A. T., Asp L., Zhang J., Navrazhina K., Pham T., Mariani J. N., Mahase S., Dutta D. J., Seto J., Kramer E. G., Ferrara N., Sofroniew M. V., & John G. R. (2012). "Astrocyte-derived VEGF-A drives blood-brain barrier disruption in CNS inflammatory disease." Journal of Clinical Investigation 122(7): 2454-2468

Azevedo F. A. C., Carvalho L. R. B., Grinberg L. T., Farfel J. M., Ferretti R. E. L., Leite R. E. P., Filho W. J., Lent R., & Herculano-Houzel S. (2009). "Equal numbers of neuronal

and nonneuronal cells make the human brain an isometrically scaled-up primate brain." Journal of Comparative Neurology 513(5): 532-541

Ballanyi K., Grafe P., & ten Bruggencate G. (1987). "Ion activities and potassium uptake mechanisms of glial cells in guinea- pig olfactory cortex slices." The Journal of Physiology 382:159-74: 159-174

Barakat L., & Bordey a. (2002). "GAT-1 and reversible GABA transport in Bergmann glia in slices." Journal of Neurophysiology 88(3): 1407-1419

Bardehle S., Krüger M., Buggenthin F., Schwausch J., Ninkovic J., Clevers H., Snippert H. J., Theis F. J., Meyer-Luehmann M., Bechmann I., Dimou L., & Götz M. (2013). "Live imaging of astrocyte responses to acute injury reveals selective juxtavascular proliferation." Nature Neuroscience 16(5): 580-586

Barres B. A., Koroshetz W. J., Chun L. L. Y., & Corey D. R. (1990). "Ion channel expression by white matter glia: The type-1 astrocyte." Neuron 5(4): 527-544

Barres B. A. (2003). "What is a glial cell?" GLIA 43(1): 4-5

Barres B. A. (2008). "The Mystery and Magic of Glia: A Perspective on Their Roles in Health and Disease." Neuron 60(3): 430-440

Battefeld A., Klooster J., & Kole M. H. P. (2016). "Myelinating satellite oligodendrocytes are integrated in a glial syncytium constraining neuronal high-frequency activity." Nature Communications 7(May): 1-13

Bauer C. K., & Schwarz J. R. (2001). "Physiology of EAG K+ Channels." The Journal of Membrane Biology 182(1): 1-15

Beattie E. C., Stellwagen D., Morishita W., Bresnahan J. C., Ha B. K., Von Zastrow M., Beattie M. S., & Malenka R. C. (2002). "Control of Synaptic Strength by Glial TNFα." Science 295(5563): 2282-2285

Becker D., Deller T., & Vlachos A. (2015). "Tumor necrosis factor (TNF)-receptor 1 and 2 mediate homeostatic synaptic plasticity of denervated mouse dentate granule cells." Scientific Reports 5(December): 1-10

Beckervordersandforth R., Rickert C., Altenhein B., & Technau G. M. (2008). "Subtypes of glial cells in the Drosophila embryonic ventral nerve cord as related to lineage and gene expression." Mechanisms of Development 125(5-6): 542-557

Beckervordersandforth R., Tripathi P., Ninkovic J., Bayam E., Lepier A., Stempfhuber B., Kirchhoff F., Hirrlinger J., Haslinger A., Lie D. C., Beckers J., Yoder B., Irmler M., & Götz M. (2010). "In vivo fate mapping and expression analysis reveals molecular hallmarks of prospectively isolated adult neural stem cells." Cell Stem Cell 7(6): 744-758

Behrendt G., Baer K., Buffo A., Curtis M. A., Faull R. L., Rees M. I., G??tz M., & Dimou L. (2013). "Dynamic changes in myelin aberrations and oligodendrocyte generation in chronic amyloidosis in mice and men." GLIA 61(2): 273-286

Bekar L. K., & Walz W. (2002). "Intracellular chloride modulates a-type potassium currents in astrocytes." GLIA 39(3): 207-216

Bekar L. K. (2004). "Complex Expression and Localization of Inactivating Kv Channels in Cultured Hippocampal Astrocytes." Journal of Neurophysiology 93(3): 1699-1709

Bekar L. K., He W., & Nedergaard M. (2008). "Locus coeruleus α-adrenergic-mediated activation of cortical astrocytes in vivo." Cerebral Cortex 18(12): 2789-2795

Bell R. D., Winkler E. A., Singh I., Sagare A. P., Deane R., Wu Z., Holtzman D. M., Betsholtz C., Armulik A., Sallstrom J., Berk B. C., & Zlokovic B. V. (2012). "Apolipoprotein e controls cerebrovascular integrity via cyclophilin A." Nature 485(7399): 512-516

Bentivoglio M., & Mazzarello P. (1999). "The history of radial glia." Brain Research Bulletin 49(5): 305-315

Bergles D. E., Jabs R., & Steinhäuser C. (2010). "Neuron-glia synapses in the brain." Brain Research Reviews 63(1-2): 130-137

Bergmann N. N. (1857). "Notiz über einige Strukturverhältnisse des Cerebellums und Rükenmarks." 8: 360-363

Bernardinelli Y., Muller D., & Nikonenko I. (2014). "Astrocyte-synapse structural plasticity." Neural Plasticity 2014

Binggeli R., & Weinstein R. C. (1986). "Membrane potentials and sodium channels: Hypotheses for growth regulation and cancer formation based on changes in sodium channels and gap junctions." Journal of Theoretical Biology 123(4): 377-401

Black J. A., Newcombe J., & Waxman S. G. (2010). "Astrocytes within multiple sclerosis lesions upregulate sodium channel Nav1.5." Brain 133(3): 835-846

Blackiston D. J., McLaughlin K. A., & Levin M. (2009). "Bioelectric controls of cell proliferation: Ion channels, membrane voltage and the cell cycle." Cell Cycle 8(21): 3527-3536

Boison D. (2008). "Adenosine as a neuromodulator in neurological diseases." Current Opinion in Pharmacology 8(1): 2-7

Bolton S., Greenwood K., Hamilton N., & Butt A. M. (2006). "Regulation of the astrocyte resting membrane potential by cyclic AMP and protein kinase A." GLIA

Bordey A., & Sontheimer H. (1997). "Postnatal development of ionic currents in rat hippocampal astrocytes in situ." Journal of Neurophysiology 78(1): 461-477

Bordey A., & Sontheimer H. (2000). "Ion channel expression by astrocytes in situ: Comparison of different CNS regions." GLIA 30(1): 27-38

Bowman C. L., Ding J.-P., Sachs F., & Sokabe M. (1992). "Mechanotransducing ion channels in astrocytes." Brain Research 584(1): 272-286

Brambilla R., Bracchi-Ricard V., Hu W.-H., Frydel B., Bramwell A., Karmally S., Green E. J., & Bethea J. R. (2005). "Inhibition of astroglial nuclear factor κB reduces inflammation and improves functional recovery after spinal cord injury." The Journal of Experimental Medicine 202(1): 145-156

Brambilla R., Persaud T., Hu X., Karmally S., Shestopalov V. I., Dvoriantchikova G., Ivanov D., Nathanson L., Barnum S. R., & Bethea J. R. (2009). "Transgenic inhibition of astroglial NF- k B improves functional outcome in experimental autoimmune encephalomyelitis by suppressing chronic central nervous system inflammation " The Journal of Immunology 182: 2628–2640

Breunig J. J., Gate D., Levy R., Rodriguez J., Kim G. B., Danielpour M., Svendsen C. N., & Town T. (2012). "Rapid genetic targeting of pial surface neural progenitors and immature neurons by neonatal electroporation." Neural Development 7(26): 1-12

Bringmann A., Pannicke T., Grosche J., Francke M., Wiedemann P., Skatchkov S. N., Osborne N. N., & Reichenbach A. (2006). "Müller cells in the healthy and diseased retina." Progress in Retinal and Eye Research 25(4): 397-424

Brown A. M., & Ransom B. R. (2007). "Astrocyte glycogen and brain energy metabolism." GLIA 55(12): 1263-1271

Brüggemann A., Stühmer W., & Pardo L. A. (1997). "Mitosis-promoting factor-mediated suppression of a cloned delayed rectifier potassium channel expressed in Xenopus oocytes." Proceedings of the National Academy of Sciences of the United States of America 94(2): 537-542

Buffo A., Rite I., Tripathi P., Lepier A., Colak D., Horn A. P., Mori T., & Götz M. (2008). "Origin and progeny of reactive gliosis: A source of multipotent cells in the injured brain." Proceedings of the National Academy of Sciences 105(9): 3581-3586

Buffo A., Rolando C., & Ceruti S. (2010). "Astrocytes in the damaged brain: Molecular and cellular insights into their reactive response and healing potential." Biochemical Pharmacology 79(2): 77-89

Bullock T., & Horridge G. A. (1965). "Structure and function in the nervous systems of invertebrates." Freeman: San Francisco.

Bundesen L. Q., Scheel T. A., Bregman B. S., & Kromer L. F. (2003). "Ephrin-B2 and EphB2 regulation of astrocyte-meningeal fibroblast interactions in response to spinal cord lesions in adult rats." The Journal of Neuroscience 23(21): 7789-7800

Bunge M. B., Bunge R. P., & Ris H. (1961). "Ultrastructural study of remyelination in an experimental lesion in adult cat spinal cord." The Journal of Biophysical and Biochemical Cytology 10(1): 67-94

Bunge M. B., Bunge R. P., & Pappas G. D. (1962). "Electron microscopic demonstration of connections between glia and myelin sheaths in the developing mammalian central nervous system." The Journal of Cell Biology 12(2): 448-453

Bunge R. P. (1968). "Glial cells and the central myelin sheath." Physiological Reviews 48(1): 197-251

Burda J. E., & Sofroniew M. V. (2014). "Reactive gliosis and the multicellular response to CNS damage and disease." Neuron 81(2): 229-248

Burda J. E., Bernstein A. M., & Sofroniew M. V. (2016). "Astrocyte roles in traumatic brain injury." Experimental Neurology 275: 305-315

Busch S. A., & Silver J. (2007). "The role of extracellular matrix in CNS regeneration." Current Opinion in Neurobiology 17(1): 120-127

Bush T. G., Puvanachandra N., Horner C. H., Polito A., Ostenfeld T., Svendsen C. N., Mucke L., Johnson M. H., & Sofroniew M. V. (1999). "Leukocyte Infiltration, Neuronal Degeneration, and Neurite Outgrowth after Ablation of Scar-Forming, Reactive Astrocytes in Adult Transgenic Mice provision of metabolic substrates for neurons, and inter-actions with endothelia to create and maintain the b." Neuron 23: 297-308

Bushong E. a., Martone M. E., Jones Y. Z., & Ellisman M. H. (2002). "Protoplasmic astrocytes in CA1 stratum radiatum occupy separate anatomical domains." The Journal of Neuroscience 22(1): 183-192

Butovsky O., Jedrychowski M. P., Moore C. S., Cialic R., Lanser A. J., Gabriely G., Koeglsperger T., Dake B., Wu P. M., Doykan C. E., Fanek Z., Liu L., Chen Z., Rothstein J. D., Ransohoff R. M., Gygi S. P., Antel J. P., & Weiner H. L. (2014). "Identification of a unique TGF-β-dependent molecular and functional signature in microglia." Nature Neuroscience 17(1): 131-143

Butt A. M., Colquhoun K., Tutton M., & Berry M. (1994). "Three-dimensional morphology of astrocytes and oligodendrocytes in the intact mouse optic nerve." Journal of Neurocytology 23(8): 469-485

Cahoy J. D., Emery B., Kaushal A., Foo L. C., Zamanian J. L., Christopherson K. S., Xing Y., Lubischer J. L., Krieg P. A., Krupenko S. A., Thompson W. J., & Barres B. A. (2008). "A Transcriptome Database for Astrocytes, Neurons, and Oligodendrocytes: A New Resource for Understanding Brain Development and Function." Journal of Neuroscience 28(1): 264-278

Camby I., Le Mercier M., Lefranc F., & Kiss R. (2006). "Galectin-1: A small protein with major functions." Glycobiology 16(11)

Cameron R. S., & Rakic P. (1991). "Glial cell lineage in the cerebral cortex: a review and synthesis." GLIA 4(2): 124-137

Campbell N., & Reece J. (2008). "Campbell Biology (8th Edition)."

Canady K. S., Ali-Osman F., & Rubel E. W. (1990). "Extracellular potassium influences DNA and protein syntheses and glial fibrillary acidic protein expression in cultured glial cells." GLIA 3(5): 368-374

Chan-Palay V., & Palay S. L. (1972). "The form of velate astrocytes in the cerebellar cortex of monkey and rat: High voltage electron microscopy of rapid Golgi preparations." Zeitschrift für Anatomie und Entwicklungsgeschichte 138(1): 1-19

Chaudhry F. A., Lehre K. P., Lookeren Campagne M. v., Ottersen O. P., Danbolt N. C., & Storm-Mathisen J. (1995). "Glutamate transporters in glial plasma membranes: Highly differentiated localizations revealed by quantitative ultrastructural immunocytochemistry." Neuron 15(3): 711-720

Chen L., Wang L., Zhu L., Nie S., Zhang J., Zhong P., Cai B., Luo H., & Jacob T. J. C. (2002). "Cell cycle-dependent expression of volume-activated chloride currents in nasopharyngeal carcinoma cells." American journal of physiology. Cell physiology 283(4): C1313-1323

Chen Y., Vartiainen N. E., Ying W., Chan P. H., Koistinaho J., & Swanson R. A. (2001). "Astrocytes protect neurons from nitric oxide toxicity by a glutathione-dependent mechanism." Journal of Neurochemistry 77(6): 1601-1610

Chittajallu R., Chen Y., Wang H., Yuan X., Ghiani C. A., Heckman T., McBain C. J., & Gallo V. (2002). "Regulation of Kv1 subunit expression in oligodendrocyte progenitor cells and their role in G1/S phase progression of the cell cycle." Proceedings of the National Academy of Sciences 99(4): 2350-2355

Chiu S. Y., & Wilson G. F. (1989). "The role of potassium channels in Schwann cell proliferation in Wallerian degeneration of explant rabbit sciatic nerves." The Journal of Physiology 408(1): 199-222

Chvátal A., Pastor A., Mauch M., Syková E., & Kettenmann H. (1995). "Distinct Populations of Identified Glial Cells in the Developing Rat Spinal Cord Slice: Ion Channel Properties and Cell Morphology." European Journal of Neuroscience 7(1): 129-142

Clark B. A., & Barbour B. (1997). "Currents evoked in Bergmann glial cells by parallel fibre stimulation in rat cerebellar slices." Journal of Physiology 502(2): 335-350

Clarke L. E., & Barres B. A. (2013). "Emerging roles of astrocytes in neural circuit development." Nature Reviews Neuroscience 14(5): 311-321

Coelho-Aguiar J. d. M., Bon-Frauches A. C., Gomes A. L. T., Veríssimo C. P., Aguiar D. P., Matias D., Thomasi B. B. d. M., Gomes A. S., Brito G. A. d. C., & Moura-Neto V. (2015). "The enteric glia: Identity and functions." GLIA 63(6): 921-935

Cone C. D. (1969). "Section of biological and medical sciences: Electroosmotic interactions accompanying mitosis initiation in sarcoma cells in vitro." Transactions of the New York Academy of Sciences 31(4 Series II): 404-427

Cone C. D., & Cone C. M. (1976). "Induction of mitosis in mature neurons in central nervous system by sustained depolarization." 192(4235): 155-158

Cone C. D. J., & Tongier M. (1971). "Control of Somatic Cell Mitosis by Simulated Changes in the Transmembrane Potential Level." Oncology 25(2): 168-182

Cook R. J., Lloyd R. S., & Wagner C. (1991). "Isolation and characterization of cDNA clones for rat liver 10-formyltetrahydrofolate dehydrogenase." Journal of Biological Chemistry 266(8): 4965-4973

Costa M. R., Kessaris N., Richardson W. D., Götz M., & Hedin-Pereira C. (2007). "The Marginal Zone/Layer I as a Novel Niche for Neurogenesis and Gliogenesis in Developing Cerebral Cortex." Journal of Neuroscience 27(42): 11376-11388

Cui W., Allen N. D., Skynner M., Gusterson B., & Clark A. J. (2001). "Inducible ablation of astrocytes shows that these cells are required for neuronal survival in the adult brain." GLIA 34(4): 272-282

Cullen D. K., Vernekar V. N., & LaPlaca M. C. (2011). "Trauma-Induced Plasmalemma Disruptions in Three-Dimensional Neural Cultures Are Dependent on Strain Modality and Rate." Journal of Neurotrauma 28(11): 2219-2233

Dallérac G., Chever O., & Rouach N. (2013). "How do astrocytes shape synaptic transmission? Insights from electrophysiology." Frontiers in Cellular Neuroscience 7(October): 1-19

Danbolt N. C. (2001). "Glutamate uptake." Progress in Neurobiology 65(1): 1-105

Darzynkiewicz Z., Gong J., Juan G., Ardelt B., & Traganos F. (1996). "Cytometry of cyclin proteins." Cytometry 25(1): 1-13

Davalos D., Grutzendler J., Yang G., Kim J. V., Zuo Y., Jung S., Littman D. R., Dustin M. L., & Gan W. B. (2005). "ATP mediates rapid microglial response to local brain injury in vivo." Nature Neuroscience 8(6): 752-758

DeAzevedo L. C., Fallet C., Moura-Neto V., Daumas-Duport C., Hedin-Pereira C., & Lent R. (2003). "Cortical radial glial cells in human fetuses: Depth-correlated transformation into astrocytes." Journal of Neurobiology 55(3): 288-298

DeCoursey T. E., Chandy K. G., Gupta S., & Cahalan M. D. (1984). "Voltage-gated K+ channels in human T lymphocytes: a role in mitogenesis?" Nature 307: 465-465

Decoursey T. E., Chandy K. G., Gupta S., & Cahalan M. D. (1987). "Mitogen induction of ion channels in murine T lymphocytes." The Journal of General Physiology 89(3): 405-420

Deiters O. (1865). "Untersuchungen über Gehirn und Rückenmark des Menschen und der Säugethiere." Braunschweig: F. Veiweg.

Deitmer J. W., & Rose C. R. (2010). "Ion changes and signalling in perisynaptic glia." Brain Research Reviews 63(1-2): 113-129

Del Rio-Hortega P. (1919). "El tercer elemento de los centros nerviosos.I.La microglia en estado nor-mal.II.Intervencion de la microglia en los procesos patologicos.III.Naturaleza probable de la microglia." Boll.Socieded Esp.Biol. 9: 69-120

Del Rio-Hortega P. (1920). "Estudios sobre la neuroglía. La microglía y su transformación en células en bastoncito y cuerpos granuloadiposos." Trab. Lab. Invest. Biol. 18: 37-82

Deller T., Haas C. A., Naumann T., Joester A., Faissner A., & Frotscher M. (1997). "Up-regulation of astrocyte-derived tenascin-C correlates with neurite outgrowth in the rat dentate gyrus after unilateral entorhinal cortex lesion." Neuroscience 81(3): 829-846

Desagher S., Glowinski J., & Premont J. (1996). "Astrocytes Protect Neurons from Hydrogen Peroxide Toxicity." The Journal of Neuroscience 16(8): 2553-2562

Deutsch B. Y. C., Krause D., & Lee S. C. (1986). "Voltage-gated potassium conductance in human T lymphocytes stimulated with phorbol ester." The Journal of Physiology 372: 405-423

Di Giorgio F. P., Carrasco M. A., Siao M. C., Maniatis T., & Eggan K. (2007). "Non-cell autonomous effect of glia on motor neurons in an embryonic stem cell-based ALS model." Nature Neuroscience 10(5): 608-614

Di Lella S., Sundblad V., Cerliani J. P., Guardia C. M., Estrin D. A., Vasta G. R., & Rabinovich G. A. (2011). "When galectins recognize glycans: From biochemistry to physiology and back again." Biochemistry 50(37): 7842-7857

Dimou L., & Götz M. (2014). "Glial Cells as Progenitors and Stem Cells: New Roles in the Healthy and Diseased Brain." Physiological Reviews 94(3): 709-737

Dimou L., & Gallo V. (2015). "NG2-glia and their functions in the central nervous system." GLIA 63(8): 1429-1451

Djukic B., Casper K. B., Philpot B. D., Chin L. S., & McCarthy K. D. (2007). "Conditional Knock-Out of Kir4.1 Leads to Glial Membrane Depolarization, Inhibition of Potassium and Glutamate Uptake, and Enhanced Short-Term Synaptic Potentiation." Journal of Neuroscience 27(42): 11354-11365

Doetsch F. (2003). "The glial identity of neural stem cells." Nature Neuroscience 6(11): 1127-1134

Doupnik C. A., Davidson N., & Lester H. A. (1995). "The inward rectifier potassium channel family." Current Opinion in Neurobiology 5(3): 268-277

Dowling P., Husar W., Menonna J., Donnenfeld H., Cook S., & Sidhu M. (1997). "Cell death and birth in multiple sclerosis brain." Journal of the Neurological Sciences 149(1): 1-11

Dringen R., Pfeiffer B., & Hamprecht B. (1999). "Synthesis of the Antioxidant Glutathione in Neurons: Supply by Astrocytes of CysGly as Precursor for Neuronal Glutathione." The Journal of Neuroscience 19(2): 562-569

Du Y., Ma B., Kiyoshi C. M., Alford C. C., Wang W., & Zhou M. (2015). "Freshly dissociated mature hippocampal astrocytes exhibit passive membrane conductance and low membrane resistance similarly to syncytial coupled astrocytes." Journal of Neurophysiology 113(10): 3744-3750

Egawa K., Yamada J., Furukawa T., Yanagawa Y., & Fukuda A. (2013). "Cl- homeodynamics in gap junction-coupled astrocytic networks on activation of GABAergic synapses." Journal of Physiology 591(16): 3901-3917

Emery B. (2010). "Regulation of Oligodendrocyte Differentiation and Myelination." Science 330(6005): 779-782

Eng L. F., Ghirnikar R. S., & Lee Y. L. (2000). "Glial Fibrillary Acidic Protein: GFAP-Thirty-One Years (1969–2000)." Neurochemical Research 25(9): 1439-1451

Enomoto K., Cossu M. F., Maeno T., Edwards C., & Oka T. (1986). "Involvement of the Ca2+-dependent K+ channel activity in the hyperpolarizing response induced by epidermal growth factor in mammary epithelial cells." FEBS Letters 203(2): 181-184

Eroglu C., & Barres B. A. (2010). "Regulation of synaptic connectivity by glia." Nature 468(7321): 223-231

Erschbamer M., Pernold K., & Olson L. (2007). "Inhibiting Epidermal Growth Factor Receptor Improves Structural, Locomotor, Sensory, and Bladder Recovery from Experimental Spinal Cord Injury." Journal of Neuroscience 27(24): 6428-6435

Etienne-Manneville S. (2006). "In vitro assay of primary astrocyte migration as a tool to study Rho GTPase function in cell polarization." Methods in Enzymology 406(1995): 565-578

Farina C., Aloisi F., & Meinl E. (2007). "Astrocytes are active players in cerebral innate immunity." Trends in Immunology 28(3): 138-145

Fazel F. S., Derakhshanrad N., Yekaninejad M. S., Vosoughi F., Derakhshanrad A., & Saberi H. (2006). "Predictive value of braden risk factors in pressure ulcers of outpatients with spinal cord injury." Acta Medica Iranica 56(1): 56-61

Fazel F. S., Derakhshanrad N., Yekaninejad M. S., Vosoughi F., Derakhshanrad A., & Saberi H. (2018). "Predictive value of braden risk factors in pressure ulcers of outpatients with spinal cord injury." Acta Medica Iranica 56(1): 56-61

Feig S. L., & Haberly L. B. (2011). "Surface-associated astrocytes, not endfeet, form the glia limitans in posterior piriform cortex and have a spatially distributed, not a domain, organization." Journal of Comparative Neurology 519(10): 1952-1969

Felix R., Sandoval A., Sánchez D., Gómora J. C., Vega-Beltrán J. L. D. l., Treviño C. L., & Darszon A. (2003). "ZD7288 inhibits low-threshold Ca2+ channel activity and regulates sperm function." Biochemical and Biophysical Research Communications 311(1): 187-192

Ferroni S., Valente P., Caprini M., Nobile M., Schubert P., & Rapisarda C. (2003). "Arachidonic acid activates an open rectifier potassium channel in cultured rat cortical astrocytes." Journal of Neuroscience Research 372: 363-372

Filous A. R., Tran A., Howell C. J., Busch S. A., Evans T. A., Stallcup W. B., Kang S. H., Bergles D. E., Lee S.-i., Levine J. M., & Silver J. (2014). "Entrapment via Synaptic-Like Connections between NG2 Proteoglycan+ Cells and Dystrophic Axons in the Lesion Plays a Role in Regeneration Failure after Spinal Cord Injury." The Journal of Neuroscience 34(49): 16369-16384

Floyd C. L., Gorin F. A., & Lyeth B. G. (2005). "Mechanical strain injury increases intracellular sodium and reverses Na+/Ca2+exchange in cortical astrocytes." GLIA 51(1): 35-46

Franze K., Grosche J., Skatchkov S. N., Schinkinger S., Foja C., Schild D., Uckermann O., Travis K., Reichenbach A., & Guck J. (2007). "Muller cells are living optical fibers in the vertebrate retina." Proceedings of the National Academy of Sciences 104(20): 8287-8292

Freedman B. D., Price M. A., & Deutsch C. J. (1992). "Evidence for voltage modulation of IL-2 production in mitogen-stimulated human peripheral blood lymphocytes . Information about subscribing to The Journal of Immunology is online at." The Journal of Immunology 149(12): 3784-3794

Friedlander D. R., Milev P., Karthikeyan L., Margolis R. K., Margolis R. U., & Grumet M. (1994). "The neuronal chondroitin sulfate proteoglycan neurocan binds to the neural cell adhesion molecules Ng-CAM/L1/NILE and N-CAM, and inhibits neuronal adhesion and neurite outgrowth." Journal of Cell Biology 125(3): 669-680

Frik J., Merl-Pham J., Plesnila N., Mattugini N., Kjell J., Kraska J., Gómez R. M., Hauck S. M., Sirko S., & Götz M. (2018). "Cross-talk between monocyte invasion and astrocyte proliferation regulates scarring in brain injury." EMBO reports: e45294-e45294

Fröhlich N., Nagy B., Hovhannisyan A., & Kukley M. (2011). "Fate of neuron-glia synapses during proliferation and differentiation of NG2 cells." Journal of Anatomy 219(1): 18-32

Fuhrmann M., Bittner T., Jung C. K. E., Burgold S., Page R. M., Mitteregger G., Haass C., Laferla F. M., Kretzschmar H., & Herms J. (2010). "Microglial Cx3cr1 knockout prevents neuron loss in a mouse model of Alzheimer's disease." Nature Neuroscience 13(4): 411-413

Fünfschilling U., Supplie L. M., Mahad D., Boretius S., Saab A. S., Edgar J., Brinkmann B. G., Kassmann C. M., Tzvetanova I. D., Möbius W., Diaz F., Meijer D., Suter U., Hamprecht B., Sereda M. W., Moraes C. T., Frahm J., Goebbels S., & Nave K.-A. (2012). "Glycolytic oligodendrocytes maintain myelin and long-term axonal integrity." Nature 485(7399): 517-517

Gadea A., Schinelli S., & Gallo V. (2008). "Endothelin-1 Regulates Astrocyte Proliferation and Reactive Gliosis via a JNK/c-Jun Signaling Pathway." Journal of Neuroscience 28(10): 2394-2408

Gallo V., Patrizio M., & Levi G. (1991). "GABA release triggered by the activation of neuron-like non-NMDA receptors in cultured type 2 astrocytes is carrier-mediated." GLIA 4(3): 245-255

Gallo V., Mangin J. M., Kukley M., & Dietrich D. (2008). "Synapses on NG2-expressing progenitors in the brain: Multiple functions?" Journal of Physiology 586(16): 3767-3781

Ganat Y. M., Silbereis J., Cave C., Ngu H., Anderson G. M., Ohkubo Y., Ment L. R., & Vaccarino F. M. (2006). "Early Postnatal Astroglial Cells Produce Multilineage Precursors and Neural Stem Cells In Vivo." Journal of Neuroscience 26(33): 8609-8621

García-Marín V., García-López P., & Freire M. (2007). "Cajal's contributions to glia research." Trends in Neurosciences 30(9): 479-487

García-Marqués J., & López-Mascaraque L. (2013). "Clonal identity determines astrocyte cortical heterogeneity." Cerebral Cortex 23(6): 1463-1472

Ge W. P., Miyawaki A., Gage F. H., Jan Y. N., & Jan L. Y. (2012). "Local generation of glia is a major astrocyte source in postnatal cortex." Nature 484(7394): 376-380

Gehring W. J., & Ikeo K. (1999). "Pax 6: Mastering eye morphogenesis and eye evolution." Trends in Genetics 15(9): 371-377

Gehrmann J., Matsumoto Y., & Kreutzberg G. W. (1995). "Microglia: Intrinsic immuneffector cell of the brain." Brain Research Reviews 20(3): 269-287

Gelfand E. W., Cheung R. K., Mills G. B., & Grinstein S. (1987). "Role of membrane potential in the response of human T lymphocytes to phytohemagglutinin." Journal of Immunology 138(2): 527-531

Genda E. N., Jackson J. G., Sheldon A. L., Locke S. F., Greco T. M., O'Donnell J. C., Spruce L. A., Xiao R., Guo W., Putt M., Seeholzer S., Ischiropoulos H., & Robinson M. B. (2011). "Co-compartmentalization of the Astroglial Glutamate Transporter, GLT-1, with Glycolytic Enzymes and Mitochondria." Journal of Neuroscience 31(50): 18275-18288

Gerdes J., Schwab U., Lemke H., & Stein H. (2018). "Production of a mouse monoclonal antibody reactive with a human nuclear antigen associated with cell proliferation." International Journal of Cancer 31(1): 13-20

Ghiani C. a., Yuan X., Eisen a. M., Knutson P. L., DePinho R. a., McBain C. J., & Gallo V. (1999). "Voltage-activated K+ channels and membrane depolarization regulate accumulation of the cyclin-dependent kinase inhibitors p27(Kip1) and p21(CIP1) in glial progenitor cells." The Journal of Neuroscience 19(13): 5380-5392

Giaume C., & McCarthy K. D. (1996). "Control of gap-junctional communication in astrocytic networks." Trends in Neurosciences 19(8): 319-325

Golgi C. (1870). "Sulla sostanza connettiva del cervello (nevroglia)." (endiconti ed.).

Gorina R., Font-Nieves M., Márquez-Kisinousky L., Santalucia T., & Planas A. M. (2011). "Astrocyte TLR4 activation induces a proinflammatory environment through the interplay between MyD88-dependent NFκB signaling, MAPK, and Jak1/Stat1 pathways." GLIA 59(2): 242-255

Götz M., Hartfuss E., & Malatesta P. (2002). "Radial glial cells as neuronal precursors: A new perspective on the correlation of morphology and lineage restriction in the developing cerebral cortex of mice." Brain Research Bulletin 57(6): 777-788

Götz M., & Sirko S. (2013). "Potential of glial cells." In: Sell S. (eds) Stem Cells Handbook. : Humana Press, New York, NY.

Goursaud S., Kozlova E. N., Maloteaux J. M., & Hermans E. (2009). "Cultured astrocytes derived from corpus callosum or cortical grey matter show distinct glutamate handling properties." Journal of Neurochemistry 108(6): 1442-1452

Graham D. I., McIntosh T. K., Maxwell W. L., & Nicoll J. A. R. (2000). "Recent Advances in Neurotrauma." Journal of Neuropathology & Experimental Neurology 59(8): 641-651

Gregory W. A., Edmondson J. C., Hatten M. E., & Mason C. A. (1988). "Cytology and neuron-glial apposition of migrating cerebellar granule cells in vitro." The Journal of Neuroscience 8(5): 1728-1738

Grissmer S., Nguyen a. N., & Cahalan M. D. (1993). "Calcium-activated potassium channels in resting and activated human T lymphocytes. Expression levels, calcium dependence, ion selectivity, and pharmacology." The Journal of General Physiology 102(4): 601-630

Grosche J., Matyash V., Möller T., Verkhratsky A., Reichenbach A., & Kettenmann H. (1999). "Microdomains for neuron-glia interaction: Parallel fiber signaling to Bergmann glial cells." Nature Neuroscience 2(2): 139-143

Grosche J., Kettenmann H., & Reichenbach A. (2002). "Bergmann glial cells form distinct morphological structures to interact with cerebellar neurons." Journal of Neuroscience Research 68(2): 138-149

Grothe B., Pecka M., & McAlpine D. (2010). "Mechanisms of Sound Localization in Mammals." Physiological Reviews 90(3): 983-1012

Guo D., Ramu Y., Klem A. M., & Lu Z. (2003). "Mechanism of Rectification in Inward-rectifier K +Channels." The Journal of General Physiology 121(4): 261-276

Gupta R. K., & Prasad S. (2013). "Early down regulation of the glial Kir4.1 and GLT-1 expression in pericontusional cortex of the old male mice subjected to traumatic brain injury." Biogerontology 14(5): 531-541

Guthrie P. B., Knappenberger J., Segal M., Bennett M. V. L., Charles A. C., & Kater S. B. (1999). "ATP Released from Astrocytes Mediates Glial Calcium Waves." 19(2): 520-528

Haas B., Schipke C. G., Peters O., Söhl G., Willecke K., & Kettenmann H. (2006). "Activity-dependent ATP-waves in the mouse neocortex are independent from astrocytic calcium waves." Cerebral Cortex 16(2): 237-246

Haas C. A., Rauch U., Thon N., Merten T., & Deller T. (1999). "Entorhinal cortex lesion in adult rats induces the expression of the neuronal chondroitin sulfate proteoglycan neurocan in reactive astrocytes." The Journal of Neuroscience 19(22): 9953-9963

Haj-Yasein N. N., Vindedal G. F., Eilert-Olsen M., Gundersen G. A., Skare O., Laake P., Klungland A., Thoren A. E., Burkhardt J. M., Ottersen O. P., & Nagelhus E. A. (2011). "Glial-conditional deletion of aquaporin-4 (Aqp4) reduces blood-brain water uptake and confers barrier function on perivascular astrocyte endfeet." Proceedings of the National Academy of Sciences 108(43): 17815-17820

Halassa M. M., Fellin T., Takano H., Dong J. H., & Haydon P. G. (2007). "Synaptic Islands Defined by the Territory of a Single Astrocyte." Journal of Neuroscience 27(24): 6473-6477

Hamby M. E., Hewett J. A., & Hewett S. J. (2006). "TGF-β1 potentiates astrocytic nitric oxide production by expanding the population of astrocytes that express NOS-2." GLIA 54(6): 566-577

Hamby M. E., Coppola G., Ao Y., Geschwind D. H., Khakh B. S., & Sofroniew M. V. (2012). "Inflammatory Mediators Alter the Astrocyte Transcriptome and Calcium Signaling Elicited by Multiple G-Protein-Coupled Receptors." Journal of Neuroscience 32(42): 14489-14510

Han X., Chen M., Wang F., Windrem M., Wang S., Shanz S., Xu Q., Oberheim N. A., Bekar L., Betstadt S., Silva A. J., Takano T., Goldman S. A., & Nedergaard M. (2013). "Forebrain engraftment by human glial progenitor cells enhances synaptic plasticity and learning in adult mice." Cell Stem Cell 12(3): 342-353

Hanani M. (2005). "Satellite glial cells in sensory ganglia: From form to function." Brain Research Reviews 48(3): 457-476

Hanani M. (2010). "Satellite glial cells in sympathetic and parasympathetic ganglia: In search of function." Brain Research Reviews 64(2): 304-327

Hansen A. J. (1985). "Effect of anoxia on ion distribution in the brain." Physiol Rev 65(1): 101-148

Harris N. G., Carmichael S. T., Hovda D. A., & Sutton R. L. (2009). "Traumatic brain injury results in disparate regions of chondroitin sulfate proteoglycan expression that are temporally limited." Journal of Neuroscience Research 87(13): 2937-2950

Harris N. G., Mironova Y. A., Hovda D. A., & Sutton R. L. (2010). "Pericontusion axon sprouting is spatially and temporally consistent with a growth-permissive environment

after traumatic brain injury." Journal of Neuropathology and Experimental Neurology 69(2): 139-154

Hartenstein V. (2011). "Morphological diversity and development of glia in Drosophila." GLIA 59(9): 1237-1252

Hartfuss E., Galli R., Heins N., & Götz M. (2001). "Characterization of CNS precursor subtypes and radial glia." Developmental Biology 229(1): 15-30

Hartline D. K. (2011). "The evolutionary origins of glia." GLIA 59(9): 1215-1236

Hartmann D., Ziegenhagen M. W., & Sievers J. (1998). "Meningeal cells stimulate neuronal migration and the formation of radial glial fascicles from the cerebellar external granular layer." Neuroscience Letters 244(3): 129-132

Hartwell L. H., & Weinert T. A. (1989). "Checkpoints : control that ensure the order of cell cycles events." Science 246(13): 629-633

Harty B. L., & Monk K. R. (2017). "Unwrapping the unappreciated: recent progress in Remak Schwann cell biology." Current Opinion in Neurobiology 47(Figure 1): 131-137

Hatakeyama J. (2004). "Hes genes regulate size, shape and histogenesis of the nervous system by control of the timing of neural stem cell differentiation." Development 131(22): 5539-5550

Hatten M. E. (1990). "Riding the glial monorail: A common mechanism for glialguided neuronal migration in different regions of the developing mammalian brain." Trends in Neurosciences 13(5): 179-184

Hatton G. I. (1999). "Astroglial modulation of neurotransmitter/peptide release from the neurohypophysis: Present status." Journal of Chemical Neuroanatomy 16(3): 201-219

Hayakawa K., Pham L. D. D., Katusic Z. S., Arai K., & Lo E. H. (2012). "Astrocytic high-mobility group box 1 promotes endothelial progenitor cell-mediated neurovascular remodeling during stroke recovery." Proceedings of the National Academy of Sciences 109(19): 7505-7510

Hayakawa K., Miyamoto N., Seo J. H., Pham L. D. D., Kim K. W., Lo E. H., & Arai K. (2013). "High-mobility group box 1 from reactive astrocytes enhances the accumulation of

endothelial progenitor cells in damaged white matter." Journal of Neurochemistry 125(2): 273-280

Healy L. M., Perron G., Won S.-Y., Michell-Robinson M. A., Rezk A., Ludwin S. K., Moore C. S., Hall J. A., Bar-Or A., & Antel J. P. (2016). "MerTK Is a Functional Regulator of Myelin Phagocytosis by Human Myeloid Cells." The Journal of Immunology 196(8): 3375-3384

Heintz N. (2004). "Gene Expression Nervous System Atlas (GENSAT)." Nature Neuroscience 7(5): 483-483

Herculano-Houzel S. (2014). "The glia/neuron ratio: How it varies uniformly across brain structures and species and what that means for brain physiology and evolution." GLIA 62(9): 1377-1391

Herrmann J. E., Imura T., Song B., Qi J., Ao Y., Nguyen T. K., Korsak R. A., Takeda K., Akira S., & Sofroniew M. V. (2008). "STAT3 is a Critical Regulator of Astrogliosis and Scar Formation after Spinal Cord Injury." Journal of Neuroscience 28(28): 7231-7243

Hertz L., & Zielke H. R. (2004). "Astrocytic control of glutamatergic activity: Astrocytes as stars of the show." Trends in Neurosciences 27(12): 735-743

Hertz L., Peng L., & Dienel G. A. (2007). "Energy metabolism in astrocytes: High rate of oxidative metabolism and spatiotemporal dependence on glycolysis/glycogenolysis." Journal of Cerebral Blood Flow and Metabolism 27(2): 219-249

Hickman S., Izzy S., Sen P., Morsett L., & El Khoury J. (2018). "Microglia in neurodegeneration." Nature Neuroscience 21(10): 1359-1369

Higashi K., Fujita A., Inanobe A., Tanemoto M., Doi K., Kubo T., & Kurachi Y. (2001). "An inwardly rectifying K+channel, Kir4.1, expressed in astrocytes surrounds synapses and blood vessels in brain." American Journal of Physiology-Cell Physiology 281(3): C922-C931

Higashimori H., & Sontheimer H. (2007). "Role of Kir4.1 channels in growth control of glia." GLIA 55(16): 1668-1679

Hille B. (1992). "Ionic channels of excitable membranes." Sunderland, Mass.: Sinauer Associates.

Hoarau J.-J., Krejbich-Trotot P., Jaffar-Bandjee M.-C., Das T., Thon-Hon G.-V., Kumar S., Gasque J. W. N., & Philippe. (2011). "Activation and Control of CNS Innate Immune Responses in Health and Diseases: A Balancing Act Finely Tuned by Neuroimmune Regulators (NIReg)." CNS & Neurological Disorders - Drug Targets 10(1): 25-43

Höltje M., Hoffmann A., Hofmann F., Mucke C., Große G., Van Rooijen N., Kettenmann H., Just I., & Ahnert-Hilger G. (2005). "Role of Rho GTPase in astrocyte morphology and migratory response during in vitro wound healing." Journal of Neurochemistry 95(5): 1237-1248

Honsa P., Pivonkova H., Harantova L., Butenko O., Kriska J., Dzamba D., Rusnakova V., Valihrach L., Kubista M., & Anderova M. (2014). "Increased expression of hyperpolarization-activated cyclic nucleotide-gated (HCN) channels in reactive astrocytes following ischemia." GLIA 62(12): 2004-2021

Houades V., Koulakoff A., Ezan P., Seif I., & Giaume C. (2008). "Gap Junction-Mediated Astrocytic Networks in the Mouse Barrel Cortex." Journal of Neuroscience 28(20): 5207-5217

Huang C., Han X., Li X., Lam E., Peng W., Lou N., Torres A., Yang M., Garre J. M., Tian G. F., Bennett M. V. L., Nedergaard M., & Takano T. (2012). "Critical Role of Connexin 43 in Secondary Expansion of Traumatic Spinal Cord Injury." Journal of Neuroscience 32(10): 3333-3338

Huang Y., & Rane S. G. (1994). "Potassium channel induction by the Ras/Raf signal transduction cascade." Journal of Biological Chemistry 269(49): 31183-31189

Iadecola C., & Nedergaard M. (2007). "Glial regulation of the cerebral microvasculature." Nature Neuroscience 10(11): 1369-1376

Ihrie R. A., & Alvarez-Buylla A. (2008). "Cells in the astroglial lineage are neural stem cells." Cell and Tissue Research 331(1): 179-191

Islas L., Pasantes-Morales H., & Sanchez J. A. (1993). "Characterization of stretch-activated ion channels in cultured astrocytes." GLIA 8(2): 87-96

Isokawa M., & McKhann G. M. (2005). "Electrophysiological and morphological characterization of dentate astrocytes in the hippocampus." Journal of Neurobiology 65(2): 125-134

Jansen L. A., Uhlmann E. J., Crino P. B., Gutmann D. H., & Wong M. (2005). "Epileptogenesis and reduced inward rectifier potassium current in tuberous sclerosis complex-1-deficient astrocytes." Epilepsia 46(12): 1871-1880

Jayakumar A. R., Tong X. Y., Ruiz-Cordero R., Bregy A., Bethea J. R., Bramlett H. M., & Norenberg M. D. (2014). "Activation of NF-κB Mediates Astrocyte Swelling and Brain Edema in Traumatic Brain Injury." Journal of Neurotrauma 31(14): 1249-1257

John G. R., Lee S. C., & Brosnan C. F. (2003). "Cytokines: Powerful regulators of glial cell activation." Neuroscientist 9(1): 10-22

Jones H. C., & Keep R. F. (1987). "The control of potassium concentration in the cerebrospinal fluid and brain interstitial fluid of developing rats." The Journal of Physiology 383(1): 441-453

Jones R. S., Minogue A. M., Connor T. J., & Lynch M. A. (2013). "Amyloid-β-induced astrocytic phagocytosis is mediated by CD36, CD47 and RAGE." Journal of Neuroimmune Pharmacology 8(1): 301-311

Kaaijk P., Pals S. T., Morsink F., Bosch D. A., & Troost D. (1997). "Differential expression of CD44 splice variants in the normal human central nervous system." Journal of Neuroimmunology 73(1): 70-76

Kafitz K. W., Meier S. D., Stephan J., & Rose C. R. (2008). "Developmental profile and properties of sulforhodamine 101-Labeled glial cells in acute brain slices of rat hippocampus." Journal of Neuroscience Methods 169(1): 84-92

Kajitani K., Nomaru H., Ifuku M., Yutsudo N., Dan Y., Miura T., Tsuchimoto D., Sakumi K., Kadoya T., Horie H., Poirier F., Noda M., & Nakabeppu Y. (2009). "Galectin-1 promotes basal and kainate-induced proliferation of neural progenitors in the dentate gyrus of adult mouse hippocampus." Cell Death and Differentiation 16(3): 417-427

Kalsi A. S., Greenwood K., Wilkin G., & Butt A. M. (2004). "Kir4.1 expression by astrocytes and oligodendrocytes in CNS white matter: A developmental study in the rat optic nerve." Journal of Anatomy 204(6): 475-485

Kamphuis W., Mamber C., Moeton M., Kooijman L., Sluijs J. A., Jansen A. H. P., Verveer M., de Groot L. R., Smith V. D., Rangarajan S., Rodríguez J. J., Orre M., & Hol E. M. (2012). "GFAP isoforms in adult mouse brain with a focus on neurogenic astrocytes and reactive astrogliosis in mouse models of Alzheimer disease." PLoS ONE 7(8): e42823

Kandel E., Schwartz J., & Jessell T. (2000). "Principles of Neural Science." McGraw-Hill Medical.

Kanemaru K., Kubota J., Sekiya H., Hirose K., Okubo Y., & Iino M. (2013). "Calcium-dependent N-cadherin up-regulation mediates reactive astrogliosis and neuroprotection after brain injury." Proceedings of the National Academy of Sciences 110(28): 11612-11617

Kang W., Balordi F., Su N., Chen L., Fishell G., & Hebert J. M. (2014). "Astrocyte activation is suppressed in both normal and injured brain by FGF signaling." Proceedings of the National Academy of Sciences 111(29): E2987-E2995

Karwoski C. J., Lu H. K., & Newman E. A. (1989). "Spatial buffering of light-evoked potassium increases by retinal Muller (glial) cells." Science 244(4904): 578-580

Kessaris N., Fogarty M., Iannarelli P., Grist M., Wegner M., & Richardson W. D. (2006). "Competing waves of oligodendrocytes in the forebrain and postnatal elimination of an embryonic lineage." Nature Neuroscience 9(2): 173-179

Kettenmann H., Backus K. H., & Schachner M. (1987). "γ-Aminobutyric acid opens Cl-channels in cultured astrocytes." Brain Research 404(1-2): 1-9

Kidd G. J., Ohno N., & Trapp B. D. (2013). "Biology of Schwann cells." In: G. Said & C. B. T. H. o. C. N. Krarup (Eds.), Handbook of Clinical Neurology (Vol. 115, pp. 55-79): Elsevier.

Kierdorf K., Erny D., Goldmann T., Sander V., Schulz C., Perdiguero E. G., Wieghofer P., Heinrich A., Riemke P., Hölscher C., Müller D. N., Luckow B., Brocker T., Debowski K., Fritz G., Opdenakker G., Diefenbach A., Biber K., Heikenwalder M., Geissmann F., Rosenbauer F., & Prinz M. (2013). "Microglia emerge from erythromyeloid precursors via Pu.1-and Irf8-dependent pathways." Nature Neuroscience 16(3): 273-280

Kim J.-Y., Jeong H. S., Chung T., Kim M., Lee J. H., Jung W. H., & Koo J. S. (2017). "The value of phosphohistone H3 as a proliferation marker for evaluating invasive breast cancers: A comparative study with Ki67." Oncotarget 8(39): 65064-65076

Kim J. V., & Dustin M. L. (2006). "Innate response to focal necrotic injury inside the blood-brain barrier." Journal of immunology (Baltimore, Md : 1950) 177(8): 5269-5277

Kimelberg H. K. (2004a). "Water homeostasis in the brain: Basic concepts." Neuroscience 129(4): 851-860

Kimelberg H. K. (2004b). "The role of hypotheses in current research, illustrated by hypotheses on the possible role of astrocytes in energy metabolism and cerebral blood flow: From Newton to now." Journal of Cerebral Blood Flow and Metabolism 24(11): 1235-1239

Kimelberg H. K. (2004c). "The problem of astrocyte identity." Neurochemistry International 45(2-3): 191-202

Kimelberg H. K. (2009). "Astrocyte Heterogeneity or Homogeneity?". In: V. Parpura & P. G. Haydon (Eds.), Astrocytes in (patho)physiology of the nervous system (pp. 1-26). Springer Science + Business Media, LLC 2009.

Kimelberg H. K. (2010). "Functions of Mature Mammalian Astrocytes: A Current View." The Neuroscientist 16(1): 79-106

Klar M., Surges R., & Feuerstein T. J. (2003). "Ih channels as modulators of presynaptic terminal function: ZD7288 increases NMDA-evoked [3H]-noradrenaline release in rat neocortex slices." Naunyn-Schmiedeberg's Archives of Pharmacology 367(4): 422-425

Ko C.-P., & Robitaille R. (2015). "Perisynaptic Schwann Cells at the Neuromuscular Synapse: Adaptable, Multitasking Glial Cells." Cold Spring Harbor Perspectives in Biology 7(10): a020503-a020503

Kofuji P., Ceelen P., Zahs K. R., Surbeck L. W., Lester H. A., & Newman E. A. (2000). "Genetic inactivation of an inwardly rectifying potassium channel (Kir4.1 subunit) in mice: Phenotypic impact in retina." The Journal of Neuroscience 20(15): 5733-5740

Kofuji P., Biedermann B., Siddharthan V., Raap M., Iandiev I., Milenkovic I., Thomzig A., Veh R. W., Bringmann A., & Reichenbach A. (2002). "Kir potassium channel subunit expression in retinal glial cells: Implications for spatial potassium buffering." GLIA 39(3): 292-303

Kole M. H. P., & Stuart G. J. (2012). "Signal Processing in the Axon Initial Segment." Neuron 73(2): 235-247

Kong S. K., Suen Y. K., Choy Y. M., Fung K. P., & Lee C. Y. (1991). "Membrane depolarization was required to induce DNA synthesis in murine macrophage cell line PU5-1.8." Immunopharmacology and Immunotoxicology 13(3): 329-339

Kreutzberg G. W. (1995). "Microglia, the first line of defence in brain pathologies." Arzneimittel-Forschung 45(3A): 357-360

Kriegstein A., & Alvarez-Buylla A. (2009). "The Glial Nature of Embryonic and Adult Neural Stem Cells." Annual Review of Neuroscience 32(1): 149-184

Kucheryavykh L. Y., Kucheryavykh Y. V., Inyushin M., Shuba Y. M., Sanabria P., Cubano L. A., Skatchkov S. N., & Eaton M. J. (2009). "Ischemia Increases {TREK-2} Channel Expression in Astrocytes: Relevance to Glutamate Clearance." Open Neurosci J 3(1): 40-47

Kucheryavykh Y. V., Kucheryavykh L. Y., Nichols C. G., Maldonado H. M., Baksi K., Reichenbach A., Skatchkov S. N., & Eaton M. J. (2006). "Downregulation of Kir4.1 inward rectifying potassium channel subunits by RNAi impairs potassium transfer and glutamate uptake by cultured cortical astrocytes." GLIA 55(3): 274-281

Kuffler S. W., & Nicholls J. G. (1966, 1966//). The physiology of neuroglial cells. Paper presented at the Ergebnisse der physiologie biologischen chemie und experimentellen pharmakologie, Berlin, Heidelberg.

Lang B., Liu H. L., Liu R., Feng G. D., Jiao X. Y., & Ju G. (2004). "Astrocytes in injured adult rat spinal cord may acquire the potential of neural stem cells." Neuroscience 128(4): 775-783

Langer J., & Rose C. R. (2009). "Synaptically induced sodium signals in hippocampal astrocytes in situ." Journal of Physiology 587(24): 5859-5877

Lau Y. T., Wong C. K., Luo J., Leung L. H., Tsang P. F., Bian Z. X., & Tsang S. Y. (2011). "Effects of hyperpolarization-activated cyclic nucleotide-gated (HCN) channel blockers on the proliferation and cell cycle progression of embryonic stem cells." Pflugers Archiv European Journal of Physiology 461(1): 191-202

Lawson L. J., Perry V. H., Dri P., & Gordon S. (1990). "Heterogeneity in the distribution and morphology of microglia in the normal adult mouse brain." Neuroscience 39(1): 151-170

Le Mercier M., Fortin S., Mathieu V., Kiss R., & Lefranc F. (2010). "Galectins and gliomas." Brain Pathology 20(1): 17-27

Lee S. H., Kim W. T., Cornell-Bell A. H., & Sontheimer H. (1994). "Astrocytes exhibit regional specificity in gap-junction coupling." GLIA 11(4): 315-325

Lenhossék M. l. (1895). "Der feinere Bau des Nervensystems im Lichte neuester Forschungen; eine allgemeine Betrachtung der Strukturprinzipien des Nervensystems, nebst einer Darstellung des feineren Baues des Rückenmarkes." (Vol. 2). Berlin: Fischer´s Medicin. Buchhandlung H. Kornfeld.

Lenz A., Franklin G. A., & Cheadle W. G. (2007). "Systemic inflammation after trauma." Injury 38(12): 1336-1345

Lenzi D., Radke K., & Wilson M. (1991). "Clonal cells from embryonic retinal cell lines express qualitative electrophysiological differences." Journal of Neurobiology 22(8): 823-836

Lenzi D., Radke K., & Wilson M. (1993). "Symmetrical segregation of potassium channels at cytokinesis." Journal of Neurobiology 24(5): 675-686

Levison S. W., Chuang C., Abramson B. J., & Goldman J. E. (1993). "The migrational patterns and developmental fates of glial precursors in the rat subventricular zone are temporally regulated." Development (Cambridge, England) 119(3): 611-622

Levison S. W., & Goldman J. E. (1993). "Both oligodendrocytes and astrocytes develop from progenitors in the subventricular zone of postnatal rat forebrain." Neuron 10(2): 201-212

Levison S. W., & Goldman J. E. (1997). "Multipotential and lineage restricted precursors coexist in the mammalian perinatal subventricular zone." Journal of Neuroscience Research 48(2): 83-94

Lewis A. S., & Chetkovich D. M. (2011). "HCN channels in behavior and neurological disease: Too hyper or not active enough?" Molecular and Cellular Neuroscience 46(2): 357-367

Liauw J., Hoang S., Choi M., Eroglu C., Choi M., Sun G. H., Percy M., Wildman-Tobriner B., Bliss T., Guzman R. G., Barres B. A., & Steinberg G. K. (2008). "Thrombospondins 1 and 2 are necessary for synaptic plasticity and functional recovery after stroke." Journal of Cerebral Blood Flow and Metabolism 28(10): 1722-1732

Lin C. S., Boltz R. C., Blake J. T., Nguyen M., Talento A., Fischer P. A., Springer M. S., Sigal N. H., Slaughter R. S., & Garcia M. L. (1993). "Voltage-gated potassium channels

regulate calcium-dependent pathways involved in human T lymphocyte activation." The Journal of Experimental Medicine 177(3): 637-645

Lin J. H. C., Lou N., Kang N., Takano T., Hu F., Han X., Xu Q., Lovatt D., Torres A., Willecke K., Yang J., Kang J., & Nedergaard M. (2008). "A Central Role of Connexin 43 in Hypoxic Preconditioning." Journal of Neuroscience 28(3): 681-695

Liu X., Zhang Z., Guo W., Burnstock G., He C., & Xiang Z. (2013). "The superficial glia limitans of mouse and monkey brain and spinal cord." Anatomical Record 296(7): 995-1007

Lotz M. M., Wang H., Song J. C., Pories S. E., & Matthews J. B. (2004). "K+ channel inhibition accelerates intestinal epithelial cell wound healing." Wound Repair and Regeneration 12(5): 565-574

Lovisolo D., Bonelli G., Baccino F. M., Peres A., Alonzo F., & Munaron L. (1992). "Two currents activated by epidermal growth factor in EGFR-T17 fibroblasts." BBA - Biomembranes 1104(1): 73-82

Ludwin S. K. (1979). "The perineuronal satellite oligodendrocyte." Acta Neuropathologica 47(1): 49-53

Lui H., Zhang J., Makinson S. R., Cahill M. K., Kelley K. W., Huang H. Y., Shang Y., Oldham M. C., Martens L. H., Gao F., Coppola G., Sloan S. A., Hsieh C. L., Kim C. C., Bigio E. H., Weintraub S., Mesulam M. M., Rademakers R., MacKenzie I. R., Seeley W. W., Karydas A., Miller B. L., Borroni B., Ghidoni R., Farese R. V., Paz J. T., Barres B. A., & Huang E. J. (2016). "Progranulin Deficiency Promotes Circuit-Specific Synaptic Pruning by Microglia via Complement Activation." Cell 165(4): 921-935

Lundgaard I., Osório M. J., Kress B. T., Sanggaard S., & Nedergaard M. (2014). "White matter astrocytes in health and disease." Neuroscience 276: 161-173

Lunn K. F., Baas P. W., & Duncan I. D. (1997). "Microtubule organization and stability in the oligodendrocyte." The Journal of Neuroscience 17(13): 4921-4932

Ma B., Xu G., Wang W., Enyeart J. J., & Zhou M. (2014). "Dual patch voltage clamp study of low membrane resistance astrocytes in situ." Molecular Brain 7(1): 1-12

Ma B., Buckalew R., Du Y., Kiyoshi C. M., Alford C. C., Wang W., McTigue D. M., Enyeart J. J., Terman D., & Zhou M. (2016). "Gap junction coupling confers isopotentiality on astrocyte syncytium." GLIA 64(2): 214-226

MacFarlane S. N., & Sontheimer H. (1997). "Electrophysiological Changes That Accompany Reactive GliosisIn Vitro." The Journal of Neuroscience 17(19): 7316-7329

MacFarlane S. N., & Sontheimer H. (2000). "Changes in ion channel expression accompany cell cycle progression of spinal cord astrocytes." GLIA 30(1): 39-48

MacVicar B. A., & Newman E. A. (2015). "Astrocyte Regulation of Blood Flow in the Brain." Cold Spring Harb. Perspect. Biol 7: 1-15

Magni M., Meldolesi J., & Pandiella A. (1991). "Ionic events induced by epidermal growth factor: Evidence that hyperpolarization and stimulated cation influx play a role in the stimulation of cell growth." Journal of Biological Chemistry 266(10): 6329-6335

Malatesta P., Hartfuss E., & Götz M. (2000). "Isolation of radial glial cells by fluorescent-activated cell sorting reveals a neuronal lineage." Development 127(24): 5253-5263

Malatesta P., Hack M. A., Hartfuss E., Kettenmann H., Klinkert W., Kirchhoff F., & Götz M. (2003). "Neuronal or glial progeny: Regional differences in radial glia fate." Neuron 37(5): 751-764

Martín-López E., García-Marques J., Núñez-Llaves R., & López-Mascaraque L. (2013). "Clonal Astrocytic Response to Cortical Injury." PLoS ONE 8(9): e74039

Marx T., Gisselmann G., Störtkuhl K. F., Hovemann B. T., & Hatt H. (1999). "Molecular cloning of a putative voltage- and cyclic nucleotide-gated ion channel present in the antennae and eyes of Drosophila melanogaster." Invertebrate Neuroscience 4(1): 55-63

Matthias K., Kirchhoff F., Seifert G., Hüttmann K., Matyash M., Kettenmann H., & Steinhäuser C. (2003). "Segregated expression of AMPA-type glutamate receptors and glutamate transporters defines distinct astrocyte populations in the mouse hippocampus." The Journal of Neuroscience 23(5): 1750-1758

Matyash V., & Kettenmann H. (2010). "Heterogeneity in astrocyte morphology and physiology." Brain Research Reviews 63(1-2): 2-10

Mazzetti S., Frigerio S., Gelati M., Salmaggi A., & Vitellaro-Zuccarello L. (2004). "Lycopersicon esculentum lectin: an effective and versatile endothelial marker of normal and tumoral blood vessels in the central nervous system." European journal of histochemistry : EJH 48(4): 423-428

McKhann G. M., D'Ambrosio R., & Janigro D. (1997). "Heterogeneity of astrocyte resting membrane potentials and intercellular coupling revealed by whole-cell and gramicidin-perforated patch recordings from cultured neocortical and hippocampal slice astrocytes." The Journal of Neuroscience 17(18): 6850-6863

Mishima T., Sakatani S., & Hirase H. (2007). "Intracellular labeling of single cortical astrocytes in vivo." Journal of Neuroscience Methods 166(1): 32-40

Mishima T., & Hirase H. (2010). "In Vivo Intracellular Recording Suggests That Gray Matter Astrocytes in Mature Cerebral Cortex and Hippocampus Are Electrophysiologically Homogeneous." Journal of Neuroscience 30(8): 3093-3100

Mittelbronn M., Dietz K., Schluesener H. J., & Meyermann R. (2001). "Local distribution of microglia in the normal adult human central nervous system differs by up to one order of magnitude." Acta Neuropathologica 101(3): 249-255

Mizee M. R., Nijland P. G., van der Pol S. M. A., Drexhage J. A. R., van het Hof B., Mebius R., van der Valk P., van Horssen J., Reijerkerk A., & de Vries H. E. (2014). "Astrocyte-derived retinoic acid: a novel regulator of blood–brain barrier function in multiple sclerosis." Acta Neuropathologica 128(5): 691-703

Møllgård K., Balslev Y., Lauritzen B., & Saunders N. R. (1987). "Cell junctions and membrane specializations in the ventricular zone (germinal matrix) of the developing sheep brain: A CSF-brain barrier." Journal of Neurocytology 16(4): 433-444

Montana R. A., Folkerth R. D., De Girolami U., Anthony D. C., Colodner K. J., & Feany M. B. (2005). "Proliferative Potential of Human Astrocytes." Journal of Neuropathology & Experimental Neurology 64(2): 163-169

Moroni R. F., Inverardi F., Regondi M. C., Pennacchio P., & Frassoni C. (2015). "Developmental expression of Kir4.1 in astrocytes and oligodendrocytes of rat somatosensory cortex and hippocampus." International Journal of Developmental Neuroscience 47: 198-205

Mosser C. A., Baptista S., Arnoux I., & Audinat E. (2017). "Microglia in CNS development: Shaping the brain for the future." Progress in Neurobiology 149-150: 1-20

Müller. (1851). "Zur Histologie der Netzhaut." Zeitschift fur Wissenschaft und Zoologie 3: 234-237

Müller J., Reyes-Haro D., Pivneva T., Nolte C., Schaette R., Lübke J., & Kettenmann H. (2009). "The principal neurons of the medial nucleus of the trapezoid body and NG2 + glial cells receive coordinated excitatory synaptic input." The Journal of General Physiology 134(2): 115-127

Müller T., Fritschy J. M., Grosche J., Pratt G. D., Mohler H., & Kettenmann H. (1994). "Developmental regulation of voltage-gated K+ channel and GABAA receptor expression in Bergmann glial cells." The Journal of Neuroscience 14(5): 2503-2514

Müller T., & Kettenmann H. (1995). "Physiology of Bergmann Glial Cells." In: R. J. Bradley, R. Harris, & B. T. Adron (Eds.), International Review of Neurobiology (Vol. 38, pp. 341-359): Academic Press.

Mummery C. L., Boonstra J., Van Der Saag P. T., & De Laat S. W. (1982). "Modulations of NA+ transport during the cell cycle of neuroblastoma cells." Journal of Cellular Physiology 112(1): 27-34

Murray a. W. (1992). "Creative blocks: cell-cycle checkpoints and feedback controls." Nature 359(6396): 599-604

Nagelhus E. A., & Ottersen O. P. (2013). "Physiological Roles of Aquaporin-4 in Brain." Physiological Reviews 93(4): 1543-1562

Neary J. T., Kang Y., Willoughby K. A., & Ellis E. F. (2003). "Activation of extracellular signal-regulated kinase by stretch-induced injury in astrocytes involves extracellular ATP and P2 purinergic receptors." The Journal of Neuroscience 23(6): 2348-2356

Nedergaard M., & Verkhratsky A. (2012). "Artifact versus reality-How astrocytes contribute to synaptic events." GLIA 60(7): 1013-1023

Neitz A., Mergia E., Eysel U. T., Koesling D., & Mittmann T. (2011). "Presynaptic nitric oxide/cGMP facilitates glutamate release via hyperpolarization-activated cyclic nucleotide-gated channels in the hippocampus." European Journal of Neuroscience 33(9): 1611-1621

Neusch C. (2006). "Lack of the Kir4.1 Channel Subunit Abolishes K+ Buffering Properties of Astrocytes in the Ventral Respiratory Group: Impact on Extracellular K+ Regulation." Journal of Neurophysiology 95(3): 1843-1852

Newlaczyl A. U., & Yu L.-G. (2011). "Galectin-3 – A jack-of-all-trades in cancer." Cancer Letters 313(2): 123-128

Nichols C. G., & Lopatin A. N. (1997). "Inward Rectifier Potassium Channels." Annual Review of Physiology 59(1): 171-191

Nishiyama A., Yang Z., Butt A., & Shakespeare W. (2005). "Astrocytes and NG2-glia : what's in a name?" Jounal of anatomy 207(6): 687-693

Nishiyama A., Komitova M., Suzuki R., & Zhu X. (2009). "Polydendrocytes (NG2 cells): Multifunctional cells with lineage plasticity." Nature Reviews Neuroscience 10(1): 9-22

Noctor S. C., Flint A. C., Weissman T. A., Dammerman R. S., & Kriegstein A. R. (2001). "Neurons derived from radial glial cells establish radial units in neocortex." Nature 409(6821): 714-720

Noctor S. C., Flint A. C., Weissman T. A., Wong W. S., Clinton B. K., & Kriegstein A. R. (2002). "Dividing Precursor Cells of the Embryonic Cortical Ventricular Zone Have Morphological and Molecular Characteristics of Radial Glia." The Journal of Neuroscience 22(8): 3161-3173

Noctor S. C., Martínez-Cerdeño V., & Kriegstein A. (2007). "Contribution of intermediate progenitor cells to cortical histogenesis." Archives of Neurology 64(5): 639-642

Norenberg M. D., Rama Rao K. V., & Jayakumar A. R. (2009). "Signaling factors in the mechanism of ammonia neurotoxicity." Metabolic Brain Disease 24(1): 103-117

Nowak L., Ascher P., & Berwald-Netter Y. (1987). "Ionic channels in mouse astrocytes in culture." J Neurosci 7(1): 101-109

Oberheim N. A., Wang X., Goldman S., & Nedergaard M. (2006). "Astrocytic complexity distinguishes the human brain." Trends in Neurosciences 29(10): 547-553

Oberheim N. A., Tian G. F., Han X., Peng W., Takano T., Ransom B. R., & Nedergaard M. (2008). "Loss of Astrocytic Domain Organization in the Epileptic Brain." Journal of Neuroscience 28(13): 3264-3276

Oberheim N. A., Takano T., Han X., He W., Lin J. H. C., Wang F., Xu Q., Wyatt J. D., Pilcher W., Ojemann J. G., Ransom B. R., Goldman S. A., & Nedergaard M. (2009). "Uniquely Hominid Features of Adult Human Astrocytes." Journal of Neuroscience 29(10): 3276-3287

Ogata K., & Kosaka T. (2002). "Structural and quantitative analysis of astrocytes in the mouse hippocampus." Neuroscience 113(1): 221-233

Oikonomou G., & Shaham S. (2011). "The glia of caenorhabditis elegans." GLIA 59(9): 1253-1263

Olsen M. L., & Sontheimer H. (2004). "Mislocalization of Kir channels in malignant glia." GLIA 46(1): 63-73

Olsen M. L., Campbell S. L., & Sontheimer H. (2007). "Differential Distribution of Kir4.1 in Spinal Cord Astrocytes Suggests Regional Differences in K+ Homeostasis." Journal of Neurophysiology 98(2): 786-793

Olsen M. L., Campbell S. C., McFerrin M. B., Floyd C. L., & Sontheimer H. (2010). "Spinal cord injury causes a wide-spread, persistent loss of Kir4.1 and glutamate transporter 1: Benefit of 17β-oestradiol treatment." Brain 133(4): 1013-1025

Orr C. W., Yoshikawa-Fukada M., & Ebert J. D. (1972). "Potassium: effect on DNA synthesis and multiplication of baby-hamster kidney cells: (cell cycle-membrane potential-synchronization-transformation)." Proceedings of the National Academy of Sciences of the United States of America 69(1): 243-247

Ouadid-Ahidouch H., Le Bourhis X., Roudbaraki M., Toillon R. A., Delcourt P., & Prevarskaya N. (2001). "Changes in the K+ current-density of MCF-7 cells during progression through the cell cycle: possible involvement of a h-ether.a-gogo K+ channel." Receptors & channels 7(5): 345-356

Ouadid-Ahidouch H. (2004). "Functional and molecular identification of intermediate-conductance Ca2+-activated K+ channels in breast cancer cells: association with cell cycle progression." AJP: Cell Physiology 287(1): C125-C134

Ouwerkerk R., Bleich K. B., Gillen J. S., Pomper M. G., & Bottomley P. A. (2003). "Tissue Sodium Concentration in Human Brain Tumors as Measured with 23Na MR Imaging." Radiology 227(2): 529-537

Oviedo N. J., & Levin M. (2007). "Smedinx-11 Is a Planarian Stem Cell Gap Junction Gene Required for Regeneration and Homeostasis." Development 134(17): 3121-3131

Pakkenberg B., & Gundersen H. J. G. (1988). "Total number of neurons and glial cells in human brain nuclei estimated by the disector and the fractionator." Journal of Microscopy 150(1): 1-20

Papadopoulos M. C., & Verkman A. S. (2013). "Aquaporin water channels in the nervous system." Nature Reviews Neuroscience 14(4): 265-277

Pardo L. A., Brüggemann A., Camacho J., & Stühmer W. (1998). "Cell cycle-related Changes in the Conducting Properties of r-eag K+ Channels." The Journal of Cell Biology 143(3): 767-775

Parpura V., & Verkhratsky A. (2014). "Introduction to Neuroglia." Morgan & Claypool Life Sciences.

Partiseti M., Korn H., & Choquet D. (1993). "Pattern of Potassium Channel Expression in Proliferating B Lymphocytes Depends upon the Mode of Activation." The Journal of Immunology 151(5): 2462-2470

Passlick S., Grauer M., Schafer C., Jabs R., Seifert G., & Steinhauser C. (2013). "Expression of the y2-Subunit Distinguishes Synaptic and Extrasynaptic GABA A Receptors in NG2 Cells of the Hippocampus." Journal of Neuroscience 33(29): 12030-12040

Pastor A., Chvátal A., Syková E., & Kettenmann H. (1995). "Glycine- and GABA-activated Currents in Identified Glial Cells of the Developing Rat Spinal Cord Slice." European Journal of Neuroscience 7(6): 1188-1198

Pedrazzi M., Melloni E., & Sparatore B. (2010). "Selective Pro-Inflammatory Activation of Astrocytes by High Mobility Group Box 1 Protein Signaling." New Insights to Neuroimmune Biology: 53-72

Pekny M., & Nilsson M. (2005). "Astrocyte activation and reactive gliosis." GLIA 50(4): 427-434

Pekny M., & Pekna M. (2014). "Astrocyte Reactivity and Reactive Astrogliosis: Costs and Benefits." Physiological Reviews 94(4): 1077-1098

Pekny M., & Pekna M. (2016). "Reactive gliosis in the pathogenesis of CNS diseases." Biochimica et Biophysica Acta - Molecular Basis of Disease 1862(3): 483-491

Pekny M., Pekna M., Messing A., Steinhäuser C., Lee J. M., Parpura V., Hol E. M., Sofroniew M. V., & Verkhratsky A. (2016). "Astrocytes: a central element in neurological diseases." Acta Neuropathologica 131(3): 323-345

Pekny M., Wilhelmsson U., Tatlisumak T., & Pekna M. (2018). "Astrocyte activation and reactive gliosis—A new target in stroke?" Neuroscience Letters(July): 0-1

Pellerin L., & Magistretti P. J. (1994). "Glutamate uptake into astrocytes stimulates aerobic glycolysis: a mechanism coupling neuronal activity to glucose utilization." Proceedings of the National Academy of Sciences 91(22): 10625-10629

Pellerin L., & Magistretti P. J. (2012). "Sweet sixteen for ANLS." Journal of Cerebral Blood Flow and Metabolism 32(7): 1152-1166

Pelvig D. P., Pakkenberg H., Stark A. K., & Pakkenberg B. (2008). "Neocortical glial cell numbers in human brains." Neurobiology of Aging 29(11): 1754-1762

Pereanu W., Shy D., & Hartenstein V. (2005). "Morphogenesis and proliferation of the larval brain glia in Drosophila." Developmental Biology 283(1): 191-203

Pérez-Cerdá F., Sánchez-Gómez M. V., & Matute C. (2015). "Pío del Río Hortega and the discovery of the oligodendrocytes." Frontiers in Neuroanatomy 9(July): 7-12

Pfrieger F. W. (2010). "Role of glial cells in the formation and maintenance of synapses." Brain Research Reviews 63(1-2): 39-46

Pivonkova H., Benesova J., Butenko O., Chvatal A., & Anderova M. (2010). "Impact of global cerebral ischemia on K+ channel expression and membrane properties of glial cells in the rat hippocampus." Neurochemistry International 57(7): 783-794

Planas A. M., Justicia C., Soriano M. A., & Ferrer I. (1998). "Epidermal growth factor receptor in proliferating reactive glia following transient focal ischemia in the rat brain." GLIA 23(2): 120-129

Ponath G., Schettler C., Kaestner F., Voigt B., Wentker D., Arolt V., & Rothermundt M. (2007). "Autocrine S100B effects on astrocytes are mediated via RAGE." Journal of Neuroimmunology 184(1-2): 214-222

Pongs O. (1999). "Voltage-gated potassium channels: From hyperexcitability to excitement." FEBS Letters 452(1-2): 31-35

Poopalasundaram S., Knott C., Shamotienko O. G., Foran P. G., Dolly J. O., Ghiani C. A., Gallo V., & Wilkin G. P. (2000). "Glial heterogeneity in expression of the inwardly rectifying K+ channel, Kir4.1, in adult rat CNS." GLIA 30(4): 362-372

Prasad M. S., & Charney R. M. (2019). "Specification and formation of the neural crest : Perspectives on lineage segregation." Wiley genesis 57: 1-21

Price M., Lee S. C., & Deutsch C. (1989). "Charybdotoxin inhibits proliferation and interleukin 2 production in human peripheral blood lymphocytes." Physiology 86: 10171-10175

Qu W. S., Wang Y. H., Ma J. F., Tian D. S., Zhang Q., Pan D. J., Yu Z. Y., Xie M. J., Wang J. P., & Wang W. (2011). "Galectin-1 attenuates astrogliosis-associated injuries and improves recovery of rats following focal cerebral ischemia." Journal of Neurochemistry 116(2): 217-226

Raap M., Biedermann B., Braun P., Milenkovic I., Skatchkov S. N., Bringmann A., & Reichenbach A. (2002). "Diversity of kir channel subunit mRNA expressed by retinal glial cells of the guinea-pig." NeuroReport 13(8): 1037-1040

Radojcic T., & Pentreath V. W. (1979). "Invertebrate glia." Progress in Neurobiology 12(2): 115-179

Rakic P. (1971). "Guidance of neurons migrating to the fetal monkey neocortex." Brain Research 33(2): 471-476

Rakic P. (1988). "Specification of cerebral cortical areas." Science 241(4862): 170-176

Ramón-Cueto A., & Avila J. (1998). "Olfactory ensheathing glia: Properties and function." Brain Research Bulletin 46(3): 175-187

Ramon y Cajal S. (1920). "Una modificación del metodo de Bielschowsky para la impregnacion de la neuroglia comum y mesoglia y algunos consejos acerca de la tecnica del oro-sublimado." Trab lab Invest Biol Univ Madr 18: 109-127

Ramon y Cajal S. (1928). "Degeneration and regeneration of the nervous system." Oxford, England: Clarendon Press.

Ransom B. R., Behar T., & Nedergaard M. (2003). "New roles for astrocytes (stars at last)." Trends in Neurosciences 26(10): 520-522

Ransom C. B., & Sontheimer H. (1995). "Biophysical and pharmacological characterization of inwardly rectifying K+ currents in rat spinal cord astrocytes." J Neurophysiol 73(1): 333-346

Rao K. V. R., Panickar K. S., Jayakumar A. R., & Norenberg M. D. (2005). "Astrocytes protect neurons from ammonia toxicity." Neurochemical Research 30(10): 1311-1318

Reichenbach A. (1989). "Glia:Neuron index: Review and hypothesis to account for different values in various mammals." GLIA 2(2): 71-77

Reichenbach A., Siegel A., Rickmann M., Wolff J. R., Noone D., & Robinson S. R. (1995). "Distribution of Bergmann glial somata and processes: implications for function." Journal fur Hirnforschung 36(4): 509-517

Reichenbach A., Derouiche A., & Kirchhoff F. (2010). "Morphology and dynamics of perisynaptic glia." Brain Research Reviews 63(1-2): 11-25

Reichenbach A., & Bringmann A. (2017). " Comparative Anatomy of Glial Cells in Mammals." In: J. H. B. T. Kaas (Ed.), Evolution of Nervous Systems (pp. 309-348). Oxford: Academic Press.

Reimann F., & Ashcroft F. M. (1999). "Inwardly rectifying potassium channels Frank Reimann and Frances M Ashcroft." Current opinion in cell biology 11: 503-508

Reyes-Haro D., Müller J., Boresch M., Pivneva T., Benedetti B., Scheller A., Nolte C., & Kettenmann H. (2010). "Neuron–astrocyte interactions in the medial nucleus of the trapezoid body." The Journal of General Physiology 135(6): 583-594

Rice M. E. (2000). "Ascorbate regulation and its neuroprotective role in the brain." Trends in Neurosciences 23(5): 209-216

Rieder C. L. (2011). "Mitosis in vertebrates: The G2/M and M/A transitions and their associated checkpoints." Chromosome Research 19(3): 291-306

Robel S., Mori T., Zoubaa S., Schlegel J. r., Sirko S., Faissner A., Goebbels S., Dimou L., & G??tz M. (2009). "Conditional deletion of ß1-integrin in astroglia causes partial reactive gliosis." GLIA 57(15): 1630-1647

Robel S., Bardehle S., Lepier A., Brakebusch C., & Gotz M. (2011a). "Genetic Deletion of Cdc42 Reveals a Crucial Role for Astrocyte Recruitment to the Injury Site In Vitro and In Vivo." Journal of Neuroscience 31(35): 12471-12482

Robel S., Berninger B., & Götz M. (2011b). "The stem cell potential of glia: Lessons from reactive gliosis." Nature Reviews Neuroscience 12(2): 88-104

Rodríguez E. M., Blázquez J. L., Pastor F. E., Peláez B., Peña P., Peruzzo B., & Amat P. (2005). "Hypothalamic Tanycytes: A Key Component of Brain–Endocrine Interaction." International Review of Cytology 247: 89-164

Roeper J., & Liss B. (2001). "Molecular physiology of neuronal K-ATP channels." Molecular Membrane Biology 18(2): 117-127

Rolls A., Shechter R., & Schwartz M. (2009). "Bright side of glial scar in CNS repair." 10: 235-241

Rose C. R., & Ransom B. R. (1996). "Mechanisms of H+ and Na+ changes induced by glutamate, kainate, and D-aspartate in rat hippocampal astrocytes." The Journal of Neuroscience 16(17): 5393-5404

Rose C. R., & Verkhratsky A. (2016). "Principles of sodium homeostasis and sodium signalling in astroglia." GLIA 64(10): 1611-1627

Roth T. L., Nayak D., Atanasijevic T., Koretsky A. P., Latour L. L., & McGavern D. B. (2014). "Transcranial amelioration of inflammation and cell death after brain injury." Nature 505(7482): 223-228

Rothstein J. D., Dykes-Hoberg M., Pardo C. A., Bristol L. A., Jin L., Kuncl R. W., Kanai Y., Hediger M. A., Wang Y., Schielke J. P., & Welty D. F. (1996). "Knockout of glutamate transporters reveals a major role for astroglial transport in excitotoxicity and clearance of glutamate." Neuron 16(3): 675-686

Roy M. L., & Sontheimer H. (1995). "Beta-Adrenergic Modulation of Glial Inwardly Rectifying Potassium Channels." Journal of Neurochemistry 64(4): 1576-1584

Ruiz M., & Ortega A. (1995). "Characterization of an Na(+)-dependent glutamate/aspartate transporter from cultured Bergmann glia." NeuroReport 6(15): 2041-2044

Rusnakova V., Honsa P., Dzamba D., Ståhlberg A., Kubista M., & Anderova M. (2013). "Heterogeneity of Astrocytes: From Development to Injury - Single Cell Gene Expression." PLoS ONE 8(8)

Rzigalinski B. A., Liang S., McKinney J. S., Willoughby K. A., & Ellis E. F. (1997). "Effect of Ca2+ on in vitro astrocyte injury." Journal of Neurochemistry 68(1): 289-296

Rzigalinski B. A., Weber J. T., Willoughby K. A., & Ellis E. F. (1998). "Intracellular Free Calcium Dynamics in Stretch-Injured Astrocytes." Journal of Neurochemistry 70(6): 2377-2385

Saab Aiman S., Tzvetavona Iva D., Trevisiol A., Baltan S., Dibaj P., Kusch K., Möbius W., Goetze B., Jahn Hannah M., Huang W., Steffens H., Schomburg Eike D., Pérez-Samartín A., Pérez-Cerdá F., Bakhtiari D., Matute C., Löwel S., Griesinger C., Hirrlinger J., Kirchhoff F., & Nave K.-A. (2016). "Oligodendroglial NMDA Receptors Regulate Glucose Import and Axonal Energy Metabolism." Neuron 91(1): 119-132

Saijo K., & Glass C. K. (2011). "Microglial cell origin and phenotypes in health and disease." Nature Reviews Immunology 11(11): 775-787

Sakaguchi M., Shingo T., Shimazaki T., Okano H. J., Shiwa M., Ishibashi S., Oguro H., Ninomiya M., Kadoya T., Horie H., Shibuya A., Mizusawa H., Poirier F., Nakauchi H., Sawamoto K., & Okano H. (2006). "A carbohydrate-binding protein, Galectin-1, promotes proliferation of adult neural stem cells." Proceedings of the National Academy of Sciences 103(18): 7112-7117

Sakry D., Karram K., & Trotter J. (2011). "Synapses between NG2 glia and neurons." Journal of Anatomy 219(1): 2-7

Scafidi J., Hammond T. R., Scafidi S., Ritter J., Jablonska B., Roncal M., Szigeti-Buck K., Coman D., Huang Y., McCarter R. J., Hyder F., Horvath T. L., & Gallo V. (2014). "Intranasal epidermal growth factor treatment rescues neonatal brain injury." Nature 506(7487): 230-234

Schafer D. P., & Stevens B. (2013). "Phagocytic glial cells: Sculpting synaptic circuits in the developing nervous system." Current Opinion in Neurobiology 23(6): 1034-1040

Schitine C., Nogaroli L., Costa M. R., & Hedin-Pereira C. (2015). "Astrocyte heterogeneity in the brain: from development to disease." Frontiers in Cellular Neuroscience 9: 1-11

Schmechel D. E., & Rakic P. (1979). "A golgi study of radial glial cells in developing monkey telencephalon: Morphogenesis and transformation into astrocytes." Anatomy and Embryology 156(2): 115-152

Schönrock L. M., Kuhlmann T., Adler S., Bitsch A., & Brück W. (1998). "Identification of glial cell proliferation in early multiple sclerosis lesions." Neuropathology and applied neurobiology 24(4): 320-330

Seifert G., Huttmann K., Binder D. K., Hartmann C., Wyczynski A., Neusch C., & Steinhauser C. (2009). "Analysis of Astroglial K+ Channel Expression in the Developing Hippocampus Reveals a Predominant Role of the Kir4.1 Subunit." Journal of Neuroscience 29(23): 7474-7488

Shieh R. C., Chang J. C., & Arreola J. (1998). "Interaction of Ba2+with the pores of the cloned inward rectifier K+channels Kir2.1 Expressed in Xenopus oocytes." Biophysical Journal 75(5): 2313-2322

Shih A. Y., Johnson D. A., Wong G., Kraft A. D., Jiang L., Erb H., Johnson J. A., & Murphy T. H. (2003). "Coordinate regulation of glutathione biosynthesis and release by Nrf2-expressing glia potently protects neurons from oxidative stress." The Journal of Neuroscience 23(8): 3394-3406

Shoukimas G. M., & Hinds J. W. (1978). "The development of the cerebral cortex in the embryonic mouse: an electron microscopic serial section analysis." J Comp Neurol 179(4): 795-830

Silver J., & Miller J. H. (2004). "Regeneration beyond the glial scar." Nature Reviews Neuroscience 5(2): 146-156

Simon C., G??tz M., & Dimou L. (2011). "Progenitors in the adult cerebral cortex: Cell cycle properties and regulation by physiological stimuli and injury." GLIA 59(6): 869-881

Simpson J. E., Ince P. G., Lace G., Forster G., Shaw P. J., Matthews F., Savva G., Brayne C., & Wharton S. B. (2010). "Astrocyte phenotype in relation to Alzheimer-type pathology in the ageing brain." Neurobiology of Aging 31(4): 578-590

Sirko S., Behrendt G., Johansson P. A., Tripathi P., Costa M., Bek S., Heinrich C., Tiedt S., Colak D., Dichgans M., Fischer I. R., Plesnila N., Staufenbiel M., Haass C., Snapyan M., Saghatelyan A., Tsai L. H., Fischer A., Grobe K., Dimou L., & Götz M. (2013). "Reactive glia in the injured brain acquire stem cell properties in response to sonic hedgehog glia." Cell Stem Cell 12(4): 426-439

Sirko S., Irmler M., Gascón S., Bek S., Schneider S., Dimou L., Obermann J., De Souza Paiva D., Poirier F., Beckers J., Hauck S. M., Barde Y. A., & Götz M. (2015). "Astrocyte reactivity after brain injury-: The role of galectins 1 and 3." GLIA 63(12): 2340-2361

Sofroniew M. V. (2009). "Molecular dissection of reactive astrogliosis and glial scar formation." Trends in Neurosciences 32(12): 638-647

Sofroniew M. V., & Vinters H. V. (2010). "Astrocytes: Biology and pathology." Acta Neuropathologica 119(1): 7-35

Sofroniew M. V. (2014). "Multiple roles for astrocytes as effectors of cytokines and inflammatory mediators." Neuroscientist 20(2): 160-172

Sonnewald U., Westergaard N., & Schousboe A. (1998). "Glutamate transport and metabolism in astrocytes." GLIA 21(1): 56-63

Sontheimer H., Trotter J., Schachner M., & Kettenmann H. (1989). "Channel expression correlates with differentiation stage during the development of Oligodendrocytes from their precursor cells in culture." Neuron 2(2): 1135-1145

Sontheimer H., Black J. A., Ransom B. R., & Waxman S. G. (1992). "Ion channels in spinal cord astrocytes in vitro. I. Transient expression of high levels of Na+ and K+ channels." Journal of Neurophysiology 68(4)

Sontheimer H. (1994). "Voltage-dependent ion channels in glial cells." GLIA 11(2): 156-172

Sontheimer H., Pappas C. A., & Haven N. (1994). "Astrocyte Na + Channels Are Required for Maintenance Na + / K + -ATPase Activity." The Journal of Neuroscience 14(5): 2464-2475

Spassky N. (2005). "Adult Ependymal Cells Are Postmitotic and Are Derived from Radial Glial Cells during Embryogenesis." Journal of Neuroscience 25(1): 10-18

Sriram K., Benkovic S. A., Hebert M. A., Miller D. B., & O'Callaghan J. P. (2004). "Induction of gp130-related cytokines and activation of JAK2/STAT3 pathway in astrocytes precedes up-regulation of glial fibrillary acidic protein in the 1-methyl-4-phenyl-1,2,3,6-tetrahydropyridine model of neurodegeneration: Key signaling pathway for ast." Journal of Biological Chemistry 279(19): 19936-19947

Stallcup W. B. (1981). "The NG2 antigen, a putative lineage marker: Immunofluorescent localization in primary cultures of rat brain." Developmental Biology 83(1): 154-165

Standen N. B., & Stanfield P. R. (1978). "A potential- and time-dependent blockade of inward rectification in frog skeletal muscle fibres by barium and strontium ions." The Journal of Physiology 280(1): 169-191

Steinhäuser C., Berger T., Frotscher M., & Kettenmann H. (1992). "Heterogeneity in the Membrane Current Pattern of Identified Glial Cells in the Hippocampal Slice." European Journal of Neuroscience 4(6): 472-484

Stellwagen D., & Malenka R. C. (2006). "Synaptic scaling mediated by glial TNF-α." Nature 440(7087): 1054-1059

Stephan J., & Friauf E. (2014). "Functional analysis of the inhibitory neurotransmitter transporters GlyT1, GAT-1, and GAT-3 in astrocytes of the lateral superior olive." GLIA 62(12): 1992-2003

Stillwell E. F., Cone C. M., & Cone Jun C. D. (1973). "Stimulation of DNA Synthesis in CNS Neurones by Sustained Depolarisation." Nature New Biology 246: 110-110

Sundelacruz S., Levin M., & Kaplan D. L. (2008). "Membrane potential controls adipogenic and osteogenic differentiation of mesenchymal stem cells." PLoS ONE 3(11): 1-15

Swanson R. A., Kauppinen W. Y., & Tiina M. (2004). "Astrocyte Influences on Ischemic Neuronal Death." Current Molecular Medicine 4(2): 193-205

Szuchet S., Nielsen J. A., Lovas G., Domowicz M. S., de Velasco J. M., Maric D., & Hudson L. D. (2011). "The genetic signature of perineuronal oligodendrocytes reveals their unique phenotype." European Journal of Neuroscience 34(12): 1906-1922

Takahashi A., Yamaguchi H., & Miyamoto H. (1993). "Change in K+ current of HeLa cells with progression of the cell cycle studied by patch-clamp technique." The American journal of physiology 265(2): C328-336

Takasaki C., Yamasaki M., Uchigashima M., Konno K., Yanagawa Y., & Watanabe M. (2010). "Cytochemical and cytological properties of perineuronal oligodendrocytes in the mouse cortex." European Journal of Neuroscience 32(8): 1326-1336

Taniike M., Mohri I., Eguchi N., Beuckmann C. T., Suzuki K., & Urade Y. (2002). "Perineuronal Oligodendrocytes Protect against Neuronal Apoptosis through the Production of Lipocalin-Type Prostaglandin D Synthase in a Genetic Demyelinating Model." The Journal of Neuroscience 22(12): 4885-4896

Thomzig A., Wenzel M., Karschin C., Eaton M. J., Skatchkov S. N., Karschin A., & Veh R. W. (2001). "Kir6.1 is the principal pore-forming subunit of astrocyte but not neuronal plasma membrane K-ATP channels." Molecular and Cellular Neuroscience 18(6): 671-690

Thulborn K. R., Davis D., Snyder J., Yonas H., & Kassam A. (2005). "Sodium MR Imaging of Acute and Subacute Stroke for Assessment of Tissue Viability." Neuroimaging Clinics of North America 15(3): 639-653

Tian G. F., Azmi H., Takano T., Xu Q., Peng W., Lin J., Oberheim N. A., Lou N., Wang X., Zielke H. R., Kang J., & Nedergaard M. (2005). "An astrocytic basis of epilepsy." Nature Medicine 11(9): 973-981

Toledo-Rodriguez M., & Markram H. (2014). "Single-Cell RT-PCR, a Technique to Decipher the Electrical, Anatomical, and Genetic Determinants of Neuronal Diversity BT ". In: M. Martina & S. Taverna (Eds.), Patch-Clamp Methods and Protocols (Vol. 1183, pp. 143-158). New York, NY: Springer New York.

Treloar H. B., Ray A., Dinglasan L. A., Schachner M., & Greer C. A. (2009). "Tenascin-C Is an Inhibitory Boundary Molecule in the Developing Olfactory Bulb." Journal of Neuroscience 29(30): 9405-9416

Tse F. W., Fraser D. D., Duffy S., & MacVicar B. A. (1992). "Voltage-activated K+ currents in acutely isolated hippocampal astrocytes." The Journal of Neuroscience 12(5): 1781-1788

Turrigiano G. G., Leslie K. R., Desai N. S., Rutherford L. C., & Nelson S. B. (1998). "Activity-dependent scaling of quantal amplitude in neocortical neurons." Nature 391: 892-892

Turrigiano G. G. (2006). "More than a sidekick: glia and homeostatic synaptic plasticity." Trends in Molecular Medicine 12(10): 458-460

Tyzack G. E., Sitnikov S., Barson D., Adams-Carr K. L., Lau N. K., Kwok J. C., Zhao C., Franklin R. J. M., Karadottir R. T., Fawcett J. W., & Lakatos A. (2014). "Astrocyte response to motor neuron injury promotes structural synaptic plasticity via STAT3-regulated TSP-1 expression." Nature Communications 5

Ullian E. M., Sapperstein S. K., Christopherson K. S., & Barres B. A. (2001). "Control of synapse number by glia." Science 291(5504): 657-661

Unichenko P., Myakhar O., & Kirischuk S. (2012). "Intracellular Na + concentration influences short-term plasticity of glutamate transporter-mediated currents in neocortical astrocytes." GLIA 60(4): 605-614

Urrego D., Tomczak A. P., Zahed F., Stühmer W., Pardo L. A., & Stuehmer W. (2014). "Potassium channels in cell cycle and cell proliferation." Phil. Trans. R. Soc. B 2014(February): 1-9

Uwechue N. M., Marx M. C., Chevy Q., & Billups B. (2012). "Activation of glutamate transport evokes rapid glutamine release from perisynaptic astrocytes." Journal of Physiology 590(10): 2317-2331

Valenzuela S. M., Mazzanti M., Tonini R., Qiu M. R., Warton K., Musgrove E. A., Campbell T. J., & Breit S. N. (2000). "The nuclear chloride ion channel NCC27 is involved in regulation of the cell cycle." Journal of Physiology 529(3): 541-552

Valverde F., & Lopez-Mascaraque L. (1991). "Neuroglial arrangements in the olfactory glomeruli of the hedgehog." Journal of Comparative Neurology 307(4): 658-674

Vargas M. R., Johnson D. A., Sirkis D. W., Messing A., & Johnson J. A. (2008). "Nrf2 Activation in Astrocytes Protects against Neurodegeneration in Mouse Models of Familial Amyotrophic Lateral Sclerosis." Journal of Neuroscience 28(50): 13574-13581

Vasek M. J., Garber C., Dorsey D., Durrant D. M., Bollman B., Soung A., Yu J., Perez-Torres C., Frouin A., Wilton D. K., Funk K., DeMasters B. K., Jiang X., Bowen J. R., Mennerick S., Robinson J. K., Garbow J. R., Tyler K. L., Suthar M. S., Schmidt R. E., Stevens B., & Klein R. S. (2016). "A complement-microglial axis drives synapse loss during virus-induced memory impairment." Nature 534(7608): 538-543

Verderio C., & Matteoli M. (2001). "ATP Mediates Calcium Signaling Between Astrocytes and Microglial Cells: Modulation by IFN- " The Journal of Immunology 166(10): 6383-6391

Verkhratsky A., Rodríguez J. J., & Parpura V. (2012). "Neurotransmitters and integration in neuronal-astroglial networks." Neurochemical Research 37(11): 2326-2338

Verkhratsky A., & Nedergaard M. (2015). "Physiology of Astroglia." (Vol. 98): Morgan & Claypool Lofe Scienes.

Verkhratsky A., & Nedergaard M. (2018). "Physiology of Astroglia." Physiological Reviews 98(1): 239-389

Virchow R. (1856). "Gesammelte Abhandlungen zyr wissenschaftlischen Medizin." Frankfurt, Germany: Verlag von Meidinger Sohn & Comp.

Virchow R. (1858). "Die Cellularpathologie in ihrer Begründung auf physiologische and pathologische Gewebelehre." (Zwanzig Vo ed.): Berlin: August Hirschwald.

Voigt T. (1989). "Development of glial cells in the cerebral wall of ferrets: Direct tracing of their transformation from radial glia into astrocytes." Journal of Comparative Neurology 289(1): 74-88

von Hilchen C. M., Beckervordersandforth R., Rickert C., Technau G. M., & Altenhein B. (2008). "Identity, origin, and migration of peripheral glial cells in the Drosophila embryo." Mechanisms of Development 125(3-4): 337-352

Wahl-Schott C., & Biel M. (2008). "HCN channels: Structure, cellular regulation and physiological function." Cellular and Molecular Life Sciences 66(3): 470-470

Wang D., & Fawcett J. (2012). "The perineuronal net and the control of cns plasticity." Cell and Tissue Research 349(1): 147-160

Wang D. D., & Bordey A. (2008). "The astrocyte odyssey." Progress in Neurobiology 86(4): 342-367

Wang E., Yin Y., Zhao M., Forrester J. V., & McCaig C. D. (2003). "Physiological electric fields control the G 1 /S phase cell cycle checkpoint to inhibit endothelial cell proliferation." The FASEB Journal 17(3): 458-460

Wang Y., Jia H., Walker A. M., & Cukierman S. (1992). "K-Current Mediation of Prolactin-Induced Proliferation of Malignant (N b2) Lymphocytes." Journal of Cellular Physiology 152: 185-189

Wanner I. B., Anderson M. A., Song B., Levine J., Fernandez A., Gray-Thompson Z., Ao Y., & Sofroniew M. V. (2013). "Glial Scar Borders Are Formed by Newly Proliferated, Elongated Astrocytes That Interact to Corral Inflammatory and Fibrotic Cells via

STAT3-Dependent Mechanisms after Spinal Cord Injury." Journal of Neuroscience 33(31): 12870-12886

Waxman S. G. (1986). "The astrocyte as a component of the node of Ranvier." Trends in Neurosciences 9: 250-253

Westergaard N., Sonnewald U., & Schousboe A. (1995). "Metabolic Trafficking between Neurons and Astrocytes: The Glutamate/Glutamine Cycle Revisited." Developmental Neuroscience 17(4): 203-211

Whittaker M. T., Zai L. J., Lee H. J., Pajoohesh-Ganji A., Wu J., Sharp A., Wyse R., & Wrathall J. R. (2012). "GGF2 (Nrg1-β3) treatment enhances NG2 + cell response and improves functional recovery after spinal cord injury." GLIA 60(2): 281-294

Wilhelmsson U., Bushong E. A., Price D. L., Smarr B. L., Phung V., Terada M., Ellisman M. H., & Pekny M. (2006). "Redefining the concept of reactive astrocytes as cells that remain within their unique domains upon reaction to injury." Proceedings of the National Academy of Sciences 103(46): 17513-17518

Wilson G. F., & Chiu S. Y. (1993). "Mitogenic factors regulate ion channels in Schwann cells cultured from newborn rat sciatic nerve." The Journal of Physiology 470(1): 501-520

Winkler B. S., Orselli S. M., & Rex T. S. (1994). "The redox couple between glutathione and ascorbic acid: A chemical and physiological perspective." Free Radical Biology and Medicine 17(4): 333-349

Wonderlin W. F., Woodfork K. A., & Strobl J. S. (1995). "Changes in membrane potential during the progression of MCF-7 human mammary tumor cells through the cell cycle." Journal of Cellular Physiology 165(1): 177-185

Woodfork K. A., Wonderlin W. F., Peterson V. A., & Strobl J. S. (1995). "Inhibition of ATP-sensitive potassium channels causes reversible cell-cycle arrest of human breast cancer cells in tissue culture." Journal of Cellular Physiology 162(2): 163-171

Wright S. H. (2004). "Generation of resting membrane potential." AJP: Advances in Physiology Education 28(4): 139-142

Wu X.-F., Liu W.-T., Liu Y.-P., Huang Z.-J., Zhang Y.-K., & Song X.-J. (2011). "Reopening of ATP-sensitive potassium channels reduces neuropathic pain and regulates astroglial gap junctions in the rat spinal cord." PAIN 152(11): 2605-2015

Wu X., Liao L., Liu X., Luo F., Yang T., & Li C. (2012). "Is ZD7288 a selective blocker of hyperpolarization-activated cyclic nucleotide-gated channel currents?" Channels 6(6): 438-442

Yan Y. P., Lang B. T., Vemuganti R., & Dempsey R. J. (2009). "Galectin-3 mediates post-ischemic tissue remodeling." Brain Research 1288: 116-124

Yao X., Hrabetova S., Nicholson C., & Manley G. T. (2008). "Aquaporin-4-Deficient Mice Have Increased Extracellular Space without Tortuosity Change." Journal of Neuroscience 28(21): 5460-5464

Yee J. M., Agulian S., & Kocsis J. D. (1998). "Vigabatrin enhances promoted release of GABA in neonatal rat optic nerve." Epilepsy Research 29(3): 195-200

Yi J. H., Katagiri Y., Susarla B., Figge D., Symes A. J., & Geller H. M. (2012). "Alterations in sulfated chondroitin glycosaminoglycans following controlled cortical impact injury in mice." Journal of Comparative Neurology 520(15): 3295-3313

Young C. C., Al-Dalahmah O., Lewis N. J., Brooks K. J., Jenkins M. M., Poirier F., Buchan A. M., & Szele F. G. (2014). "Blocked angiogenesis in Galectin-3 null mice does not alter cellular and behavioral recovery after middle cerebral artery occlusion stroke." Neurobiology of Disease 63: 155-164

Zaheer A., Yorek M. A., & Lim R. (2001). "Effects of Glia Maturation Factor Overexpression in Primary Astrocytes on MAP Kinase Activation, Transcription Factor Activation, and Neurotrophin Secretion." Neurochemical Research 26(12): 1293-1299

Zamanian J. L., Xu L., Foo L. C., Nouri N., Zhou L., Giffard R. G., & Barres B. A. (2012). "Genomic Analysis of Reactive Astrogliosis." Journal of Neuroscience 32(18): 6391-6410

Zanotti S., & Charles a. (1997). "Extracellular calcium sensing by glial cells: low extracellular calcium induces intracellular calcium release and intercellular signaling." Journal of Neurochemistry 69(2): 594-602

Zhan Y., Paolicelli R. C., Sforazzini F., Weinhard L., Bolasco G., Pagani F., Vyssotski A. L., Bifone A., Gozzi A., Ragozzino D., & Gross C. T. (2014). "Deficient neuron-microglia signaling results in impaired functional brain connectivity and social behavior." Nature Neuroscience 17(3): 400-406

Zheng K., Bard L., Reynolds J. P., King C., Jensen T. P., Gourine A. V., & Rusakov D. A. (2015). "Time-Resolved Imaging Reveals Heterogeneous Landscapes of Nanomolar Ca2+in Neurons and Astroglia." Neuron 88(2): 277-288

Zheng Y. J., Furukawa T., Ogura T., Tajimi K., & Inagaki N. (2002). "M phase-specific expression and phosphorylation-dependent ubiquitination of the ClC-2 channel." Journal of Biological Chemistry 277(35): 32268-32273

Zhou M., Tanaka O., Suzuki M., Sekiguchi M., Takata K., Kawahara K., & Abe H. (2002). "Localization of pore-forming subunit of the ATP-sensitive K+-channel, Kir6.2, in rat brain neurons and glial cells." Molecular Brain Research 101: 23-32

Zhou M. (2005). "Development of GLAST(+) Astrocytes and NG2(+) Glia in Rat Hippocampus CA1: Mature Astrocytes Are Electrophysiologically Passive." Journal of Neurophysiology 95(1): 134-143

Zhou M., Xu G., Xie M., Zhang X., Schools G. P., Ma L., Kimelberg H. K., & Chen H. (2009). "TWIK-1 and TREK-1 Are Potassium Channels Contributing Significantly to Astrocyte Passive Conductance in Rat Hippocampal Slices." The Journal of Neuroscience 29(26): 8551-8564

Zhu X., Bergles D. E., & Nishiyama A. (2007). "NG2 cells generate both oligodendrocytes and gray matter astrocytes." Development 135(1): 145-157

Zhu X., Hill R. A., & Nishiyama A. (2008). "NG2 cells generate oligodendrocytes and gray matter astrocytes in the spinal cord." Neuron Glia Biology 4(1): 19-26

Zhu X., Hill R. A., Dietrich D., Komitova M., Suzuki R., & Nishiyama A. (2011). "Age-dependent fate and lineage restriction of single NG2 cells." Development 138(4): 745-753

6 List of Figures

7 Glossary

°C	degree Celsius
µl	micro litre
µm	micro meter
µM	micro Molar
2pLSM	2 photon laser scanning microscope
ACSF	artificial cerebrospinal fluid
ADK	adenosine kinase
AFB	Atipamezol/Flumazenil/Buprenorphine
Aldh1l1	aldehyde dehydrogenase 1 family, member L1
AMPA	alpha-amino-3-hydroxy-5-methyl-4-isoxazolepropionic acid
AP-1	activator protein 1
APOE	apolipoprotein E
AQP4	aquaporin 4
ATP	adenosine triphosphate
ATPase	adenosine triphosphatase
Ba^{2+}	barium
BAC	bacterial artificial chromosome
$BaCl_2$	barium chloride
BBB	blood-brain barrier
BK	big conductance
Ca^{2+}	calcium
$CaCl_2$	calcium chloride
cAMP	cyclic adenosine monophosphate
CC	corpus callosum
CD	cluster of differentiation
Cdc	cell division control protein
CDK	cyclin-dependant kinases
c-fos	AP-1 transcription factor subunit

CGE	caudal ganglionic eminence
c-kit	tyrosine-protein kinase kit
Cl^-	chloride
cm	centimetres
c-myc	avian myelocytomatosis viral oncogene homolog
CNS	central nervous system
CO_2	carbon dioxide
CSPGs	chondroitin sulphate proteoglycans
DAMP	danger-associated molecular pattern
dG_r	effective resting membrane conductance
DiI	3H-Indolium
DNA	deoxyribonucleic acid
DNTM	DNA (cytosine-5)-methyltransferase
dpi	days post injury
dV_r	effective resting membrane potential
E1	embryonic day 1
EAAT	excitatory amino acid transporter
eGFP	enhanced green fluorescent protein
EGFR	epidermal growth factor receptor
EGTA	triethylene glycol diamine tetra acetic acid
E_i	equilibrium potential
E_K	potassium equilibrium potential
Emx1	empty spiracles homeobox 1
FGF	fibroblast growth factor
GABA	gamma-aminobutyric acid
GAT	GABA transporter
GFAP	glial fibrillary acidic protein
GFP	green fluorescent protein
GLAST	glutamate aspartate transporter
Gln	glutamine

GLT	glutamate transporter
Glu	glutamate
G-phase	gap phase
G_r	resting membrane conductance
GS	glutamine-synthetase
Gsh2	glutathione synthetase 2
GTPase	guanosine triphosphate hydrolase enzyme
H^+	hydrogen
HCN	hyperpolarisation-activated cyclic nucleotide-gated
HCO_3^-	hydrogen carbonate
Hepes	2-[4-(2-hydroxyethyl)piperazin-1-yl]ethane sulfonic acid
hERG	human Ether-a-go-go Related Gene
Hes	hairy and enhancer of split
HIP	hippocampus
HMGB1	high-mobility group box 1
Hy	hypothalamus
Hz	Hertz
I	current
i.p.	intraperitoneal
i.v.	intravenous
I_a	transient potassium currents
I_d	delayed rectifying current
I_h	hyperpolarization-activated cation current
IK	intermediate conductance
IL	interleukin
IV-curve	Current/voltage-curve
J	juxtavascular
K^+	potassium ion
K_{2P}	two-pore-domain potassium channel
K_{ATP}	ATP-sensitive potassium channel

KCl	potassium chloride
kg	kilograms
KH_2PO_4	monobasic potassium phosphate
kHz	kilo Hertz
K_{ir}	inwardly rectifying potassium channel
K_v	voltage activated potassium channel
Lgals	Lectin, Galactoside-Binding, Soluble
LGE	lateral ganglionic eminence
LI	cortical layer I
LII	cortical layer II
LIII	cortical layer III
LIV	cortical layer IV
LPS	lipopolysaccharide
LSO	lateral superior olive
LTP	long term potentiation
LV	cortical layer V
LV	cortical layer V
LVI	cortical layer VI
LVI	cortical layer VI
M	molar
mCherry	monomeric cherry fluorescent protein
MCT	monocarboxylate transporter
mg	milligram
$MgCl_2$	magnesium chloride
MGE	medial ganglionic eminence
mGluR	metabotropic glutamate receptors
MHC	major histocompatibility complex
ml	millilitre
mM	millimolar
mm	millimetre

MMF	Medetomidin/Midazolam/Fentanyl
MNTB	medial nucleus of the trapezoid body
M-phase	mitosis-phase
mRNA	messenger ribonucleic acid
ms	millisecond
mV	millivolt
mW	milliwatt
MΩ	Mega Ohm
n.s.	not significant
nA	nano ampere
Na^+	sodium ion
Na_2-ATP	adenosine 5′-triphosphate disodium salt hydrate
Na_2HPO_4	disodium hydrogen phosphate
NaCl	sodium chloride
NADP	nicotinamide adenine dinucleotide phosphate
NaH_2PO_4	sodium dihydrogen phosphate
$NaHCO_3$	sodium hydrogen carbonate
NaOH	sodium hydroxide
Na_v	voltage activated sodium channels
N-CoR	nuclear receptor co-repressor 1
NFIA	nuclear factor 1 A-type
NFκB	nuclear factor kappa-light-chain-enhancer of activated B cells
NG2	neuron-glial antigen 2
NH_4^+	ammonium
Nj	non-juxtavascular
Nkx2.1	thyroid transcription factor 1
nm	nano meter
NMDA	N-Methyl-D-Aspartate
nS	nano Siemens
O_2	oxygen

p1	postnatal day 1
PB	phosphate buffer
PFA	paraformaldehyde
pH	potentia hydrogenii
PKA	protein kinase
PNS	peripheral nervous system
R	resistance
Raf	serine/threonine-protein kinase
RAGE	receptor for advanced glycation end products
Ras	rat sarcoma (GTP-ase)
r-eag	rat ether-à-go-go
Rho	Ras homologue
R_{in}	input resistance
ROS	reactive oxygen species
RT-PCR	real time - polymerase chain reaction
RT-qPCR	real time – quantitative polymerase chain reaction
s	second
S1	primary somatosensory cortex
S2	secondary somatosensory cortex
Shal	potassium voltage-gated channel subfamily D
Shh	sonic hedgehog
SK	small conductance
Sox9	sex determining region Y-box 9
S-phase	synthesis-phase
STAT	signal transducer and activator of transcription
SUR	ATP-binding cassette transporter sub-family C
TBI	traumatic brain injury
TCA	tricarboxylic acid
TGF-β	transforming growth factor beta
Th	thalamus

TL649	DyLight649 conjugated *Lycopersicon esculentum* (tomato) lectin
TLR	toll-like receptor
TNFα	tumour necrosis factor alpha
TREK	potassium channel subfamily K member 2
TWIK	potassium channel subfamily K member 1
V	voltage
V3	third ventricle
VEGF	vasoactive endothelial growth factor
VL	lateral ventricle
V_r	resting membrane potential

8 Appendix

Chemical Suppliers

Agarose	(A9539-250G; Sigma Aldrich Chemie GmbH)
Alexa Fluor® 568 hydrazide	(A10437; Thermo Fisher Scientific Inc.)
$BaCl_2$ dihydrate	(31125-500G-R; Sigma Aldrich Chemie GmbH)
Bovine Serum Albumin	(A7906-100G; Sigma Aldrich Chemie GmbH)
$CaCl_2$ dihydrate	(C5080-500G; Sigma Aldrich Chemie GmbH)
D-(+)-Glucose	(G7528-1KG; Sigma Aldrich Chemie GmbH)
EGTA	(E-1219; Invitrogen GmbH)
Heparin	(Meditech Vertriebs GmbH)
Hepes	(H7523-250G; Sigma Aldrich Chemie GmbH)
KCl	(P9333-500G; Sigma Aldrich Chemie GmbH)
K-Gluconate	(P1847-500G; Sigma Aldrich Chemie GmbH)
KH_2PO_4	(P5655-100G; Sigma Aldrich Chemie GmbH)
L-ascorbic acid	(A4544-100G; Sigma Aldrich Chemie GmbH)
$MgCl_2$	(M2670-100G; Sigma Aldrich Chemie GmbH)
myo-Inositol	(I5125-500G; Sigma Aldrich Chemie GmbH)
Na_2-ATP	(A26209-1G; Sigma Aldrich Chemie GmbH)
NaCl	(S7653-1KG; Sigma Aldrich Chemie GmbH)
NaH_2PO_4	(S8282-500G; Sigma Aldrich Chemie GmbH)
$NaHCO_3$	(S6297-250G; Sigma Aldrich Chemie GmbH)
Na-pyruvate	(P2256-100G; Sigma Aldrich Chemie GmbH)
PFA	(0335.3; Carl Roth GmbH + Co. KG)
Saponin	(47036-250G-F; Sigma Aldrich Chemie GmbH)
Sucrose	(S7903-1KG; Sigma Aldrich Chemie GmbH)
TritonX100	(3051.4; Carl Roth GmbH + Co. KG)
ZD7288	(BN0631; Biotrend Chemichalien GmbH)

9 Acknowledgements

Firstly, I want to thank my supervisor **PD Dr. Lars Kunz** for constantly supporting me during the last years with his encouragement, enthusiasm, guidance, interesting discussions and expertise. Your reassurance and kind words helped me to be aware of what I can achieve and reassured me to believe in myself and in what I do through all ups and downs of my PhD.

I especially want to thank **Prof. Dr. Benedikt Grothe** for giving me the opportunity to work on my favourite cells, the astrocytes. Thank you for all the great discussions we had, your expertise and input and for always lending an open ear. Moreover, thank you for being the second referee of my PhD thesis and a member of my TAC.

Also I want to thank **Prof. Dr. Magdalena Götz** for providing together with Benedikt the great topic of my PhD thesis and for being a member of my TAC. Thank you for the great suggestions and discussions about new approaches from a different perspective.

Moreover, I want to thank my other TAC member **Prof. Dr. Christian Wahl-Schott** for all the great suggestions and especially for his input on HCN channels.

Of course there are also many other people that accompanied me the last years.

Thank you…..

… Dr. **Olga Alexandrova, Karin Fischer, Hilde Wohlfrom** and **Bea Stiening** for all your technical advice and support in the lab and for teaching me so much.

… the whole **GSN Team** for always helping out if I had and any questions and for all the organizational effort you put into events, teaching, administration and supporting us students.

… to the my lab peers **Dr. Sonja Brosel** and **Dr. Stephan Keplinger** for always having a helping hand and made working in the lab a lot of fun.

…to my fellow office inmates **Dieter**, **Helge**, **Dani**, **Barbara**, **Diana** and **Shreya** who made the time at the university an especially great and fun one. Thanks for always listening, supporting and especially for all the joking around.

… an meine Mutter die mir ermöglicht hat da zu sein wo ich jetzt bin und mich immer auf jegliche Art und Weise unterstützt. An meine Schwester die mir immer den Rücken freigehalten und ganz besonders immer dann einen kühlen Kopf bewahrt hat wenn ich es nicht konnte. Und natürlich meinem Freund Florian, für die viele Geduld und die moralische Unterstützung.

10 Short CV

11 Affidativ

Eidesstattliche Versicherung/Affidavit

Hiermit versichere ich an Eides statt, dass ich die vorliegende Dissertation

„Electrophysiological characterisation and expression pattern of ion channels in astrocytes before and after traumatic brain injury“

selbstständig angefertigt habe, mich außer der angegebenen keiner weiteren Hilfsmittel bedient und alle Erkenntnisse, die aus dem Schrifttum ganz oder annähernd übernommen sind, als solche kenntlich gemacht und nach ihrer Herkunft unter Bezeichnung der Fundstelle einzeln nachgewiesen habe.

I hereby confirm that the dissertation

“Electrophysiological characterisation and expression pattern of ion channels in astrocytes before and after traumatic brain injury“

is the result of my own work and that I have only used sources or materials listed and specified in the dissertation.

München, den

Munich, Date 22.07.2019 ----------

Stefanie Götz